Dissertations (2016-Present)   Dissertations

8-2022

Preclinical Development of Novel Chemotherapeutic Agent AC1LPSZG: Formulation Optimization, in Vitro Characterization, and in Vivo Pharmacokinetics

Ritu Gupta

PRECLINICAL DEVELOPMENT OF NOVEL CHEMOTHERAPEUTIC AGENT

AC1LPSZG: FORMULATION OPTIMIZATION, *IN VITRO*

CHARACTERIZATION, AND *IN VIVO* PHARMACOKINETICS

DISSERTATION

Presented in Partial Fulfillment of the Requirements for

the Degree Doctor of Philosophy in the Graduate School

of Texas Southern University

By

Ritu Gupta

Texas Southern University

2022

Approved By

Huan Xie, Ph.D.
_____
Chairperson, Dissertation Committee

Gregory H. Maddox, Ph.D.
_____
Dean, The Graduate School

Approved By

Huan Xie, Ph.D.   06/15/2022

Chairperson, Dissertation Committee   Date

Dong Liang, Ph.D.   06/15/2022

Committee Member   Date

Yuanjian Deng, Ph. D.   06/15/2022

Committee Member   Date

Song Gao, Ph.D.   06/15/2022

Committee Member   Date

PRECLINICAL DEVELOPMENT OF NOVEL CHEMOTHERAPEUTIC AGENT AC1LPSZG: FORMULATION OPTIMIZATION, *IN VITRO* CHARACTERIZATION, AND *IN VIVO* PHARMACOKINETICS

By

Ritu Gupta

Texas Southern University, 2022

Professor Huan Xie, PhD, Advisor

Preclinical development of novel chemotherapeutic agent AC1LPSZG, a mammalian target of rapamycin (mTOR) inhibitor, involved development of sensitive reverse-phase ultra-performance liquid chromatography (UPLC) and LC-MS/MS methods for quantification of AC1LPSZG in *in vitro* study samples and rat plasma, respectively. Pharmacokinetic studies were done in SD rats after intravenous injection of cosolvent formulations. The resulting pharmacokinetic parameters were analyzed using non-compartmental analysis (NCA) and two-compartmental modeling.

Poly (D, L-lactic-co-glycolic acid) (PLGA) is most used biodegradable synthetic polymer for nano drug delivery due to its non-toxic and biodegradable nature, and tunable release properties. PLGA nanoparticles (NPs) were prepared by 'nanoprecipitation' technique using a nonionic surfactant poloxamer P188. The particle size, size distribution, and zeta potential of prepared nanoparticles were analyzed using dynamic light scattering

1

(DLS). The drug entrapment efficiency (%EE) was accessed by ultra-sonication of lyophilized NPs with acetonitrile and analyzing the drug content using UPLC. Design of Experiments (DoE) strategy using Design Expert® software (version 13) was successfully used to optimize PLGA (50:50) based NPs of AC1LPSZG. Optimized batch was prepared using 5 mg drug and 4 mL aqueous phase volume with EE of 41.2%, NP size of 124 nm, drug load of 2.6% and zeta potential of – 15 mV. We conclude similar DOE approaches can help to understand and optimize innovative manufacturing processes, needed for the quality by design (QbD) preparation of other nano-formulations.

The *in vitro* drug release was tested in phosphate buffer pH 6.8 for 72 hours, employing USP-4 apparatus CE7-smart (SOTAX®) incorporated with Float-A-Lyzer dialysis cells at 300 kDa molecular weight cut–off (MWCO), flow rate 16 mL/min and temperature 37°C. Different surfactants were explored to enhance the drug solubility and accelerate the *in vitro* drug release. The influence of three different surfactants: SLS (Sodium Lauryl Sulfate-anionic), Tween 80 (non-ionic) and CTAB (Cetyltrimethylammonium bromide- cationic) on drug solubility, sink conditions and dissolution behavior was demonstrated. The solubility improvement was in the order of SLS > Tween80 > CTAB and dissolution efficiency was improved with the increase of surfactant concentration. The developed *in vitro* drug release method was able to discriminate among different release profiles. In brief, similar discriminatory test method can be used as a quality control tool to identify critical formulation and process parameters

and can also be used as a surrogate for bioequivalence studies if a predictive *IVIVC* (*In vitro In vivo* correlation) is obtained.

TABLE OF CONTENTS

LIST OF TABLES

LIST OF FIGURES

LIST OF ABBREVIATIONS

- -2 Log Likelihood (-2LL)
- % Coefficient of Variation or Precision (% CV)
- % Relative Error of Accuracy (% RE)
- 2FI (2-Factor Interaction)
- Akaike's Information Criteria (AIC)
- Analysis of Variance or Fisher Test (ANOVA)
- Area Under the Plasma Concentration-Time Curve to Infinity (AUC∞)
- Bayesian Information Criteria (BIC)
- Biopharmaceutics Classification System (BCS)
- Blood Urea Nitrogen (BUN)
- Concentration after complete dissolution of NPs (Cd)
- Central Composite Design (CCD)
- Cetrimonium Bromide or Hexadecyltrimethylammonium Bromide (CTAB)
- Clearance (CL)
- Coefficient Of Determination (R^2)
- Collision Cell Exit Potential (CXE)
- Collision Energy (CE)
- Critical Material Attributes (CMAs)
- Critical Quality Attributes (CQAs)
- Saturation Solubility of Drug
- Decluttering Potential (DP)
- Design Of Experiment (DoE)
- Difference Factor (F1)
- Differential Scanning Calorimetry (DSC)

- Dimethyl Sulfoxide (DMSO)

- Dissolution Efficiency (DE)

- Drug Loading (DL)

- Elimination Rate (K_{el})

- Encapsulation Efficiency (EE)

- Enhanced Permeability and Retention (EPR)

- Entrance Potential (EP)

- Glass Transition Temperature (T_g)

- Half-Life ($T_{1/2}$)

- Heat Capacity (Cp)

- Heater Gas (Gas 2)

- ICH (International Council for Harmonization of Technical Requirements for Pharmaceuticals for Human Use)

- Internal Standard (IS)

- Lactate Dehydrogenase (LDH)

- Limit of Detection (LOD)

- Liquid Chromatography-Tandem Mass Spectrometry (LC-MS/MS

- Lower Limit of Quantitation (LLOQ)

- Malondialdehyde (MDA)

- Mammalian Target of Rapamycin (mTOR)

- Mean Residence Time (MRT)

- Mean Squared Error (MSE)

- Melting Point (MP)

- Membrane Molecular Weight Cutoff (MWCO)

- Model Selection Criteria (MSC)

- Molecular Weight Cut–Off (MWCO)

- Multiple Reaction Monitoring (MRM)

- Nano Drug Delivery Systems (NDDS)

- Nanoparticles (NPs)

- Nebulizer Gas (Gas 1)

- Non-Compartmental Analysis (NCA)

- Non-Small Cell Lung Cancer (NSCLC)

- Novel Chemical Entity (NCE)

- One Variable/Factor at A Time (OVAT Or OFAT)

- Peak Exposure (C_{max})

- Pharmacokinetic (PK)

- Phosphate-Buffered Saline (PBS)

- Plackett–Burman Designs (PBDs)

- Plasma Creatinine (PC)

- PLGA (50:50) or (50:50)

- PLGA (75:25) or (75:25)

- Poly (Glycolic Acid) (PGA)

- Poly (L-Lactic Acid) (PLA),

- poly (lactic-co-glycolic acid) (PLGA)

- Poly(E-Caprolactone) (PCL)

- Polydispersity Index (PdI)

- Polyethylene Glycols (PEG)

- Polyvinyl Alcohol (PVA)

- Polyvinylpyrrolidone (PVP)

- Predicted Residual Error Sum of Squares (PRESS)

- Process Analytical Technology (PAT)

- Process Parameters (CPPs)

- Quality by Design (QbD)

- Quality Target Product Profile (QTPP

- Quality Target Product Profile (QTPP)
- Rapid Expansion of a Supercritical Solution into A Liquid Solvent' (RESOLV)
- Rapid Expansion of Supercritical Solutions (RESS)
- Resomer® RG 503H (Resomer)
- Response Surface Methods (RSMs)
- Similarity Factor (F2)
- Sodium Lauryl Sulfate (SLS)
- Sprague-Dawley (SD) Rats
- Spray Freeze Drying (SFD)
- TdT dUTP Nick End Labeling Assay
- Terminal deoxynucleotidyl transferase (TdT) deoxyuridine triphosphate (dUTP) Nick End Labeling Assay (TUNEL)
- Thermogravimetry (TG or TGA)
- Tween® 80 (Polyoxyethylene (80)
- Ultra-Performance Liquid Chromatography (UPLC)
- United States Pharmacopoeia (USP)
- Volume Of Distribution (V_d)

VITAE

EDUCATION

- Texas Southern University, Houston, TX, USA — PhD (Pharmaceutical Sciences) (2017 – 2022)
- Uttarakhand Technical University, Dehradun, UK, India — PhD (Pharmaceutics) (2010 – 2013)
- UP Technical University, Lucknow, UP, India — M. Pharm (Pharmaceutics) (2004 – 2006)
- MJP Rohilkhand University, Bareilly, UP, India — B. Pharm (Pharmacy) (1999 – 2003)

PROFESSIONAL EXPERIENCE

- Texas Southern University, Houston, TX, USA— Graduate Research Assistant (2017 – 2022)
- Invertis University, Bareilly, India — Associate Professor (Aug 2015 – Aug 2017)
- IIMT, Greater Noida, India — Associate Professor (Aug 2013 – Aug 2015)
- RKGIT, Ghaziabad, UP, India — Assistant Professor (Jan 2007 – July 2013)

ACKNOWLEDGEMENTS

First and foremost, I would like to thank my esteemed supervisor Dr. Huan Xie for her invaluable supervision, tutelage, and for her unwavering support and believing in me. I would like to extend my sincere thanks to Dr. Dong Liang for his insightful comments and suggestions at every stage of this research project. My gratitude extends to my dissertation committee members Dr. Song Gao and Dr. Yuanjian Deng who supported me and offered deep insight into the study.

I would also like to express my gratitude to Dr. Yuan Chen who helped me in becoming accustomed to the lab and in finalizing this project. I would like to show my deep appreciation to Dr. Mahua Sarkar for her critique that influenced the progress and final shape of my experimental methods. I would like to offer my special thanks to Dr. Jing Ma for her kind help and all the support she provided throughout the study.

I express my appreciation to Dr. Du Ting for providing technical support. I would also like to thank my seniors Dr. Xiuqing Gao, Dr. Ololade Tosin Awosemo and my colleagues Maria Rincon Nigro, Robin Sunsong, Maryam Hoseini Zare and Imoh Etim for their valuable and timely support throughout my study.

I am very grateful to the College of Pharmacy and Health Sciences at Texas Southern

CHAPTER 1 INTRODUCTION

1.1 Nanotechnology and Nano drug delivery systems (NDDS)

Nanotechnology is an emerging technology that encompasses a broad range of FDA-regulated products, including foods, cosmetics, and drug delivery systems. Materials in the nanoscale range (at least one dimension in size range of 1 to 100 nm) (Figure 1.1) are unique as they can exhibit different physical, chemical, or biological properties compared to their larger-scale counterparts. "Nanotechnology products" are the products that contain or are manufactured using materials in the nanoscale range, as well as the products that contain or are manufactured using materials exhibiting dimension-dependent phenomena (FDA & Nanotechnology, 2014).

Nano drug delivery systems (NDDS) are formulation approaches to improve therapeutic efficacy and safety of conventional dosage forms (Ventola, 2017). These NDDS may improve therapeutic drug performance by enhancing drug solubility, minimizing gastric degradation, controlling drug release or extending circulation time for greater drug accumulation (Deng et al., 2019). NDDS can dodge the physiological barriers like immune clearance, renal clearance, mechanical, enzymatic, and pH degradation to achieve higher drug levels at lower doses. Passive targeting of NDDS utilizes well known 'enhanced permeability and retention (EPR)' effect characterized by increased vascular permeability and poor lymphatic drainage of the tumor microenvironment (e.g., Doxil®,

Baxter Healthcare Corp.). Active targeting is based on receptor-ligand binding (Gupta et al., 2021). NDDS attached to a suitable ligand (e.g., antibodies, proteins) can bind to receptors present on specific cells (e.g., trastuzumab binds to HER2 receptors) (Attia et al., 2019).

Based on the integrity of particles, the NDDS can be classified into two broad categories, nonrigid nanoparticles (NPs) and rigid NPs. The nonrigid NPs consist of relatively soft structures easily disrupted by external forces. Lipid-based NPs such as liposomes and solid lipid NPs are categorized as nonrigid NPs. Rigid NPs are known to possess significant mechanical strength compared with nonrigid NPs and encompass polymeric NPs, carbon nanotubes, and metal-based NPs (Mahato, 2017).

1.2 Polymeric NDDS

Polymeric NDDS are being enormously investigated for a range of delivery routes like oral (Sonaje et al., 2010), transdermal (Rao et al., 2015), vaginal (Leyva-Gomez et al., 2018), ocular (Sánchez-López et al., 2017) and parenteral (Joshi & Muller, 2009) routes to treat a range of diseases such as diabetes (Wong et al., 2020), malaria (Guo et al., 2013), tuberculosis (Hwang et al., 2015) and cancer (Awasthi et al., 2018). They possess better targeting abilities, higher encapsulation efficiency and long-term storage capabilities than other nano-carriers (Kammari et al., 2017). Polymeric NDDS can be classified as nanospheres or nanocapsules. Nanospheres consist of polymeric matrices, whereas the nanospheres consist of vesicles (generally oily) covered with polymers (Mahato, 2017).

Polymeric NDDS may consist of natural, synthetic, or semisynthetic polymers. Natural polymers consist of chitosan (Lima et al., 2018; Ozturk & Kiyan, 2020), alginate (Sanna et al., 2012), albumin (Li et al., 2015; Shubhra et al., 2014), hyaluronic acid (HA)(Choi et al., 2010), collagen (Grant et al., 2014), and gelatin (Sahoo et al., 2015). Ethyl cellulose (Basta et al., 2020) and cellulose acetate (Beisl et al., 2019) are some semisynthetic polymers used for NPs preparation. Synthetic polymers can be classified as biodegradables and nonbiodegradables. Biodegradable polymers self-degrade over time due to hydrolysis and therefore require no surgical removal. Poly(ε-caprolactone) (PCL), poly(L-lactic acid) (PLA), poly(glycolic acid) (PGA) and Poly(D,L-lactic-co-glycolic acid) (PLGA) are examples of biodegradable polymers. PLGA is the most used biodegradable polymer because of its non-toxic and biodegradable nature and tunable release properties (Taghavi et al., 2017). Polyacrylamide (Sandland et al., 2021) and polystyrene (Balbi et al., 2017) are examples of nondegradable polymers used for NPs preparation.
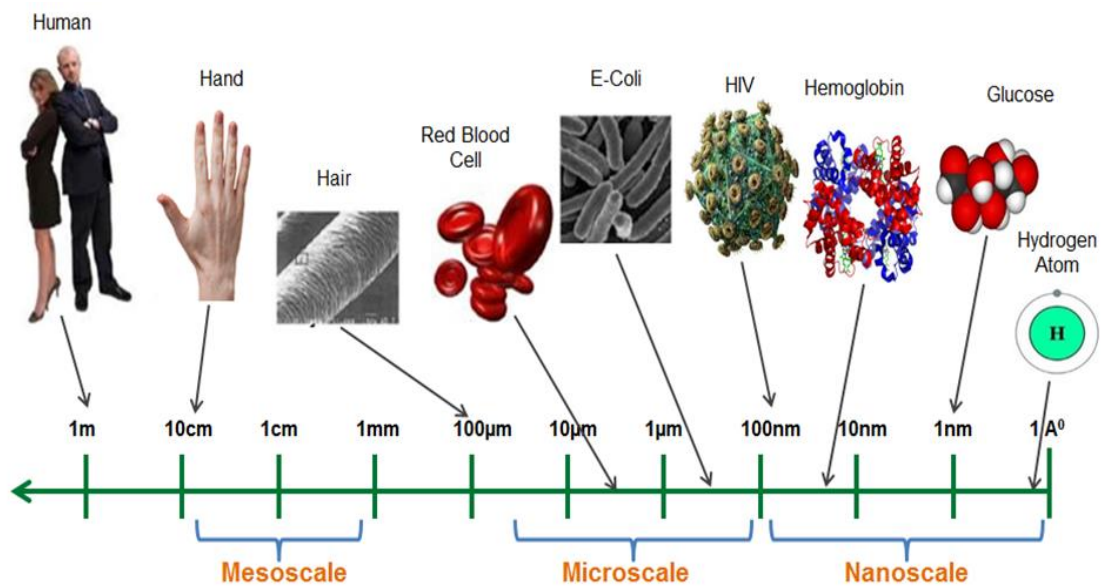
Figure 1. 1: Nanoscale Illustration

(Reference: https://shayonano.com/wp-content/uploads/2014/10/FAQ-1.png)

1.3 <u>Preparation of Polymeric NDDS</u>

The selection of appropriate method for NPs preparation depends on the physicochemical properties of the drug and polymer. Small laboratory-scale methods include two broad categories: top-down approaches (dispersion of preformed polymers) and bottom-up (polymerization of monomers) strategies. Large-scale NPs preparation methods include supercritical fluid technology and spray drying. Preparation methods using preformed polymer include emulsion-solvent evaporation, emulsion-solvent diffusion, nanoprecipitation, salting out, and nonaqueous phase separation methods (Kammari et al., 2017).

1.3.1 Emulsion-Solvent Evaporation Method

This is a two-step method mainly used for lipophilic drugs (Figure 1. 2). The first step involves emulsifying polymer solution into an aqueous phase and the second step requires evaporation of the organic solvent. Solvent evaporation results in precipitation of nanospheres that are collected by ultracentrifugation. Nanosphere size depends on the type and concentration of surfactant, homogenization time and speed, phase ratio, and polymer concentration (Desgouilles et al., 2003; Urbaniak & Musiał, 2019).
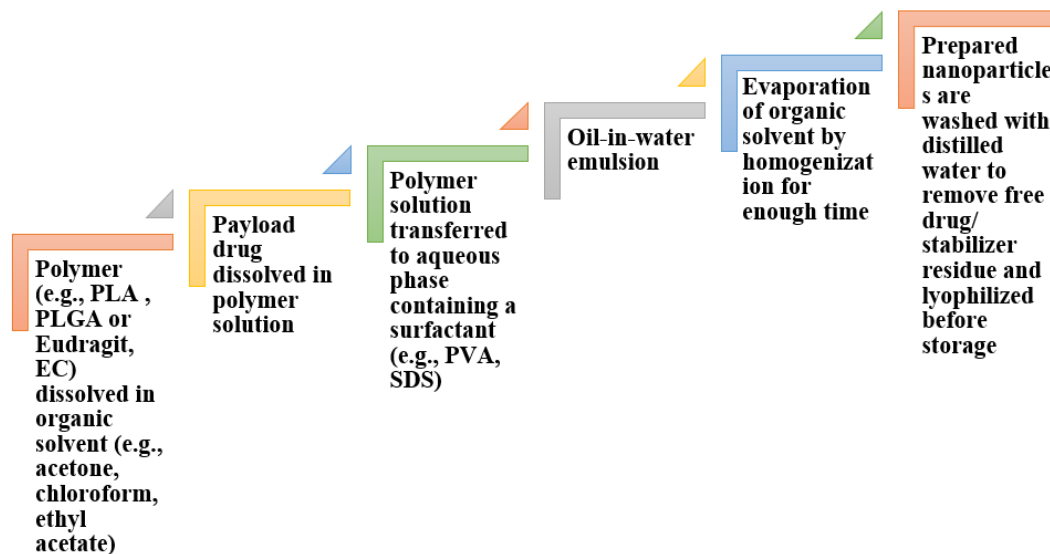
Figure 1. 2: Emulsion-Solvent Evaporation Method

1.3.1.1 Double Emulsion-Evaporation Method

The emulsion-solvent evaporation method suffers from poor entrapment efficiency of hydrophilic drugs. Introduction of additional water phase in the above technique enables incorporation of hydrophilic drugs (Figure 1. 3) (Lamprecht et al., 2000; Ritu & Meenakshi, 2013). These double emulsions are also called "emulsions of emulsions," where dispersed phase droplets contain smaller droplets of another dispersed phase (Iqbal et al., 2015).
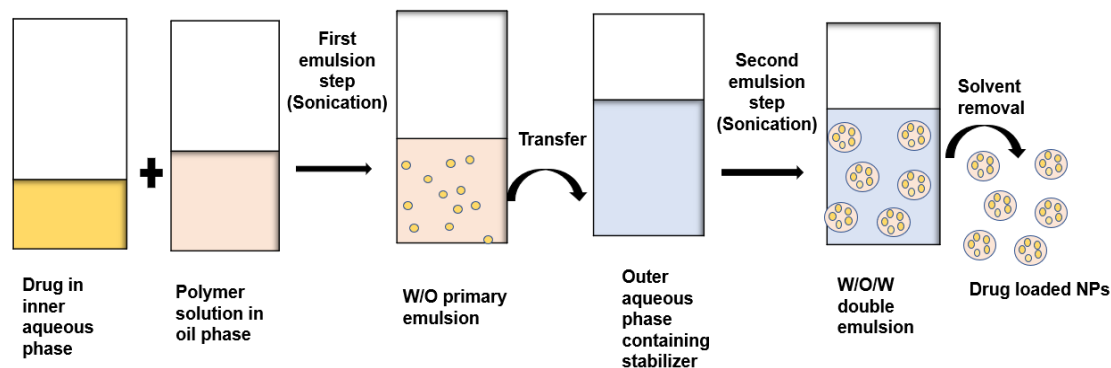
Figure 1. 3: Double Emulsion- Evaporation Method

1.3.1.2 Emulsions-Solvent Diffusion Method

This method is a modification of the solvent-evaporation method as shown in Figure 1. 4 (Zhang et al., 2009). It offers several advantages, such as high encapsulation efficiency, narrow size distribution, no need for homogenization, high batch-to-batch reproducibility, and easy scaleup. However, it becomes difficult to eliminate large volumes of water, and this method is not suitable for water-soluble drugs due to their leakage into the external aqueous phase (Quintanar-Guerrero et al., 2012).
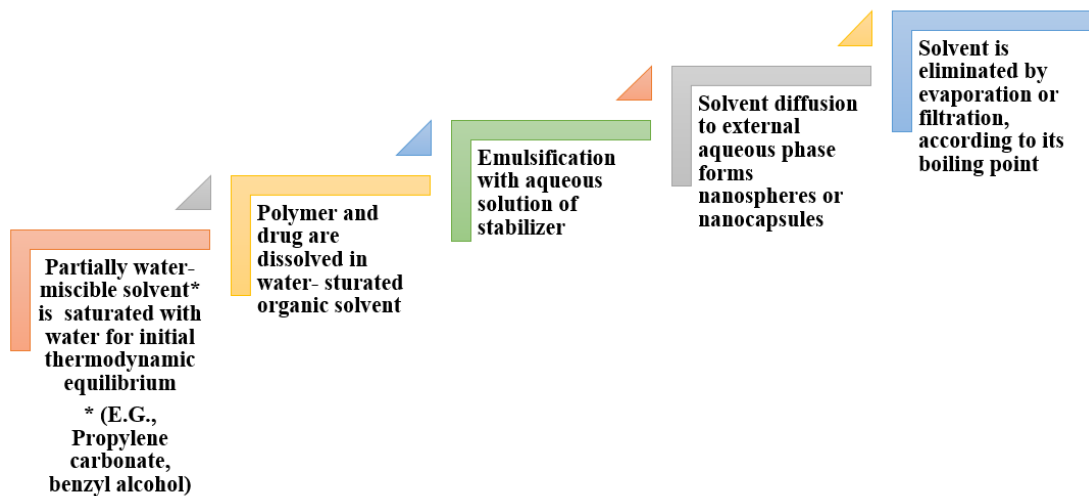
Figure 1. 4: Emulsions-Solvent Diffusion Method

1.3.1.3 Spontaneous Emulsification Solvent Diffusion Method

This method is also a modification of the solvent-evaporation method using a mixture of two organic solvents (Figure 1. 5) (Chen et al., 2014). This method can produce small particles, but there are some disadvantages, such as the presence of the considerable amount of toxic residual organic solvent and particles tend to aggregate during the solvent-evaporation process. In a modified spontaneous emulsification solvent diffusion method, use two water-miscible organic solvents (e.g., ethanol/acetone or methanol/acetone) instead of a mixture of water-miscible and less water-miscible organic solvents (Murakami et al., 1999) can avoid these problems.

| Polymer is dissolved in a mixture of water-miscible organic solvent (e.g., acetone) and less water-miscible organic solvent (e.g., dichloromethane) | | Polymeric solution is slowly poured into aqueous phase containing emulsifier and agitated by stirrer | | Interfacial turbulence is created and emulsion droplets are formed in aqueous phase | | Acetone quickly diffuses out from each emulsion droplet reducing it to nanometer size | | Subsequent evaporation of water-immiscible organic solvent solidifies droplets to form polymeric nanoparticles |

Figure 1. 5: Spontaneous Emulsification Solvent Diffusion Method

1.3.2 Solvent Displacement / Nanoprecipitation method

The solvent displacement / nanoprecipitation method is well suited for most poorly soluble drugs. The underlying principle involves interfacial deposition of the polymer after displacement of organic solvent from an oil phase to an aqueous phase (Figure 1. 6) (Zielinska et al., 2020). The polymer concentration in the organic phase, rates of organic phase into the aqueous phase, type, and concentration of surfactant affect the particles size and encapsulation efficiency (Alshamsan, 2014; Gaonkar et al., 2017; Saadati & Dadashzadeh, 2014; Sahin et al., 2017).
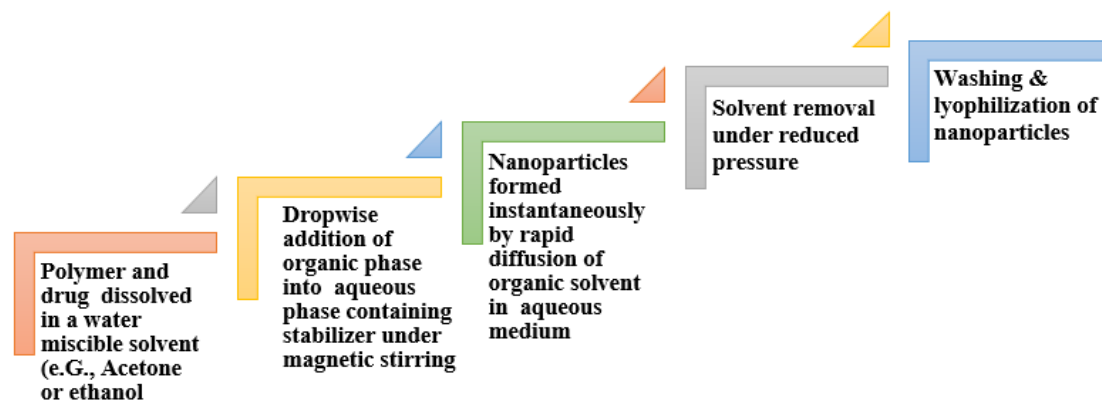
Figure 1. 6: Solvent Displacement / Nanoprecipitation method

1.3.3 Salting Out Method

This method is based on separating a water-miscible organic solvent (salting out) from an aqueous solution. Initially, a high concentration of salts hinders the miscibility of the organic phase into an aqueous gel and leads to o/w emulsion. Subsequently, the reverse salting-out effect results in hardening of NPs. The addition of sufficient aqueous phase to o/w emulsion lowers the ionic strength of electrolyte and causes migration of hydrophilic organic solvent from the oil phase to the aqueous phase (Figure 1.7) (Lim & Hamid, 2018). Salting out does not require an increase in temperature and, therefore may be helpful for heat-sensitive substances (Wang et al., 2016). Several manufacturing parameters can be varied, including stirring rate, internal/external phase ratio, the concentration of polymers in the organic phase, type of electrolyte concentration, and type of stabilizer in the aqueous phase. This technique has advantages like high encapsulation efficiency, high yield, small

particle size, and easy scale-up. Main disadvantages include unsuitability to lipophilic

drugs and extensive washing steps (Allémann et al., 1992; Galindo-Rodriguez et al., 2004;

Galindo-Rodríguez et al., 2005; Mendoza-Muñoz et al., 2012).

Polymer and drug dissolved in a water-miscible organic solvent (e.G., Ethanol, acetone,tetra hydrofuran (THF))

Aqueous phase consists of a colloidal stabilizer* and saturated solution of salting out agent** to form a viscous gel

Oil phase emulsified in aqueous phase gel under strong shearing force by overhead mechanical stirrer

Oil/water emulsion is diluted with sufficient volume of water to enhance solvent diffusion

Hardening of NPs

Solvent removed by evapoartion under reduced pressure

Ultra-centrifugation and repeated washing to eliminate both salting-out agent and stabilizer

Figure 1. 7: Salting Out Method

 *Polyvinylpyrrolidone (PVP) or hydroxyethyl cellulose

**electrolytes; magnesium chloride and calcium chloride, or non-electrolytes; sucrose. Electrolytes should not be soluble in an organic solvent.

1.3.4 Nonaqueous Phase Separation Method

This method is suitable for both hydrophilic and lipophilic drugs; hydrophilic drugs

are dissolved in the aqueous phase, and lipophilic drugs are dissolved in the polymer

solution. The basic principle behind this method is use of a second organic solvent such as

silicone oil (miscible with the first organic solvent but nonsolvent for the drug) (Figure 1.

8). It decreases polymer solubility, and phase separation of polymer results in adsorption of polymer coacervate onto drug molecules (Kammari et al., 2017).
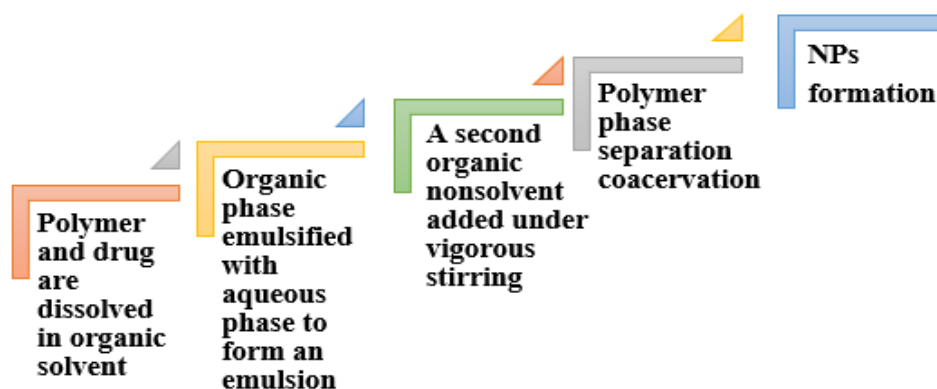
Figure 1. 8: Nonaqueous Phase Separation Method

1.3.5 Supercritical Fluid Technologies

Any substance above its critical temperature and critical pressure is called a supercritical fluid (SCF) (Soh & Lee, 2019). These fluids have very low viscosity, high diffusivity, and high compressibility (Akbari et al., 2020). They can diffuse through solids like a gas and dissolve materials like a liquid (Figure 1. 9). Carbon dioxide and water are the two most common SCFs. Supercritical fluid (SCF) technologies like 'rapid expansion of supercritical solutions' (RESS), 'gas-antisolvent' (GAS) (Esfandiari & Ghoreishi, 2013), 'supercritical fluid-antisolvent' (SAS) (Campardelli et al., 2015) and its various modifications are being developed to design drug delivery systems including NPs due to

SCF's inert, economical, non-toxic, and environmentally friendly properties (Chakravarty et al., 2019; Meziani et al., 2009).

A pressurized SCF solvent containing shell material and drug is released through a small nozzle

Rapid expansion & abrupt pressure drop causes desolvation of shell material

formation of a coating layer around drug
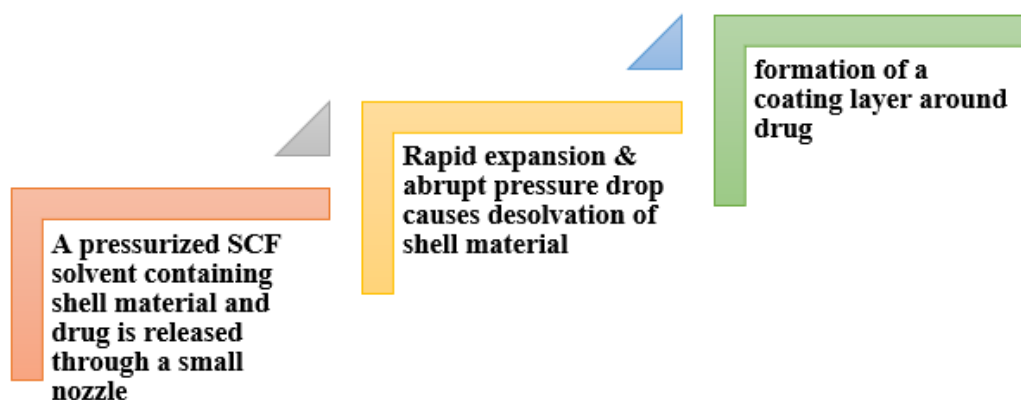
Figure 1. 9: Rapid Expansion of Supercritical Solutions (RESS) Method

*A prerequisite for this technology is that the drug should effectively dissolve in the SCF.

A modification of the classical RESS method is 'rapid expansion of a supercritical solution into a liquid solvent' (RESOLV). It involves a rapid expansion of supercritical solution into a liquid instead of an air or gas phase (Sun et al., 2001). An SCF can also be used as an antisolvent and may lead to precipitation of dissolved substrate from a liquid solvent (Chakravarty et al., 2019; Meziani et al., 2009).

1.3.6 Spray Drying

Spray drying is a widely known technology that can transform liquids (solutions, suspension, emulsions, pastes, slurries, or melts) into solid powders at the nano range (Figure 1. 10). The size distribution depends on formulation parameters such as concentration and nature of wall material (e.g., gums, proteins, modified starch, polyvinyl alcohol, Pluronic F127, PEG 1000, Tween 80) and process parameters such as drying gas flow rate, relative spray rate, inlet, and outlet temperature and location of powder collection (Abdel-Mageed et al., 2019; Draheim et al., 2015; Jafari et al., 2008; Li et al., 2010).

Polymer and drug are dissolved or emulsified in an organic solvent

Spraying through a nozzle

Droplets are dried simultaneously to produce NPs
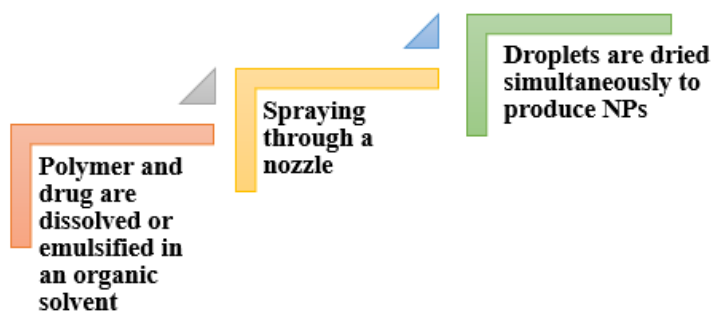
Figure 1. 10: Spray Drying

1.3.6.1 Spray Freeze Drying (SFD)

In spray freeze drying, spray drying technology is combined with lyophilization or freeze-drying. This modified method consists of three steps: the atomization of feed solution into liquid nitrogen to form nano-droplets, freezing, and the lyophilization of frozen droplets after the evaporation of liquid nitrogen (Ali & Lamprecht, 2014; Wang et al., 2012).

1.3.7 Emulsion Polymerization Method

In this method, monomers (e.g., acrylate polymers) emulsion droplets are polymerized in the presence of a drug to produce NPs. During polymerization, low viscosity monomer droplets gradually convert into a sticky polymer-monomer mixture, and then, further, increase in internal viscosity results in solid particles (Figure 1. 11) (Lovell & Schork, 2020). Primary loci in the emulsion polymerization process are continuous aqueous phase, monomer droplets, monomer-swollen micelles (if surfactant concentration is above CMC), and polymer particles (Lovell & Schork, 2020). Parameters that affect polymerization include monomer concentration, surfactant concentration and type, initiator amount, feeding mode, and reaction temperature (Zhang et al., 2015). Microemulsion polymerization, precipitation polymerization, and suspension polymerization are some specific forms of this process (Kotti & Kiparissides, 2010). Microemulsions, optically transparent and thermodynamically stable systems, require much more surfactant than classic emulsions to stabilize a large internal interfacial area. These microemulsions may be polymerized using chemical, photochemical, and high-energy gamma radiation

techniques. Polymerization of O/W microemulsions is termed "microemulsion polymerization", whereas polymerization of W/O microemulsions is termed "inverse microemulsion polymerization". Inverse microemulsion polymerization is used in water-soluble polymers (Kade & Tirrell, 2014; Pavel, 2004; Zhang & Yang, 2015).

Emulsification of monomer* into an aqueous solution of surfactant by applying shear

Monomer droplets are formed and stabilized by adsorption of surfactant at monomer-water interface

Above critical micelle concentration (CMC) surfactant micelles** are formed

Monomer-swollen micelles formed by absorption of monomer molecules into hydrophobic interior

Free-radical initiators enter into monomer-swollen micelles to begin polymerization

Polymer particles stabilized by adsorbed surfactant molecules

Figure 1. 11: Emulsion Polymerization Method

* Monomer is usually relatively insoluble in water, and drug is either dissolved or dispersed in the monomer prior to emulsification, ** spherical aggregates of typically 50−100 surfactant molecules

1.4 Characterization of Polymeric NDDS

1.4.1 Particle size

Fine particles and molecules always remain in random thermal motion, known as Brownian motion. They diffuse at a speed corresponding to their size; smaller particles diffuse faster than the larger ones. Dynamic Light Scattering (DLS), also referred as photon correlation spectroscopy (PCS) or quasi-elastic light scattering (QELS), is a technique that measures the diffusion of particles moving under Brownian motion.

When the NPs are illuminated by a narrow beam of laser, the intensity of light scattered at a specific angle fluctuates with time and is detected using a sensitive avalanche photodiode detector (APD). A digital autocorrelator generates a correlation function (based on the Stokes-Einstein equation) to convert the intensity changes in terms of particle size and size distribution (Carvalho et al., 2018; Holzer et al., 2009).

As Brownian movement depends on temperature, precise temperature control is essential for accurate size measurements. Sample concentrations should be chosen such that the results are independent of the concentrations taken. With very low sample concentrations, not enough light is scattered for measurement. On the other hand, with high sample concentrations, the light scattered by one particle is scattered by another one (known as multiple scattering) and sample cannot freely diffuse due to particle interactions. Maximum and minimum sample concentrations depend on the size of particles. Recommended minimum sample concentrations for 100 nm to 1 µm size particles is 0.01g/l

$(10^{-3}$ % mass), and maximum sample concentration is 1% mass (assuming density of $1g/cm^3$). DLS requires a larger number of particles thus providing much better statistics than SEM. Low instrument cost and short measurement time are additional advantages of this technique (Bootz et al., 2004; MalvernZetasizer & Performance; ZetasizerNano & Manual, 2003)

1.4.2 Zeta Potential

The charge acquired by a particle or molecule in a specific dispersion medium is referred as zeta potential. Particles with high charge magnitudes are more stable as due to similar charges as they repel each other and resist aggregation. Thus, particle stability can be modified by altering pH, type of ions, and ionic concentration using certain additives (e.g., surfactants and polyelectrolytes). When charged particles are dispersed in a liquid an electric double layer is developed around them instantaneously. The inner layer composed of oppositely charged ions is tightly coupled to the core of the particle and called 'stern layer'. The second outermost layer composed of both opposite and same charge ions is loosely bound to the particle and called as 'diffuse layer'. Within the diffuse layer, at the particle-liquid interface, there is a hypothetical plane or boundary called 'slipping plane' or 'shear plane'. Any ions within this slipping plane will move with the moving particle while in an electric field. The zeta-potential is the potential difference between the electric double layer around moving particles and the layer of dispersant (aqueous or organic liquid) at the slipping plane (Bhattacharjee, 2016).
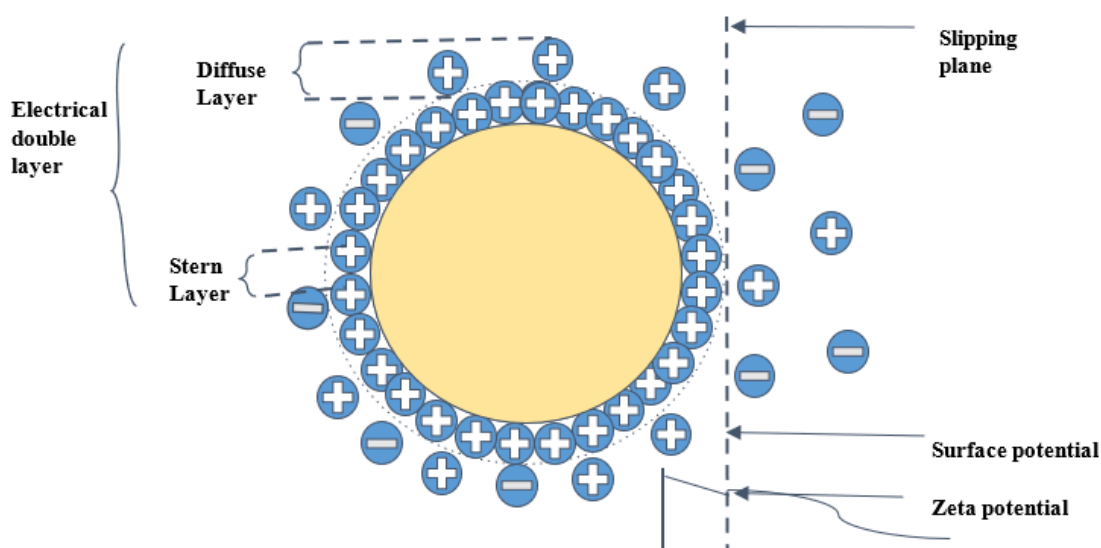
Figure 1. 12: Electrical Double Layer with Zeta Potential

Zeta potential is measured using Laser Doppler Electrophoresis, a combination of two techniques: Electrophoresis and Laser Doppler Velocimetry. An electric field is applied across the electrode pair at each end of the cell filled with nanoparticle dispersion. Charged particles start moving towards oppositely charged electrodes. Particles' velocity is measured per unit field strength and expressed as electrophoretic mobility. Dynamic Light Scattering (DLS) is the most common technique for measuring the electrophoretic mobility of NPs. Laser Doppler electrophoresis measures small frequency shifts in the

scattered light due to the movement of particles in an applied electric field. The frequency shift Δf is expressed by the following equation 1:

$$\Delta f = \frac{2v \sin(\theta/2)}{\lambda} \qquad \text{Equation (1)}$$

where v is velocity of moving particle, θ is light scattering angle and λ is laser wavelength. The measured electrophoretic mobility (UE) is converted to zeta potential (ζ) through Henry's equation.

$$UE = \frac{2\varepsilon\zeta F(ka)}{3\eta} \qquad \text{Equation (2)}$$

where ε and η are dielectric constant and viscosity of the dispersant respectively while F(ka) is Henry function (Carvalho et al., 2018; Kaszuba et al., 2010)

1.4.3 Thermal Analysis (DSC & TGA)

Differential scanning calorimetry (DSC) and thermogravimetry (TG or TGA) are two most common thermal analysis techniques.

1.4.3.1 Differential Scanning Calorimetry (DSC)

Differential scanning calorimetry (DSC) is a useful technique for the determination of thermal events, thermal degradation, oxidative stability, and water loss of materials. It can also be used to determine the glass transition of polymers, an important thermal event indicating the miscibility of polymer blends. Glass transition temperature (Tg) is a temperature at which amorphous materials shows transition from a brittle state to a viscous

state (Tomoda et al., 2020). DSC is widely used to demonstrate that the drug encapsulated in polymeric NPs is present in molecular dispersion (dissolved state) form, in contrast to a crystalline form of pure drug (Panyam et al., 2004; Sindhu et al., 2015; Yallapu et al., 2010).

DSC instruments measure temperature and heat flow corresponding to different material transitions as a function of time and temperature. They can be of two types based on the mechanism of operation- heat-flux DSC and power-compensated DSC. In heat-flux DSC, an empty reference pan and a sample-loaded pan both are kept onto a thermoelectric disk. This thermoelectric disk is surrounded by a furnace heated at a linear heating rate. Due to the heat capacity (Cp) of the sample, a temperature difference arises between the sample and the reference pan. Area thermocouples measure this temperature difference and modified Ohm's law (thermal equivalent) is used to know the heat flow between sample and reference pans. Where q is heat flow between sample pan and reference pan, ΔT is temperature difference, and R is resistance of thermoelectric disk.

$$q = \frac{\Delta T}{R} \qquad \text{Equation (5)}$$

In a power-compensated DSC, sample and reference pans are placed in separate furnaces and separate heaters are used to heat both. The difference in thermal power required to maintain sample and reference at the same temperature is plotted against temperature or time (Gill et al., 2010).

1.4.3.2 Thermogravimetry TGA

Thermal behavior of NPs is characterized by thermogravimetry (TGA) to determine their thermal and oxidative stability, water content, and chemical composition. Sample mass is observed against time or temperature to monitor the physical and chemical changes in the sample under a controlled environment, either in an isothermal furnace or by temperature change (decrease or increase) at a constant rate. TGA is a destructive technique and not suitable for volatile samples (Shi et al., 2018; Sindhu et al., 2015; Tansık et al., 2013; Tomoda et al., 2020; Tukulula et al., 2015).

1.4.4 Drug Loading (DL) and Entrapment Efficiency (EE)

In the direct method for entrapment efficiency determination, the drug present within the NPs is calculated after dissolving them in acetonitrile and analyzing them using UPLC. In the indirect method, the amount of free drug is analyzed in the supernatant recovered during the washing step using the following formula (Seju et al., 2011; Sun et al., 2015). Drug load can be calculated considering the weight of prepared NPs.

$$\% \ EE \ (Indirect) = \frac{Amount \ of \ drug \ encapsulated \ X100}{Amount \ of \ drug \ initially \ taken \ to \ prepare \ NPs} \qquad \text{Equation (6)}$$

$$\% \, DL = \frac{Amount \; of \; drug \; encapsulated \; X100}{Weight \; of \; prepared \; NPs}$$

Equation (7)

1.4.5 *In Vitro* Dissolution for NDDS

In vitro dissolution becomes an indispensable quality control tool to predict the *in vivo* physiologic response of NDDS. Knowledge of the BCS class of a drug alone is not adequate to predict the complex bi- or tri-phasic *in vitro* release profiles. As formulation parameters (critical material attributes, CMAs) and process parameters (critical process parameters, CPPs), in addition to drug properties (solubility and permeability) complicate the drug release from NDDS (Kamaly et al., 2016). CMAs and CPPs are formulation and process parameters respectively that can ensure the critical quality attributes (CQAs) (e.g., particle size, size distribution, zeta potential, and % encapsulation efficiency) of NDDS (Chiesa et al., 2018; Krull et al., 2017; Schubert & Müller-Goymann, 2003; Stevens et al., 2015). A well established *in vitro* release method can help recognize CMAs and CPPs during the early stage of the formulation development (Bastogne, 2017). Depending on the preparation technique CMAs can include surfactant concentrations, drug-polymer ratio, drug-lipid ratio, organic to aqueous phase ratio and CPPs can include processing temperature, flow rate, sonication time, stirring rate, flow, injection rate.

Two dissolution pairs can be compared using a quantitative approach known as 'dissolution efficiency' (DE) (Khan, 2011) or two qualitative approaches known as

'similarity factor' (f2) and 'difference factor' (f1). An f2-value between 50-100 and an f1-value between 0-15 make the two dissolution profiles similar. Similarity factor is a very popular comparison parameter among researchers as even a small difference in profiles results into a big drop in f2-value, being it a log function parameter(Anderson et al., 1998; FDA & SUPAC, 1997; Kassaye & Genete, 2013; Shah et al., 1998; Zhang et al., 2010; Zuo et al., 2014). Such type of studies help to compare the generic formulations with innovator drug product and assist in development of generic NDDS formulations(Tang et al., 2019; Yuan et al., 2017).
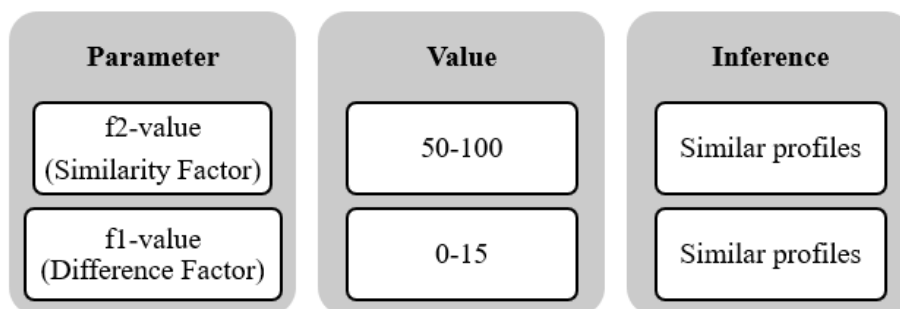
Figure 1. 13: Model independent approaches (F1&F2) for dissolution profile comparison

$$f_2 = 50 \cdot \log \left\{ \left[1 + \frac{1}{n} \sum_{t=1}^{n} (R_t - T_t)^2 \right]^{-0.5} \times 100 \right\}$$

Equation (8)

$$f_1 = \left\{ \left[\sum_{t=1}^{n} |R_t - T_t| \right] / \left[\sum_{t=1}^{n} R_t \right] \right\} \times 100$$

Equation (9)

$$DE = \frac{\int_{t_1}^{t_2} y \cdot dt}{y_{100} \times (t_2 - t_1)} \times 100$$

Equation (10)

where n is total number of dissolution time points, R_t sand T_t are mean % drug dissolved at time t for reference and test formulations respectively, y is % drug dissolved, y_{100} is maximum dissolution. Area under the curve ($\int_{t1}^{t2} y.\,dt$) is evaluated using trapezoid (model independent) or model dependent methods (Anderson et al., 1998).

1.4.6 Factors affecting *In Vitro* Dissolution of NDDS

There are several factors related to NDDS that affect the *in vivo* performance of products. These factors include the Biopharmaceutics Classification System (BCS) of drug, size and shape, formulation parameters, environmental conditions, biocompatibility and residual solvents.

Biopharmaceutics Classification System (BCS) of drug

The BCS is based on drugs' solubility and intestinal permeability. It can reflect the oral bioavailability and *in vivo* performances of NDDS. Most feasible drug delivery technologies can be chosen based on BCS class of a drug (Figure 13) (FDA & M9, 2018). The revised BCS classification system—known as the developability classification system (DCS)—provides the significance of particle size in the determination of dissolution-rate limited absorption(Butler & Dressman, 2010). DCS class IIa drugs have 'dissolution rate-limited' absorption and it is possible to achieve their complete oral absorption by size reduction. DCS class IIb drugs have 'solubility-limited' absorption, their bioavailability depends on gastric pH. They would remain incompletely absorbed unless formulated in solubilized dosage forms.
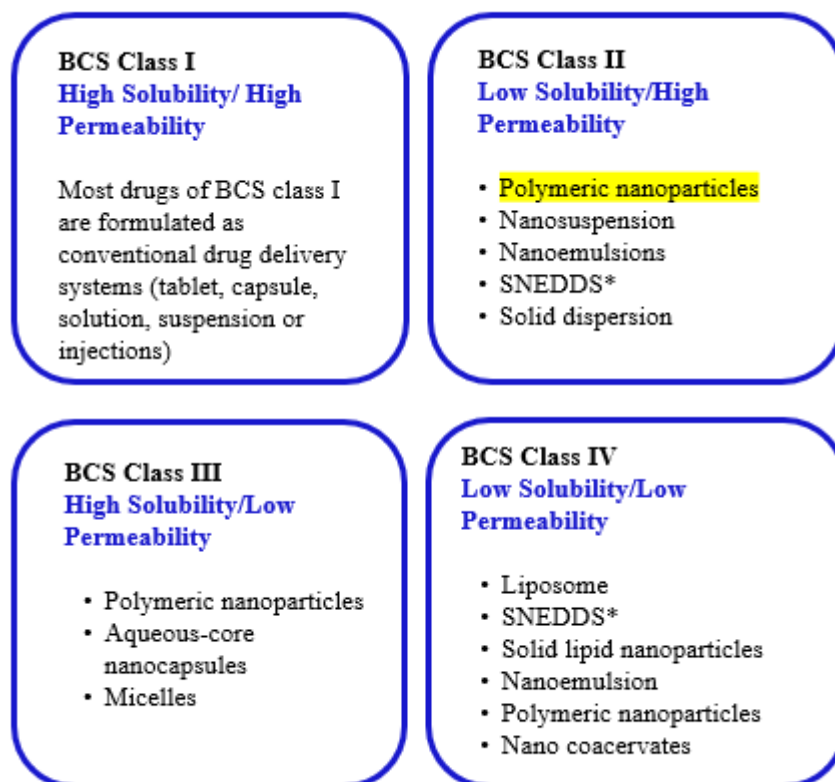
Figure 1. 14: Nano drug delivery systems (NDDS) for various BCS classes.

Size and shape of NPs

Size and shape can influence cytotoxicity and *in vivo* drug release from NPs. Needle-shaped NPs may induce greater cytotoxicity than the spherical NPs (Zhang et al., 2017) and small size particles adsorb more biomolecules (protein-corona) (Xiong et al., 2013). Such type of toxicity and irritancy may influence the *in vivo* drug release because of cell edema and the presence of inflammatory cells (e.g., macrophages and neutrophils) (Zolnik & Burgess, 2008).

Formulation parameters

Various formulation parameters (e.g., drug/ polymer ratio, stabilizer concentration, choice of solvent, organic to aqueous solvent ratio, lipid ratio), as well as process parameters (e.g., preparation technique, rate of stirring and solvent removal, temperature), may be modified to get desired release profile from NDDS (Sedighi et al., 2019; Sharma et al., 2014).

In Vivo Environment and Protein-Corona

Spatiotemporal (controlled by site and time) interactions of environment and biological factors form a spontaneous layer of biomolecules in the vicinity of NPs called "protein-corona." Various NPs properties e.g., shape, size, topology, surface charge and hydrophobicity directly influence the nature of its protein-corona. NPs attached to its protein-corona act as a biological unit that will interact with various barriers (physical, chemical, or immunological) inside the body influencing its biodistribution (Behzadi et al., 2014; Jain et al., 2017). NP surface modifications can reduce the nonspecific binding and aggregations (Bagwe et al., 2006). Polyethylene glycol (PEG) modifications is a highly tested approach to increase NP circulation time and avoid immune recognition (Fam et al., 2020; Suk et al., 2016).

To develop a biorelevant *in vitro* drug release method for NDDS, it becomes very crucial to study the effect of biorelevant concentrations of plasma proteins and other blood components such as bile salts, cholesterol, and phospholipids (Lu et al., 2019; Wallenwein

et al., 2019; Yeo et al., 2019; Zhang et al., 2019). Depending on the environment and specific use of NPs special test setup may be required e.g., two-stage drug release to simulate the drug release in circulation on the way to the target site (Xu et al., 2012), donor-acceptors vesicle pair can be used to simulate drug release to phospholipid cell membrane (Shabbits et al., 2002).

For realistic dissolution testing, sink conditions are usually recommended to achieve fast and complete dissolution. To attain the sink condition, the drug's saturation solubility, in the selected dissolution medium, should be more than thrice the drug concentration. (Phillips et al., 2012). Cosolvents (e.g., PEG 400) (Bala et al., 2006; Phillips et al., 2012), enzyme (e.g., pepsin) (Anand et al., 2011) or surfactants, synthetic (e.g., Tween 80, SLS, CTAB) or biorelevant (bile salts, phospholipids) can be added for poorly water-soluble drugs to achieve clinically relevant solubility and reach sink conditions (Anand et al., 2011; Huang et al., 2018; USP43NF38, 2020; Weng et al., 2020). Hence, the solubility/stability of drugs should be tested in the target media (under relevant hydrodynamic conditions) before dissolution testing of the actual dosage form to identify such issues at the earliest. However, in some cases, non-sink conditions are maintained to obtain slow dissolution rates and discriminatory dissolution profiles (Liu et al., 2013).

Biocompatibility

Some excipients can be cytotoxic when used in high concentrations. *In vivo* enzyme markers such as lactate dehydrogenase (LDH) (Madani et al., 2020) or

immunohistochemical techniques such as TdT dUTP Nick End Labeling assay or TUNEL (Mo & Lim, 2005) can be used to test the biocompatibility of such excipients.

Residual Solvents

NDDS preparation usually involves the use of different organic solvents. Residual solvents can affect drug particle size, wettability, and dissolution, and can have toxic effects. Based on individual health and environmental hazards Q3C document of ICH (International Council for Harmonization of Technical Requirements for Pharmaceuticals for Human Use) classifies existing solvents into three classes and recommends their acceptable limits. This guideline is applicable to all routes of administration and all dosage forms (FDA & ICHQ3C, 2017; FDA & Q3C, 2018; ICH, 2019) (FDA & Liposome, 2018). Specific guidelines have also been set forth to identify residual impurities in NDDS(FDA & Safety, 2014).

Dikpati et al. (Dikpati et al., 2020) have provided useful recommendations to minimize residual solvents in NDDS. These include the use of class III solvents (e.g., ethyl acetate, acetone, dimethyl sulfoxide), solvent-limiting preparation techniques (e.g., supercritical fluid technology, microfluidics, high pressure homogenization) (Anton et al., 2012; Paliwal et al., 2014), use of disposable measuring devices and multiple purification steps (e.g., size exclusion chromatography, electrophoresis, dialysis, ultrafiltration) (Paliwal et al., 2014; Robertson et al., 2016).

1.4.6.1 Accelerated *in vitro* release testing

Sustained release NDDS may release drugs for several days to months. Accelerated *in vitro* drug release tests can predict 'real-time' release and speed up the analyses (Shen et al., 2016). However, researchers need to be cautious as applied stress conditions (extreme pH values, elevated temperature) can also alter the drug release mechanism (Shameem et al., 1999; Zackrisson et al., 1995; Zolnik et al., 2006).

1.4.7 *In Vitro* Drug Release Methods For NDDS

Drug release from NDDS can be established using either *in vivo* or *in vitro* (acellular or cellular) tests as shown in Figure 1.14. Dialysis membrane methods are extensively utilized *in vitro*-acellular tests, use of the continuous flow method (USP 4 apparatus) is a promising trend (Figure 1.15) (Gupta et al., 2021)
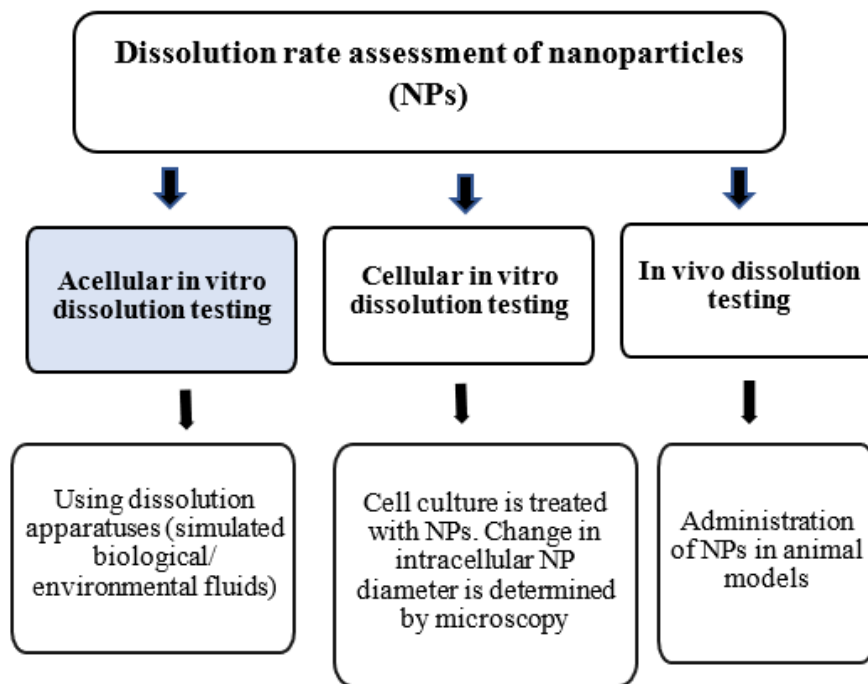
Figure 1. 15: Dissolution rate assessment of NPs
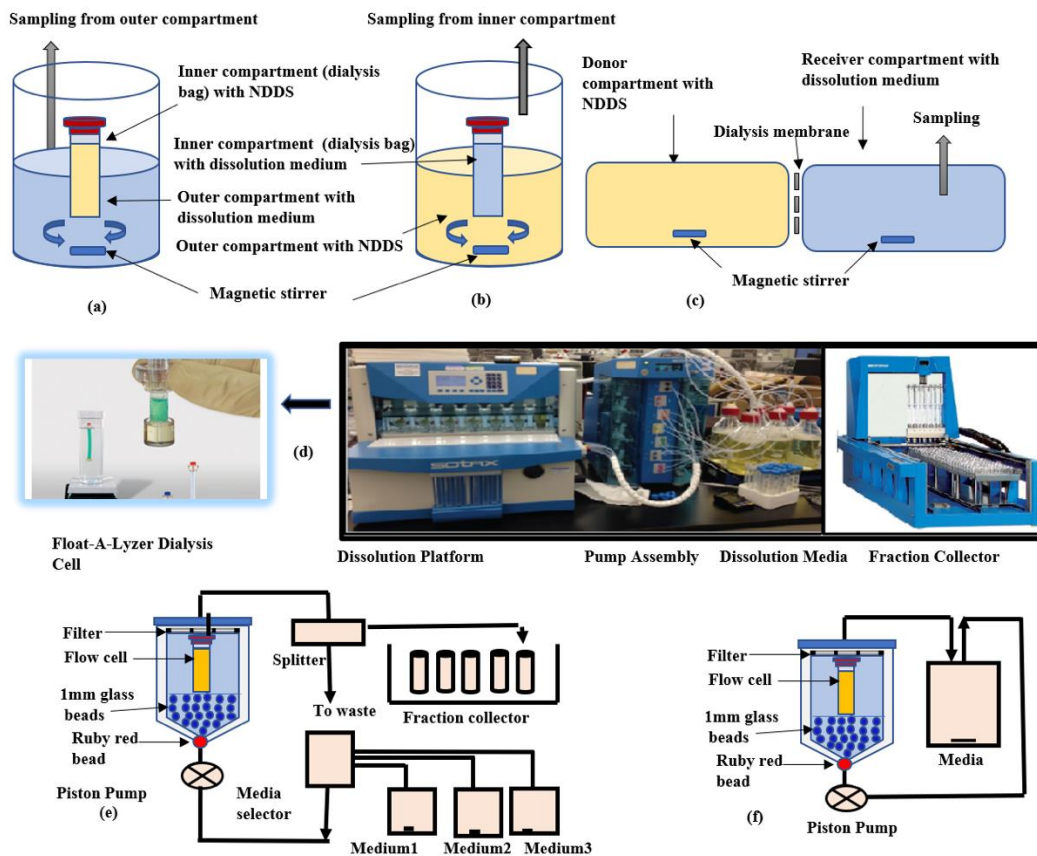
Figure 1. 16 :(a) Dialysis method: NPs are filled inside dialysis bag and samples are collected from outer medium reservoir. **(b) Reverse dialysis method**: opposite to above discussed set-up. **(c) Side by side dialysis method**: donor and receiver compartments are set apart using dialysis membrane. **(d) USP 4 (Flow Through Cell)**. (e) Open Loop System: continuous flow of fresh solvent helps maintain the infinite sink conditions. (f) Close Loop System: small media volume re-circulates to overcome the limit of quantitation issues of poorly soluble drugs.

1.4.7.1 Dialysis membrane methods

In dialysis membrane methods, NPs are placed inside the pretreated dialysis bag that is placed in an outer media compartment. Drug release samples can be collected from the outer compartment agitated with a magnetic stirrer (Figure 1.15a). In the reverse dialysis method, NPs are placed in the outer media compartment and samples are taken from media inside the dialysis bag. Such type of setup provides excellent sink conditions (Figure 1.15b) (Calvo et al., 1996; Xu et al., 2012). In the side-by-side dialysis method, the membrane separates equal volume donor and receiver compartments (Figure 1.15c) (Chidambaram & Burgess, 1999). Dialysis bag methods can also be combined with USP apparatus 1 and USP apparatus 2 (Bhagav et al., 2011).

Membrane molecular weight cutoff (MWCO), the ratio between donor and acceptor cell volumes, and stirring conditions, are governing parameters in dialysis methods. Pore size should be such that it prevents leakage of NPs but can allow easy drug passage (100 times the molecular size of drug) (Shen & Burgess, 2013; Xu et al., 2012). The limitations associated with these methods are potential membrane binding of a drug, leakage of NPs and media from improperly sealed dialysis bags, incomplete drug release in case of high equilibration times or non-sink conditions and inaccurate results if instead the dissolution membrane becomes rate-limiting of dialysis process (D'Souza, 2014; Heng et al., 2008).

1.4.7.2 Sample and separate methods

The NPs are added directly into the release medium held in a beaker or USP apparatus 1 or 2 (Gao et al., 2013; Sievens-Figueroa et al., 2012; Weng et al., 2020). In some cases, NPs may be filled into gelatin capsule shells (Saroj & Rajput, 2018). At specified time intervals, dispersed NPs are separated from media using different separation techniques like ultracentrifugation, ultrafiltration, or combination of both, and subsequent supernatant/filtrate is analyzed for drug release (Ham et al., 2009; Morales-Cruz et al., 2012). However, it is quite difficult to efficiently separate NPs from release media. Long and high-speed ultracentrifugation can destabilize NPs leading to accelerated drug release and filters may get clogged during filtration (Kim et al., 1997; Shen & Burgess, 2013).

1.4.7.3 Continuous flow method or USP 4 apparatus

In this method, NPs suspension is filled in specially designed ready-to-use dialysis cells e.g., Float-A-Lyzer® G2 cells (made of cellulose ester). The cell dimension and molecular weight cutoff can be selected as per the type of dosage forms (Figure 1.15d). In an open loop configuration, fresh solvent circulates continuously to maintain the infinite sink conditions. This setup is useful for easy IVIVC development for poorly soluble drugs (Figure 1.15e). In a closed loop configuration, a small volume of media recirculates through the dialysis cells to overcome the problem of the limit of quantification (Brown, 2005; Forrest et al., 2018; Tang et al., 2019). (Figure 1.15f)

1.5 <u>Cosolvent formulation for pharmacokinetic profile investigation</u>

Preliminary preclinical evaluation of a novel chemical entity (NCE) requires formulating an aqueous solution formulation. This would allow easy administration to preclinical species and ensure uniformity of content. However, majority of NCEs have poor aqueous solubility that necessitates the use of some formulation strategies to improve its aqueous solubility. Such strategies may include development of cosolvent-based systems, suspensions, emulsions, etc. Cosolvent-based approach is widely used simple approach to formulate poorly soluble drugs for the purpose of establishing preliminary pharmacokinetic profiles. It involves rational use of different solvents for drug solubilization via vortexing or sonication (with or without use of heat). Examples of various cosolvents used include different grades of polyethylene glycols (PEG), propylene glycols; glycerol; diethylene glycol monoethyl ether (Transcutol®), pyrrolidones and alcohol etc. (Shah et al., 2014).

1.6 Background of compound AC1LPSZG

Adenosquamous carcinoma is a rare subtype of non-small cell lung cancer (NSCLC). Development of targeted therapies for adenosquamous carcinoma has received rising attention in recent years. The mammalian target of rapamycin (mTOR) is one such promising target selectively dysregulated in NSCLC (Fumarola et al., 2014). mTOR regulates the cell growth, proliferation, metabolism and lies upstream/ downstream of many frequently mutated oncogenic pathways. Several mutations (gain or loss of function) may cause hyperactivation of mTOR pathway and result in various cancers. mTOR inhibitors, alone or in combination with Rapamycin (firstly described mTOR inhibitor) are being evaluated in ongoing clinical trials(Hua et al., 2019). mTOR, a protein kinase, along with other different proteins, forms two distinct protein complexes known as mTOR complex 1 and 2 (mTORC1 and mTORC2) that regulate different cellular processes (Cargnello et al., 2015; Mabuchi et al., 2015; Paoloni et al., 2010; Yoon & Choi, 2016) (Figure 1.17).
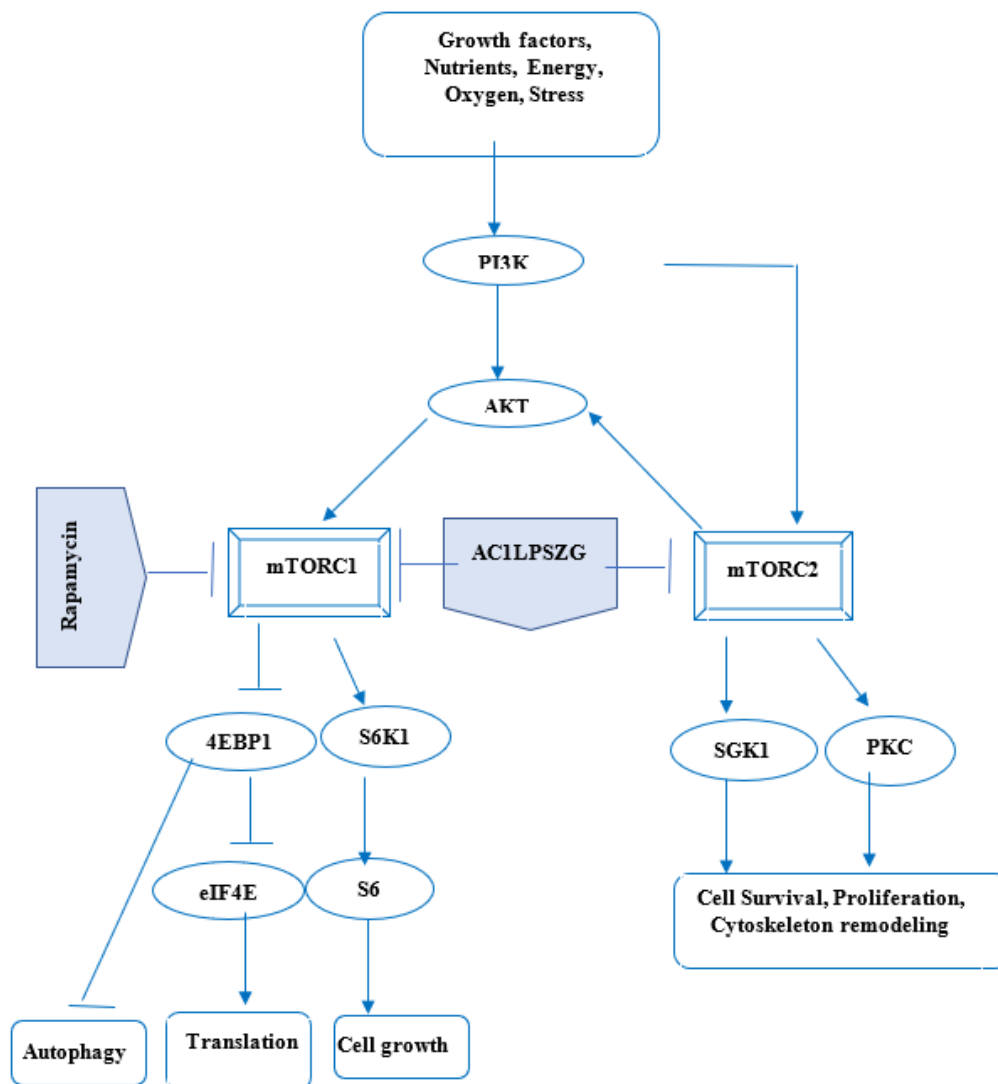
Figure 1. 17: mTOR signaling pathway

The recently identified synthetic compound AC1LPSZG is a new generation mTORC1/2 inhibitor. In preliminary *in vitro* studies, AC1LPSZG significantly reduced the

viability of HTB-lung tumor cells (2). This study has revealed the anti-NSCLC potential of AC1LPSZG and drives its further preclinical development. AC1LPSZG is (2E)-3-(4-bromophenyl)-2-(phenylsulfonyl)-N-(pyridine-3-ylmethyl) prop-2-enamide with molecular formula $C_{21}H_{17}BrN_2O_3S$ (Figure 1.17). Lipinski's rule of five suggests that AC1LPSZG is a drug-like compound. Its molecular weight is 456 Da (<500 Da), partition coefficient (log P) value is 3.47 (<5), one hydrogen bond donor (<5) and 5 hydrogen bond acceptors (<10). The software predicted its strongest pKa(acid) value is 11.0 ±0.5 and its strongest pKa(base) value is 4.7 ±0.1.
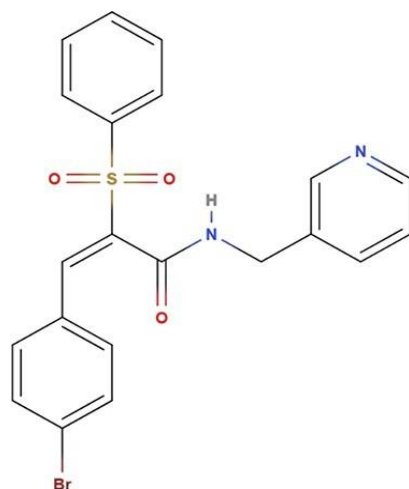
Figure 1. 18 : Chemical structure of Compound AC1LPSZG

1.7 Specific aims of this project

To further develop AC1LPSZG for future clinical application, we designed the preclinical studies with the following specific aims:

1.7.1 Specific Aim 1: To develop ultra-performance liquid chromatography (UPLC) and liquid chromatography-tandem mass spectrometry (LC-MS/MS) assays for the analysis of AC1LPSZG concentration *in vitro* and *in vivo.*

1.7.2 Specific Aim 2: To develop an optimized AC1LPSZG co-solvent formulation for *in vivo* study and obtain the pharmacokinetic profile after intravenous administration.

1.7.3 Specific Aim 3.1: To develop AC1LPSZG loaded PLGA nanoparticles using Design of Experiment (DoE).

1.7.4 Specific Aim 3.2: To study *in vitro* drug release profile of AC1LPSZG loaded PLGA nanoparticles using USP 4 apparatus.

CHAPTER 2 ITERATURE REVIEW

2.1 Cosolvent systems for Pharmacokinetic Studies

Pharmacokinetic profile of a novel lactone-stabilized camptothecin (CPT) analog, named CZ48, was compared in cosolvent system containing dimethyl sulfoxide: polyethylene glycol 400: ethanol (2:2:1 by volume) and in nanosuspensions using both PBS and human plasma (Dong et al., 2019).

A simulated stomach duodenum model was used to predict the effect of fluid volume and prandial gastric flow patterns on nifedipine pharmacokinetics using capsules filled with cosolvent mixture of polyethylene glycol (PEG) and glycerin (Honigford et al., 2019).

Compared with commercial tablets, the co-solvent formulation of riluzole (comprising of 15% v/v PEG 400, 20% v/v propylene glycol and 10% v/v glycerin) showed a faster rate of absorption and sustained pharmacokinetics with significantly longer elimination half-life (Sarkar et al., 2018).

2.2 <u>PLGA Nanoparticle Applications</u>

Poly (lactic-co-glycolic acid) (PLGA) is an FDA-approved biodegradable polymer and several PLGA based products have already been approved by FDA against a variety of diseases including PLGA microparticles (e.g., Lupron Depot® for prostate cancer and endometriosis, Somatuline® Depot for acromegaly, and Bydureon BCise® for type 2 diabetes) and PLGA implants (e.g., Zoladex® for Breast-Cancer, Ozurdex® for Diabetic macular edema and Eligard® for advanced prostate cancer) (Pardeshi et al., 2021).

The application of PLGA based NPs is a promising approach to treat a variety of diseases (Danhier et al., 2012) and is explored to deliver a variety of pharmaceuticals including haloperidol (Budhian et al., 2005), insulin (Zhang et al., 2012), Docetaxel (Patel et al., 2018), bone morphogenetic protein (BMP-2)(del Castillo-Santaella et al., 2019), curcumin (Duse et al., 2019), vitamin E (Varga et al., 2019), paclitaxel (Morelli et al., 2019), thiazolidinedione (Monge et al., 2020) and atorvastatin (Grune et al., 2021).

2.3 <u>Mechanisms of Drug Release from PLGA Based Systems</u>

Many PLGA-based delivery systems have been developed for a variety of drugs with delivery spans ranging from days to years. PLGA is a water-insoluble polymer (Kitchell & Wise, 1985) but multiple mechanisms lead to drug release from PLGA-based drug delivery systems. Different mechanisms may dominate at different time points and at

different locations within the same system. There are four true rate controlling release mechanisms (Fredenberg et al., 2011):

- Diffusion through water-filled pores

- Diffusion through the polymer

- Erosion (no drug transport)

- Osmotic pumping

2.3.1 Diffusion through water-filled pores

When polymer is in contact with water (*in vitro* or *in vivo*), it starts absorbing it to create small water-filled pores within the polymer matrix. The size and number of these pores increase with time constructing a porous network of connected water-filled pores to allowing drug release (Mochizuki et al., 2008). It is a dominant release mechanism for large hydrophilic drugs (e.g., proteins) because they cannot easily diffuse through hydrophobic polymer and the osmotic pressure is usually compensated by swelling polymer. This release mechanism mainly depends on the porous structure of polymer and the processes governing pore formation or pore closure (Zhang et al., 2018). Diffusion through water-filled pores is mostly used to describe the initial stage of drug release(burst release phase), prior to the beginning of the polymer erosion (Liu et al., 2019).

2.3.2 Diffusion through polymer

In contrast to diffusion through water-filled pores, the diffusion through a polymer depends on the physical state (instead of the porous structure) of the polymer. This is the dominant release mechanism for small hydrophobic molecules during polymer transitioning from a glass-like vitreous stage to a more plastic rubbery state. Low molecular weight polymers have higher diffusivity due to more flexible polymer chains (Karlsson et al., 2001; Wischke & Schwendeman, 2008). The glass transition temperature (T_g) of PLGA in delivery systems may be lower than that of the original polymer due to degradation during processing, sterilization and the plasticizing effects of additives, water or residual water (Blasi et al., 2005; In Pyo Park & Jonnalagadda, 2006; Loo et al., 2004; Ricci et al., 2005; Sun et al., 2013).

2.3.3 Erosion (no drug transport)

Erosion could be the dominant release mechanism for low molecular weight PLGA formulations (Corrigan & Li, 2009) (Körber, 2010). Erosion involves the 'mass loss' after hydrolytic degradation of the polymer. Relative rates of water diffusion into the polymer matrix and polymer erosion determine if the erosion is a surface or bulk phenomenon. When water diffusion into the polymer matrix is faster, bulk erosion takes place. On the other side, when polymer erosion is faster, surface erosion takes place. PLGA is well known to undergo hydrolytic degradation via bulk erosion (Jain et al., 2010) . Hydrolysis

of ester bonds generates shorter chain alcohols and intermediate acids (lactic acid and glycolic acid) throughout the polymer. These acid monomers diffuse into the surrounding release medium. Concurrently, bases from bulk medium (phosphate buffer pH 7.4) diffuse into the polymer matrix to neutralize the acids, but at a slower rate, resulting in a net drop of system pH. Since hydrolytic cleavage of ester bond is a proton-catalyzed reaction this low system pH further accelerates the polymer degradation termed as autocatalysis. Diffusional path lengths for acids and bases will depend on the size of the PLGA-based system and determine if autocatalytic will occur or not. Autocatalysis can accelerate the drug release and can also inversely affect the stability of some drugs (Klose et al., 2006; Siepmann et al., 2005).

Polymer erosion may lead to drug release without transport. Assuming homogenous drug distribution throughout the polymer, drug release profiles identical to polymer loss (erosion) were reported (Shah et al., 1992). When the drug is not molecularly dispersed within the polymer system, the drug (crystalline or amorphous aggregates) will first dissolve and then subsequently diffuse out of the polymer into the surrounding bulk medium (Klose et al., 2006). Maintenance of sink conditions for hydrophobic drugs is very critical so that concentration does not reach saturation and concentration gradient is maintained (Fredenberg et al., 2011).

2.3.4 Osmotic pumping

This is a less common release mechanism for PLGA-based delivery systems (Hu et al., 2018). Osmotic pumping is defined as the drug transport due to osmotic pressure created by water absorption into a non-swelling system. Such type of transport is based on the convection instead of a drug diffusion (Gu et al., 2016). And, the rate of water influx should be equal to the rate of water efflux after an initial equilibrium period (Fredenberg et al., 2011). It is possible for hydrophobic polymers with high molecular weights, high viscosity and high lactide to glycolide ratio (100:0 or 85:15) as swelling and erosion will be minimal. However, most delivery systems use low molecular weight PLGA, and any osmotic pressure is balanced out by volume increase due to significant polymer swelling (Gu et al., 2016; Murphy & Lampe, 2018). Osmotic transport depends on the length of channels while diffusive transport depended on both the length and the area of channels (Fredenberg et al., 2011; Sun et al., 2021).

2.4 Factors/ Processes affecting Drug Release from PLGA Based Systems

Researchers have been working for a long time to understand the impact of various factors that influence the drug release profile from PLGA-based delivery systems. Polymer composition, molecular weight, polymer dispersity, temperature, processing and sterilization conditions, drug solubility, drug loading and drug-drug/ polymer interaction are some important factors.

2.4.1 Polymer Composition (lactide to glycolide ratio)

The rate of *in vivo* degradation of PLGA depends on the molar ratio of lactic acid to glycolic acid. Release patterns from PLGA-based systems can be modified by simply altering this ratio (Kitchell & Wise, 1985). The degradation rate of polymers prepared with a greater percentage of hydrophobic lactic acid (e.g., PLGA 75:25) decreases due to decreased ability of water molecules to diffuse into copolymers leading to slower hydrolysis (Keles et al., 2015). In addition, lactic acid is optically active and optically pure enantiomer is preferred for drug delivery due to accelerated hydrolysis from polymers prepared with racemic mixture (Amann et al., 2010; Kitchell & Wise, 1985).

2.4.2 Molecular Weight and Dispersity

Both polymer molecular weight and polymer dispersity (molecular weight distribution) influence the rate of hydrolysis. PLGA with higher molecular weight and lower polymer dispersity showed a small initial release and a longer sustained release phase (Kitchell & Wise, 1985).

2.4.3 Temperature

The kinetics of PLGA hydrolysis is temperature dependent. An increase in temperature increases the degradation of PLGA with any lactide to glycolide ratio (50/50, 75/25 or 100/0) (Keles et al., 2015).Agrawal et. al. (1997) demonstrated that activation energies for hydrolytic degradation of PLGA were distinctly different at temperatures

below and above glass transition temperature (T_g). It was recommended that results derived from tests performed at temperatures above T_g should not be used to predict PLGA degradation at temperatures below T_g (Agrawal et al., 1997).

2.4.4 Processing and sterilization

Processing and sterilization can affect the chemistry and morphology of PLGA, altering the hydrolysis rate and consequently remodeling the release rate of entrapped drugs. Supercritical carbon dioxide processing (at ambient temperatures and moderate pressures) results in a porous morphology due to escaping gas bubbles from solidifying polymer. It also causes a drop in glass transition temperature (T_g) to influence the hydrolysis rates of polymer (Keles et al., 2015).

Gamma irradiation of PLGA 50:50 microparticle increased its degradation rate, as revealed by FTIR imaging. Gel permeation chromatography (GPC) showed a decrease in molecular weight of PLGA 50:50 and DSC analysis exhibited a decrease in glass transition temperature (T_g) with increased dose of gamma irradiation. All these findings indicated that gamma irradiation brings about severe changes in polymer morphology. It reduces the overall molecular weight of polymer matrix due to a chain scission degradation mechanism (Keles et al., 2015).

2.4.5 Drug Solubility

Hydrolytic degradation of PLGA involves two steps: diffusion of water into the polymer matrix (swelling) and its hydrolysis reaction. Effective diffusion rate (diffusion coefficient) of water into the polymer matrix and, the effective reaction rate for hydrolysis were studied for various drugs with differing water solubilities. The highest rates of diffusion (swelling) and degradation (hydrolysis) were obtained for a hydrophilic drug while lower values were obtained for a relatively hydrophobic drug with low solubility. Nevertheless, release rates of all drugs were not explained by their water solubility and a better understanding of their release pattern and relation with water is solicited (Siegel et al., 2006).

2.4.6 Drug Loading

Drug loading in PLGA matrix-based delivery systems depends on drug solubility. Kitchell and Wise (1985) demonstrated that system durations may vary from 30 days to 1600 days for the drugs with solubilities ranging from 4000 μg/ml to 0.02 μg/ml. They suggested that soluble macromolecules (e.g., proteins and peptides) will be released quite rapidly. PLGA systems with low drug content may provide long-term delivery of such molecules (Kitchell & Wise, 1985).

2.4.7 Drug–drug or drug-polymer interactions

Drug-drug interaction (physical or chemical) or high affinity of a drug for the polymer may result in an incomplete drug release (Wong et al., 2001).

2.5 *In Vitro* **Drug Release from PLGA based NPs**

- Dexamethasone-loaded PLGA NPs were prepared using solvent emulsification-evaporation method and *in vitro* drug release was tested using Franz vertical diffusion static cells in phosphate buffer (pH 7.4) PLGA NPs showed a sustained release profile with only 42% drug released in 600 min. In contrast, free dexamethasone showed a release rate close to 100% in just 120 min followed by a rapid decline in drug (Ribeiro et al., 2021).

- PLGA (50:50) (Resomer® RG 503H, MW34 kDa) NPs significantly improved the *in vitro* drug release of poorly water-soluble drug Zaleplon prepared via emulsification–solvent evaporation technique. Drug release profiles were established using 5-cm dialysis sac (spectra-por, cut-off 12–14 KDa) and PBS (pH 7.4) as release medium. Longer sonication time during the emulsification step of preparation resulted in NPs with a large number of pores and released drug more quickly. A significant decline in initial burst release (from 36% to 24%) was observed in increasing PLGA concentrations (from 2.5% to 10%) due to particles

with smaller pore size and more tortuous entanglement of polymer chains. Whereas NPs prepared with higher concentrations of stabilizer (1% and 1.5% w/v PVA) had smaller size and higher surface area, thus, showing significantly higher initial burst effect than formulations prepared with lower stabilizer concentrations (0.5% w/v PVA) (Haggag et al., 2021).

- Docetaxel NP formulations were developed using PLGA (50:50) polymer (with acid terminal group and low-molecular-weight 6,700 Da) by modified emulsification solvent evaporation technique. *In vitro* drug release was tested in PBS buffer with sample and separate method. Both, PLGA NPs and PLGA–PEG NPs displayed biphasic release profiles with an initial burst release for the first 24 h of the test. PLGA–PEG NPs demonstrated a higher and faster drug release profile compared to PLGA NPs with an overall 25% and 49% drug release after 5 days, respectively (Rafiei & Haddadi, 2017).

- PLGA (Resomer RG 50:50 H; Mw 40–75 kDa, inherent viscosity 0.45–0.6 dl/g) NPs and PLGA–PEG blend NPs of curcumin were prepared by single-emulsion solvent-evaporation technique. The *in vitro* drug release was evaluated in phosphate-buffered saline (PBS) (0.01 M, pH 7.4) using a sample and separate method. Both NPs sustained the drug release, PLGA NPs released the drug more slowly than PLGA–PEG blend NPs. PLGA–PEG NPs demonstrated a biphasic

release pattern with a burst release of 21% in initial 24 h followed by a sustained release of 56.9% for nine days. Drug release from PLGA NPs was more progressive with no biphasic profile. Only 5.8% of curcumin was released in the first 24 h and a total of 37% drug was released over nine days (Khalil et al., 2013).

- Donepezil NPs were formulated by solvent emulsification diffusion– evaporation method utilizing PLGA 50:50 (RH 503, Molecular weight 35–40 kDa). *In vitro* release study was done using a dialysis tube (MW cut off 2000 Da) in PBS (pH 7.4). Donepezil-loaded NPs showed a biphasic release pattern, an early burst effect observed within 30 min followed by sustained drug release over a period of 25 days. While donepezil solution (control) released 61.49% drug in only 240 min. Cumulative percentage drug release from PLGA NPs depended on drug-polymer ratio. It increased from 76.11% to 92.03 % by decreasing drug-polymer ratio from 1:10 to 1:1. Coating of PLGA NPs with 1% polysorbate 80 slightly lowered the drug release (87.42% for drug-polymer ratio 1:1) (Bhavna et al., 2014).

2.6 USP 4 as Discriminatory *In Vitro* Dissolution Method

The lack of robust and biorelevant *in vitro* drug release methods for NDDS prompts the researchers to select arbitrary release methods. USP 4 emerges as a promising solution due to various advantages including its discriminatory capabilities. Much efficient simulation of intraluminal hydrodynamics is possible due to options to change media composition, pH, temperature, and flow rate over the course of the entire test (Gite et al., 2016). Moreover, sampling and media changes are done without disturbing test hydrodynamics and no additional filtration step is required (D'Arcy et al., 2010; Eaton et al., 2012; Heng et al., 2008; Singh & Aboul-Enein, 2006; Yoshida et al., 2015). Provision of 1-mm glass beads and a red ruby bead in the conical part of the dissolution cell provides excellent flow symmetry and uniformity (Kakhi, 2009). Studies summarized in Table 2.1 support that USP 4 has discriminatory potential for *in vitro* drug release from NDDS. However, more research is needed to confirm its suitability in testing different drugs delivered through different NDDS (e.g., polymeric NPs, liposomes) and to justify its regulatory standing.

Table 2. 1: Discriminatory potential of USP 4 for *in vitro* drug release from NDDS

NDDS	*In Vitro* Release Methods	Study Findings	Reference
Cefuroxime Axetil NPs	• USP 4 (flow rate 16 ml/min; 0.2-µm disc filter) • USP 1 (100 rpm) • USP 2 (100 rpm) • Dialysis bag (12-14 kDa MWCO)	USP apparatus 4 was testified to be unequivocally the most robust dissolution method to differentiate dissolution rate ratios of Cefuroxime Axetil NPs and unprocessed drug.	(Heng, Cutler et al. 2008)
Dexamethasone Liposomes	• USP 4 (flow rate 16 ml/min; 50 kDa MWCO) • Dialysis sac (50 rpm; 50 kDa MWCO) • Reverse dialysis sac (50 rpm; 50 kDa MWCO)	USP apparatus 4 was able to discriminate between solution, suspension, and the extruded and non-extruded liposomes.	(Bhardwaj and Burgess 2010)
Griseofulvin NP-laden stripfilms	• USP 4 (flow rate 16 ml/min; 0.2-µm disc filter) • USP 1 (50, 100, and 150 rpm)	Researchers validated the particle-size discriminatory nature of USP 4 using Griseofulvin NP-laden stripfilms to suggest that its potential to provide similar results for other BCS Class II drugs.	(Sievens-Figueroa, Pandya et al. 2012)
Atorvastatin NPs	• USP 4 (glass-bead mixing; flow rate 8,16 ml/min) • Dialysis bag in USP 1 (75, 100, and 125 rpm; MWCO NA) • Dialysis bag in USP 4 (8,16 mL/min)	USP 4 dissolution method established for Atorvastatin NPs using modified sample loading (glass-bead mixing with NPs) was found to be discriminatory.	(Gite, Chogale et al. 2016)
Doxorubicin liposome	• USP 4 (flow rate 16 ml/min; 10–300 kDa MWCO)	USP 4 assay distinguished between generic parenteral liposome formulations and innovator Doxorubicin liposome product Doxil®.	(Yuan, Kuai et al. 2017)
Amphotericin B liposome	• USP 4 (flow rate 16 ml/min; 300 kDa MWCO)	USP 4 assay was able to differentiate marketed liposome formulation of Amphotericin B AmBisome® and other in-house formulations.	(Tang, Srinivasan et al. 2019)

2.7 Drug Pharmacokinetics from PLGA based NPs

- PLGA NPs of Zaleplon demonstrated higher plasma concentrations, improved bioavailability, lower clearance, and longer half-life when compared with marketed tablet and drug suspension in rabbits. The oral bioavailability of PLGA NPs was 3.42-fold higher than the marketed tablet and 2.75-fold higher than the drug suspension. Also, drug-loaded NPs showed significantly higher peak exposure (C_{max}) of 29.31 ng/ml than a marketed tablet (10.86 ng/ml) and a free drug suspension (13.27ng/ml). Total AUC was found to be 2135 ng·h/ml for Zaleplon NPs compared to the marketed tablet (625 ng·h/ml) and the drug suspension (802 ng·h/ml) (Haggag et al., 2021).

- The pharmacokinetic parameters of Apremilast loaded PLGA NPs were compared with pure drug suspension in Wistar albino rats (weighing 180–220g) after oral administration (dose 2 mg/kg). Oral bioavailability of PLGA NPs was 2.25-fold higher than the pure drug suspension without significant change in peak exposure (C_{max}). Long term retention of NPs was confirmed by significant decrease in elimination rate (K_{el}), increase in half-life ($T_{1/2}$) and mean residence time (MRT). Gender-specific absorption of Apremilast was indicated by five times higher bioavailability in female rats than in male rats (Anwer et al., 2019).

- Noncompartmental analysis was used to study the important pharmacokinetic parameters in 8-week-old female BALB/c mice after intravenous administration of docetaxel-loaded NPs and free drug solution at a dose level of 5 mg/kg. PLGA and PLGA–PEG NPs demonstrated an increase in serum exposure (AUC) and a decrease in elimination rate (K_{el}). The volume of distribution (V_d) was decreased from 383 ml (free drug solution) to 150 and 290 mL for PLGA and PLGA–PEG NPs respectively. Both types of NPs showed significant decreases in clearance (3.6-fold and 5-fold respectively) and significant increases in mean residence time (MRT) (2.4-fold and 4.8-fold), respectively, compared to free drug solution (Rafiei & Haddadi, 2017).

- Curcumin-loaded PLGA NPs and PLGA–PEG NPs were administered orally in rats, and their pharmacokinetics were compared with curcumin aqueous suspension. PLGA and PLGA–PEG NPs increased curcumin bioavailability by 15.6-fold and 55.4-fold, respectively, and increased curcumin half-life from 1 h to 4 and 6 h, respectively. The Cmax was increased 2.9-fold and 7.4-fold, respectively. Both NP formulations decreased the distribution and the metabolism of curcumin, more prominently by PLGA–PEG NPs (Khalil et al., 2013).

- Pharmacokinetics of cyclosporine-loaded NPs was determined in male SD rats (weighing 200–240 g) using oral gavage (15 mg/kg body weight). Relative

bioavailability (AUC_{0-inf}) of cyclosporine NPs was 119.2% compared to Sandimmune Neoral® capsules. Drug loaded NPs exhibited sustained drug release for 5 days with C_{max} at 24 h, in contrast to marketed formulation with a sharp C_{max} within 2 h and a 3-day drug release profile. NPs showed significantly less nephrotoxicity, evidenced by lower values of plasma creatinine (PC), blood urea nitrogen (BUN), and malondialdehyde (MDA) in rat plasma and kidney (Italia et al., 2007).

CHAPTER 3 DESIGN OF THE STUDY

3.1 Design of experiments (DoE) for Formulation Optimization

In the context of pharmaceuticals, optimization can be defined as the application of systematic approaches to propose the best combination of formulation and/or process variables to get the best formulation (with best outcomes or response variables). The traditional one variable/factor at a time (OVAT or OFAT) approach involves the study of one single variable/factor at a time. Because of its inability to explain two-factor interactions this approach become invalid when multiple variables are changed simultaneously. Apart from that, it is highly time-consuming and uneconomical due to unnecessary runs. Design of experiments (DoE) may provide solutions to these inherent limitations of OVAT approach and deliver better results with fewer experimental runs. Design of experiments (DoE) is a collection of statistical tools (such as screening designs and optimization designs) coupled with mathematical models, and graphical optimization to thoroughly understand relationship between significant input variables and tested responses (N. Politis et al., 2017; Vera Candioti et al., 2014).

As per FDA "quality should not be tested into finished products, it should be built-in or should be by design" (FDA & PAT, 2004). DoE is an integral component of pharmaceutical and analytical quality by design (QbD). Other elements of QbD approach include process analytical technology (PAT), quality target product profile (QTPP), critical quality attributes (CQAs), risk assessment, control strategy, and design space (Nayak et al.,

2019). Process analytical technology (PAT) is a regulatory framework that broadly integrates chemical, physical, mathematical, microbiological, and risk analysis to enhance the understanding and control of manufacturing process. (FDA & PAT, 2004). Quality target product profile (QTPP) of a pharmaceutical product is summary of quality characteristics that must be achieved to ensure its safety and efficacy (Fukuda et al., 2018; ICH & Q8(R2), 2009; Zhang & Mao, 2017). Critical quality attributes (CQAs) are physical, chemical, biological or microbiological properties that must lie within set specifications to ensure quality (e.g., particle size, shape) (Fukuda et al., 2018; Sangshetti et al., 2017). ICH defines design space as "multidimensional combination and interaction of input variables; critical material attributes (CMAs) and process parameters (CPPs) that have been demonstrated to provide assurance of quality" (ICH & Q8(R2), 2009). Any change within the approved design space is not subject to regulatory post-approval submission(ICH & Q8(R2), 2009). DoE can help identify CMAs (e.g., drug: polymer ratio, surfactant conc) and critical process parameters or CPPs (e.g., temperature, flow rate). These CMAs and CPPs subsequently help achieve desired CQAs (e.g.,) to realize quality target product profile (QTPP) and, ultimately establish a design space. (Amadeo et al., 2014; Zhang & Mao, 2017).

3.1.1 Selection of experimental design

The choice of a design should be based on available resources, time, cost and a permissible limit on Type I and Type II errors for hypotheses testing. The experimenter should choose a design with a number of runs less than allowed by the budget, to keep the scope for the addition of some center points runs (to check curvature in a two-level screening design) and repeat some design points considering unplanned experimental mistakes (Fontdecaba et al., 2014; Rüttimann & Wegener, 2015). Screening designs (full or fractional Factorial design, Plackett–Burman designs (PBDs) or Taguchi designs) are useful for screening of a large number of input variables to identify a few significant ones. But these are low-resolution designs and can support only linear responses. However, if a nonlinear response is detected, more complex response surface methods (RSMs) such as Central composite designs (CCD) or Box–Behnken designs become necessary to get an idea about local shape of response surface. Besides having main effect and two-factor interaction terms RSMs may also have quadratic and cube terms to explain the curvature in response (Kauffman et al., 2015; N. Politis et al., 2017; NIST; Subra & Jestin, 2000). DoE optimization methodology can be presented as stepwise sequence as described in Figure 3.1.
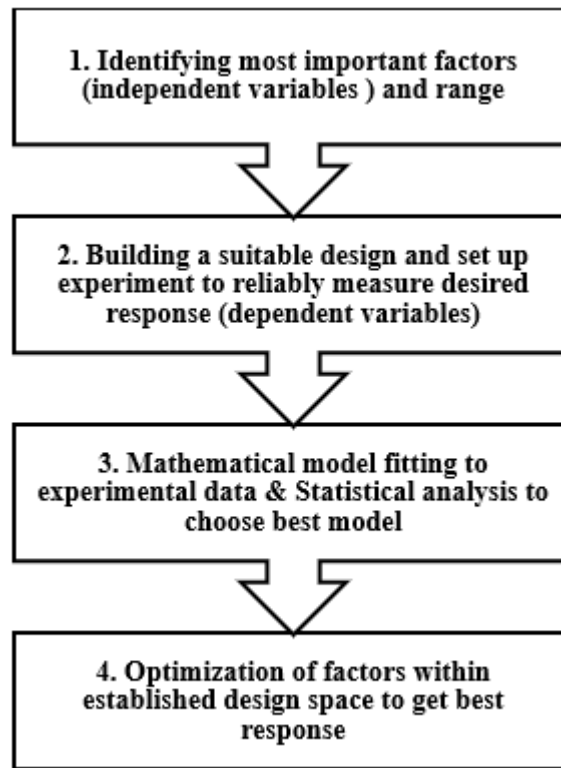
Figure 3. 1: Stepwise sequence of DoE optimization methodology

3.1.2 Box-Wilson Central Composite Design or Central Composite Design (CCD)

Central composite design (CCD), a response surface design can appropriately establish a correlation between the independent variables and the responses by fitting them into the second order polynomial equations.

$$Y = \beta_0 + \beta_1 X_1 + \beta_2 X_2 + \cdots + \beta_k X_k + \beta_{11} X_1^2 + \beta_{22} X_2^2 + \cdots \beta_{kk} X_k^2 + \beta_{12} X_1 X_2 + \cdots +$$

$$\beta_{k-1,k} X_{k-1} X_k + \varepsilon \qquad\qquad \text{Equation 3.1}$$

Here, Y represents the response, k is the total number of factors, β_0 is an intercept,

β represent the coefficient values (regressors) for linear, quadratic, and interaction effects

and ε represents the error associated with model (Dutka et al., 2015; Sadhukhan et al.,

2016). A CCD design requires five levels of each factor: high (+1), low (-1), (+α), (-α) and

mid-center (0) level and comprises of three type of design points (Figure 3.2).

a) 2^k factorial design points (consisting of all possible combinations of +1 and

   −1 levels of each factor)

b) $2k$ axial/star points (to generate quadratic terms)

c) n center points or replicate terms (independent estimate of pure experimental

   error(Kowalski et al., 2002))

Thus, total number of experiments designed by CCD will be (Asghar et al., 2014):

$$N = k^2 + 2k + n \qquad\qquad \text{Equation 3.2}$$

Axial or Star Point

$(0,+\alpha)$

Factorial Point
$(+1,+1)$

$(-1,+1)$

Center point
$(0,0)$

$(-\alpha,0)$ $(+\alpha,0)$

$(-1,-1)$ $(+1,-1)$

$(0,-\alpha)$
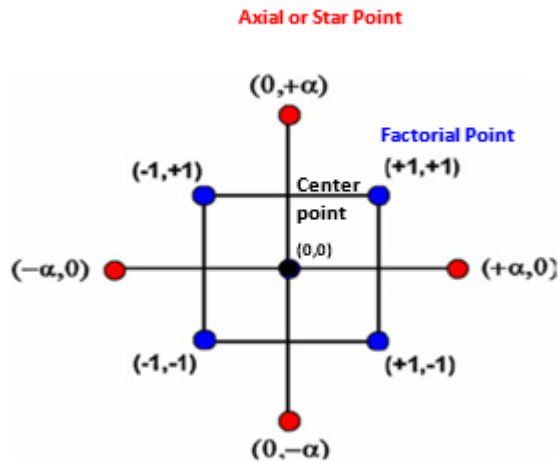
Figure 3. 2: Three types of CCD design points: a)2^k design or factorial points; b)$2*k$ axial or star points and c) n center points ($\alpha= \sqrt{k} =1.41$ which gives a spherical design; K = number of factors)

where N is the total number of experiments, k is the number of factors studied, and n is the number of replicate center points. Rotatability is a desired property for response surface designs (quadratic model designs). It means that prediction variance at any specific design point will depend only upon its distance from center point, not on the direction. Such designs can be rotated around the center without changing the variance of predicted response value.

In CCD, star or axial points allow for the estimation of curvature (or pure quadratic effect) present in response of interest. They establish new higher extremes, at a distance α (alpha) from center point and are useful in defining the area of operability. The value of α

determines the location of star points within experimental domain and it depends on the number of experimental runs within the factorial part of design (Equation 3.3). A CCD design with α=1 is a simpler 'face-centered CCD'. The axial points are present on the face of square itself thus, this design tests only three factor levels. It can give reasonably good predictions within the design space but poor predictions for estimates of quadratic coefficients (not a rotatable design). 'Circumscribed CCD' design with an α value of √ k is sufficient to maintain the rotatability of design and precisely estimate the pure quadratic coefficients (Asghar et al., 2014; Singh et al., 2011). The 'inscribed CCD' is a scale-down circumscribed CCD design where axial points are located at upper and lower bounds (±1) specified for factors. The design points shrink as each factor level is divided by α to generate such design. Like circumscribed CCD they also use five factor levels and are rotatable designs (Zhang & Xiaofeng, 2009).

$$\alpha = [\text{Number of factorial runs}]^{\frac{1}{4}} \qquad \text{Equation 3.3}$$
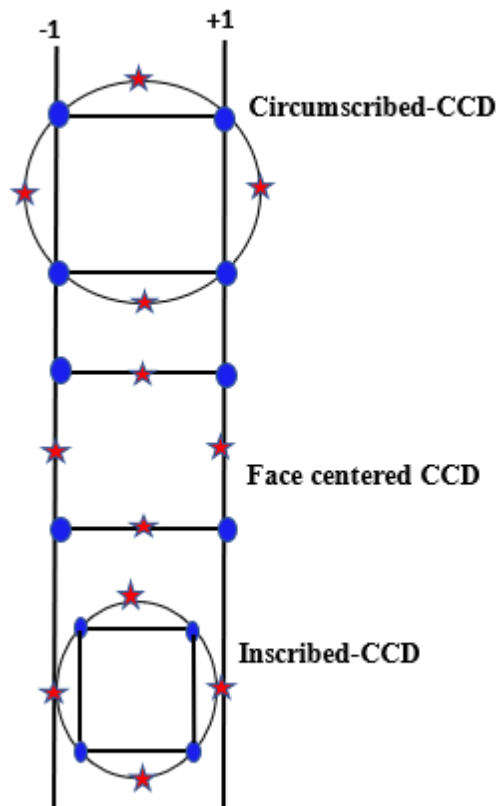
Figure 3. 3: Three types of CCD designs

(Reference: https://www.itl.nist.gov/div898/handbook/pri/section3/pri3361.htm)

'Resolution' of a design refers to the degree to which the main effects are confounded or aliased with two-factor or three-factor interaction terms. CCDs are resolution V designs, where neither main effects nor two-factor interaction terms are aliased with any other main effect or two-factor interaction terms. However, two-factor

interactions are confounded with some three-factor interactions (Kowalski et al., 2002; Vining et al., 2005). 'Robustness' is the ability of a process not to break down when some observations are missed out. CCD designs are robust enough to missing observations. It means they can give reliable predictions even in the absence of some design points (factorial/axial/central) without impacting the power much (E.I et al., 2021; Oladugba & Nwanonobi, 2021).

3.2 Materials

3.2.1 Chemicals, Drugs and Animals

- Synthetic compound AC1LPSZG was a gift sample from Baylor College of Medicine, Houston, TX, USA.

- Acetonitrile (LC-MS grade) purchased from Avantor Performance Materials, LLC, PA, USA, water (LC-MS grade) purchased from EMD Millipore Corp., MA, USA, and formic acid purchased from Sigma-Aldrich, St, Louis, MO, USA were used to prepare UPLC and LC-MS/MS mobile phases.

- Griseofulvin (Sigma-Aldrich, St. Louis. MO, USA) was used as internal standard solution in UPLC and LC-MS/MS assay for AC1LPSZG analysis.

- Poly (D, L-lactide-co-glycolide) lactide: glycolide 50:50 (molecular weight 30,000-60,000), Poly (D, L-lactide-co-glycolide) lactide: glycolide 73:25 (molecular weight

66,000-107,000) and Resomer® RG 503H, Poly (D, L-lactide-co-glycolide), acid terminated, lactide: glycolide 50:50 (molecular weight 24,000-38,000), all were purchased from Sigma-Aldrich, St, Louis, MO, USA and used as biodegradable polymers for nanoparticle preparation.

- For cosolvent formulation the solvents DMSO, PEG400, and saline solution were purchased from Millipore Sigma (St. Louis, MO) and Transcutol HP was obtained from Gattefosse (Paramus, NJ).

- Acetone (VWR Chemicals, PA, USA) was used as organic solvent during nanoparticle preparation.

- Kolliphor® P188 (Poloxamer 188 or Lutrol® F68) was used as surfactant and sucrose was used as lyoprotectant during nanoparticle preparation, both were bought from Sigma-Aldrich St, Louis, MO, USA).

- Potassium phosphate monobasic (or potassium dihydrogen phosphate, KH_2PO_4), potassium chloride (KCl), sodium acetate (CH_3COONa), all were obtained from Sigma-Aldrich, St, Louis, MO, USA and used for buffer preparations during pH-stability studies. Hydrochloric acid (36.5-38%) was procured from Aqua Solutions, TX, USA and sodium hydroxide(10N) was purchased from Avantor Performance Materials, LLC, PA, USA.

- Potassium phosphate monobasic-sodium phosphate dibasic buffer (pH7.4) was purchased from Fisher Scientific, NJ, USA. Ethanol was obtained from Sigma-Aldrich, St, Louis, MO, USA.

- Hexadecyltrimethylammonium bromide (or Cetrimonium bromide, CTAB) (Sigma-Aldrich, St, Louis, MO, USA), Tween® 80 (Polyoxyethylene (80) Sorbitan Monooleate) (EMD Chemicals Inc., NJ, USA) and Sodium lauryl sulfate (Bio-Rad Laboratories, CA, USA) were used as solubilizers during dissolution studies.

- Labrasol ALF (PEG-8 Caprylic/Capric triglycerides) (Gattefosse, CS, France), Polyethylene glycol-400 (PEG-400) (Wood Scientific Inc, Houston, TX, USA) Propylene glycol (PCCA, Houston, TX, USA) and Isopropyl alcohol (VWR Chemicals, PA, USA) were used as cosolvent wash.

- Diethyl ether (EMD Chemicals, Inc., NJ, USA), dichloromethane (VWR Chemicals, PA, USA), chloroform (Sigma-Aldrich, St, Louis, MO, USA) and ethyl acetate (Fisher Scientific, NJ, USA) were used during liquid-liquid extraction.

- Sprague-Dawley (SD) rats (male, 150-174g) were purchased from Envigo RMS, LLC, (Indianapolis, IN, USA) and were used in the pharmacokinetic studies of compound AC1LPSZG.

- Anesthesia cocktail comprised of acepromazine, ketamine and xylazine, procured from Sigma-Aldrich (St, Louis, MO, USA), and used to anesthetize the rats during the jugular vein cannulation surgery.

- 1000 U/ml Heparin sodium solution (Sagent Pharmaceuticals, Schaumberg, IL, USA) was diluted with aqueous normal saline (sodium chloride solution, 0.85%) (Sigma-Aldrich., St, Louis, MO, USA) to prepare various concentrations (100 U/mL, 20 U/ml) for pharmacokinetic studies. Heparinized microcentrifuge tubes (coated

with 1000 U/ml) were prepared for blood sample collection and storage. Jugular vein cannulas were flushed using 100 U/ml of heparin solution after each sampling. 10 U/ml of heparin solution was given after each sample withdrawal to replenish the body fluid.

3.2.2 Supplies

- 20 ml clear disposable scintillation vials (VWR, West Chester, PA, USA) were used during preparation step and to store standard stock solutions of AC1LPSZG and griseofulvin.

- Glass syringe, 5ml, with metal Luer-lock tip was purchased from Poulten & Graf Gmbh, Wertheim, Germany used for nanoprecipitation preparation method.

- Spectra/Por® Float-A-Lyzer G2 dialysis cells (cellulose ester, amber color cap, 1ml, 300 kDa molecular weight cut–off (MWCO)) were purchased from Spectra Labs, CA, USA.

- Whatman™ membrane filters (cellulose acetate, 47 mm, 0.45 µm) (GE Healthcare UK Ltd., Buckinghamshire, UK) were used to filter harsh mobile phases or aggressive organic solvent-based solutions.

- CTV-0910P-100 µL Polypropylene Vial, 9mm screw thread, bought from Chrom Tech, MN, USA were used in UPLC assays.

- 2 ml Screw top vials and screw cap (Agilent, CA, USA) were used for collection of dissolution samples.

- Microcentrifuge tubes (clear, 2 ml and 1.5 ml) (VWR International LLC., Radnor, PA, USA) were used for working standard solution preparation, washing of NPs, blood sample collections and plasma sample storage.

- Pipette tips (20 µl, 200 µl, 1000 µl) were purchased from VWR International LLC., Radnor, PA, USA to be used with appropriate pipette to accurately measure and transfer the solutions.

- Powder-free latex examination gloves purchased from VWR International LLC., Radnor, PA, USA were used during all experiments.

- 6" Cotton tipped applicators used to stop bleeding during animal surgeries were purchased from Dynarex Corporation, Orangeburg, NY, USA.

- Kendall curity Gauze sponges (3 in x 3 in) purchased from Tyco Healthcare, Mansfield, MA, USA were used to stop bleeding and to clean up the wounds during animal surgeries.

- Face masks were purchased from AlphaProTech, Inc (Salt lake City, UT, USA) to protect from infection while performing animal experiments.

- Sterile tuberculin slip tip syringes (1 mL) assembled with PrecisionGlide™ 23G needles purchased from Becton Dickinson & Co (Franklin Lakes, NJ, USA) or 23G 0.5" blunt needles purchased from Sai Infusion Technologies (Lake Villa, IL) were used for intramuscular injection of anesthetic cocktail and for withdrawal of blood samples from experimental rats respectively.

- Silk surgical sutures from Henry Schein Inc (Melville, NY, USA) were used for securing the jugular vein cannula and closing the incisions during animal surgeries.

3.2.3 Equipment, Apparatus, and Software

- New Classic Balance (Model: MS104S /03) (120g, 0.1mg) and XPR 225 Dual Range balance (Model: XPR225DU) (121g, 0.01mg) from Mettler Toledo, Greifensee, Switzerland were used to weigh drugs and chemicals.

- Syringe pump (Model: NE-300) (New Era Pump Systems, Inc., Farmingdale, NY) attached with Heidolph magnetic stirrer (Heidolph Instruments Gmbh & co., Germany) was used for nanoprecipitation method of nanoparticle preparation.

- Malvern Zetasizer Nano-ZS (Model: ZEN 3600) (Malvern Instrument Ltd, Worcestershire, UK) was used for particle size and zeta potential measurements.

- Eppendorf centrifuge 5417R (Rotor no. F45-30-11) from CE, Germany was used for nanoparticle wash and sample analysis by UPLC and LC-MS/MS.

- Hot plate stirrers (NO97042-634) (VWR, Troemner LLC, USA) were used to heat and /or stir solutions during nanoparticle preparation.

- Bath sonicator (B2500A-MTH) from VWR International, West Chester, PA, USA was used for entrapment efficiency experiment and for dissolving polymers.

- Lyophilizer (Vir Tis SP Scientific BenchTop Pro with Omnitronics™) (Model: BTP-95GEVW), USA was used to lyophilize NPs.

- Thermo-Scientific –86°C Freezer, CA, USA was used during particle lyophilization and to store plasma samples.

- Bench top stability chamber (Model: PH09-DA), Darwin Chambers, St. Louis, MO, USA was used for stability studies.

- Shimadzu Auto Differential Scanning Calorimeter DSC-60A, Koyoto, Japan was used for thermal analysis of drug and excipients.

- JEOL JSM-6010LA Scanning Electron Microscope (SEM) was used to examine the external morphology of NPs.

- Water bath (Type: 89032-203) from VWR, PA, USA was used during stability studies.

- VWR pulsing vortex mixer (Model: 945320), Henry, Troemner, LLC, USA and Vortex bench mixer, Benchmark Scientific Inc, Edison, NJ, USA were used for simple mixing of all liquid samples.

- SOTAX® CE7-smart dissolution testing unit (Sotax, AG, Aesch, Switzerland) was used for nanoparticle dissolution studies.

- ThermoScientific pH meter with Orion ROSS pH electrodes (Thermo Fischer Scientific Inc., Mettler Toledo, LLC, USA) was used for buffer pH measurement.

- UPLC system consisting of:

  o Waters Acquity UPLC® BEH Shield RP18 column (2.1 X 50mm, 1.7μm, 100 Å). Waters, Milford, MA, USA)

- o Waters Acquity UPLC® Sample Manager FTN-H (Model: K18FTP125G, Waters, Milford, MA, USA)

- o Waters Acquity UPLC® Quaternary Solvent Manager (Model: A19Q5P493A, Waters, Milford, MA, USA)

- o Waters Acquity UPLC® Photodiode Array Detector (Model: M184PD004A, Waters, Milford, MA, USA)

- o Empower software (EM9BA01540, Waters, Milford, MA, USA)

- LC-MS/MS system consisting of

  - o 4000 QTRAP® triple quadrupole mass spectrometer equipped with a Turbo Ion Spray ion source (AB SCIEX, Redwood City, CA, USA)

  - o Analyst® Software 1.6.2 (Redwood City, CA, USA) was used to control the LC-MS/MS system and to acquire data from.

  - o Waters ACQUITY UPLC HSS T3 C_{18} column (50 mm x 3 mm i.d., 1.8μm, 100 Å)

- WinNonlin v8.1, Pharsight Corp, Mountain View, CA, USA software was used for noncompartmental pharmacokinetics data analysis.

- DDSolver, a free add-in program for Microsoft Excel was used for modelling and comparison of *in vitro* drug release profiles.

- JMP software for Windows (Free version) was used to perform statistical analysis.

3.3 Methods

3.3.1 Preparation of Cosolvent System

Optimized   cosolvent system for AC1LPSZG was prepared by vortexing the solvents DMSO: PEG400: Transcutol HP: Saline solution in the ratio of 10:30:30:30 (v/v) (Chen et al., 2022).

3.3.2 Preparation of PLGA-AC1LPSZG-NPs

Poly (D, L-lactic-co-glycolic acid) (PLGA), a biodegradable, non-toxic polymer was used for nanoparticle preparation. Acetone was a choice of organic solvent as at a given polymer concentration acetone has reported to produce smaller particles(Legrand et al., 2007). 3% Poloxamer P188 (or Pluronic F68) was used as a stabilizer. In the preliminary experiments this concentration produced significantly smaller particles. Previous studies also reported that Poloxamer P188 can produce smaller particles compared to other surfactants (Cohen-Sela et al., 2009).

Solvent Displacement / nanoprecipitation method was used to prepare PLGA NPs of poorly water-soluble model drug AC1LPSZG. Briefly, 60 mg PLGA was dissolved in 2mL acetone. 5mg AC1LPSZG was dissolved in above prepared polymer solution and then added dropwise into the aqueous phase containing stabilizer (3% Poloxamer P188) under

magnetic stirring (0.3 ml/min, 30°C, 750 rpm) using syringe pump (Model: NE-300) (New Era Pump Systems, Inc., Farmingdale, NY) attached with Heidolph magnetic stirrer (Heidolph Instruments Gmbh & co., Germany). NPs were formed instantaneously by interfacial deposition of polymer due to rapid diffusion of water miscible organic solvent (acetone) into the aqueous medium. Solvent removal was done under magnetic stirring on hot plate stirrers (NO97042-634) (VWR, Troemner LLC, USA) at 60°C, 400 rpm for 3hours. NPs were washed three times with water at 14000 rpm, 4°C for 45 minutes using Eppendorf centrifuge 5417R (Rotor no. F45-30-11) from CE, Germany and lyophilized (SP Scientific BenchTop Pro with OmnitronicsTM) using 10% sucrose as lyoprotectant.

3.3.3 Particle Size & Zeta Potential Measurement

Malvern Zetasizer Nano-ZS (Model: ZEN 3600) (Malvern Instrument Ltd, Worcestershire, UK) was used for particle size and zeta potential measurements. Disposable polystyrene folded capillary cell (DTS0012, Malvern) cell was rinsed with dispersant before use. Recommended minimum sample concentrations for 100nm to 1µm size particles is 0.01g/l or 10^{-3} % mass. About 1ml of sample was slowly filled into one of the sample ports of the folded capillary cell with the help of micro-pipettor avoiding any air bubbles. When the sample started to emerge from the second sample port, the stoppers were inserted onto both the ports. Any excess liquid spilt onto electrodes was removed using tissue paper. The cell area lid of the instrument was opened, and folded capillary cell

was pushed into the cell holder so as the polished optical surface was facing the front of instrument (indicated by a small triangle at the top of cell). The cell area lid was closed, and measurements were done in triplicate. Milli Q water was used as a dispersion medium during all measurements.

3.3.4 Drug Loading (DL) and Entrapment Efficiency (EE)

In the direct method for entrapment efficiency determination, 20 mg NPs were sonicated with 1.5ml acetonitrile for 5min (Bath sonicator, B2500A-MTH, VWR International, West Chester, PA, USA) to dissolve the PLGA and then centrifuged at 11,000 rpm, 4°C for 10 min in cooling centrifuge (Eppendorf centrifuge 5417R, Rotor no. F45-30-11, CE, Germany) to precipitate out the sucrose lyoprotectant. Supernatant was collected and analyzed under Waters Acquity UPLC system after suitable dilution and centrifuging again at 11,000 rpm, 4°C for 10 minutes.

In the indirect method, the amount of free drug was analyzed in the supernatant recovered during the washing step. The entrapment efficiency and drug loading were calculated using the following formula (Seju et al., 2011; Sun et al., 2015).

$$\% \, EE = \frac{Amount \; of \; drug \; encapsulated \; X100}{Amount \; of \; drug \; initially \; taken \; to \; prepare \; NPs} \qquad \text{Equation (6)}$$

$$\% \, DL = \frac{Amount \; of \; drug \; encapsulated \; X100}{Weight \; of \; prepared \; NPs} \qquad\qquad \text{Equation (7)}$$

3.3.5 *In vitro* drug release study

A close loop type USP 4 apparatus CE7-smart (SOTAX®) incorporated with 22.6 mm dissolution cells (14 mL) and piston pump (Sotax™CP7-35/CP7-300) was used for *in vitro* drug release studies. A known amount of NPs was suspended in 1 ml of respective dissolution medium and filled in Float-A-Lyzer dialysis cells with cut off size of 300 kDa. 100 ml of dissolution medium was filled in each media bottle. The test method was loaded manually- sample volume, flow rate of release medium and temperature were set at 16 mL/min, 37°C and 200µl respectively. When the Prep I was completed the Float-A-Lyzer cells were inserted into the dissolution assembly. After the completion of Prep II step, the test was started. At predetermined time intervals the samples were withdrawn and assayed using UPLC after suitable dilution. Experiments were done in triplicate and data were presented as the mean ± SEM.

3.3.6 Differential Scanning Calorimetry (DSC)

In a heat flux type DSC (Shimadzu DSC-60A), an empty reference pan and a sample loaded pan both were kept onto a thermoelectric disk. The disk was heated at a linear heating rate and generated temperature difference (due to heat capacity of sample)

between the sample and the reference pan was measured by area thermocouples and converted to the heat flown.

3.3.7 *In Vivo* Studies

The pharmacokinetic (PK) studied were done by intravenous administration of cosolvent formulation to Sprague-Dawley (SD) rats at a dose of 5 mg/kg dose level. Blood samples were collected via jugular vein cannulation at predetermined time-points and stored with heparin sodium anticoagulant. Drug concentrations were analyzed by a validated LC-MS/MS method ((Chen et al., 2022)). Relevant pharmacokinetic parameters were calculated by using WinNonlin v8.1 (Pharsight Corp, Mountain View, CA, USA) software. All animal studies were approved by the Institutional Animal Care and Use Committee (*IACUC*) at Texas Southern University (TSU protocol #9136 approved on 11 July 2020) and were conducted according to the National Institute of Health "Guide for the Care and Use of Laboratory Animals, 8th Edition" (Gao et al., 2021).

CHAPTER 4 RESULTS AND DISCUSSIONS

4.1 Analytical Methods

4.1.1 UPLC method

UPLC method was used for *in vitro* sample analysis (dissolution studies and entrapment efficiency determination) of AC1LPSZG -loaded PLGA nanoparticles (PLGA-AC1LPSZG-NPs). Griseofulvin was selected as the internal standard (IS) based on properties comparable to AC1LPSZG (Table 4.1). The calibration curve of UPLC assay for AC1LPSZG in neat solution has good linearity (Coefficient of determination (r^2) ≥ 0.999) over the range of 5-100 µg/mL (Figure 4.1). Lower limit of quantification (LLOQ) was 5 µg/mL. Waters, ACQUITY UPLC BEH C18 (50mm x 2.1mm i.d., 1.7 µm, 100 Å) column was used with PDA detector (285nm). The retention times for AC1LPSZG and IS were 2.16 and 2.62 min respectively. Mobile phase A was 0.1% formic acid in water, Mobile phase B was 0.1% formic acid in acetonitrile at a flow rate of 0.5 mL/min and Injection volume of 10µL. The solvent gradient profile is shown in Table 4.2. A representative UPLC chromatogram for AC1LPSZG and IS both at conc = 10 ug/ml is shown in Figure 4.2.
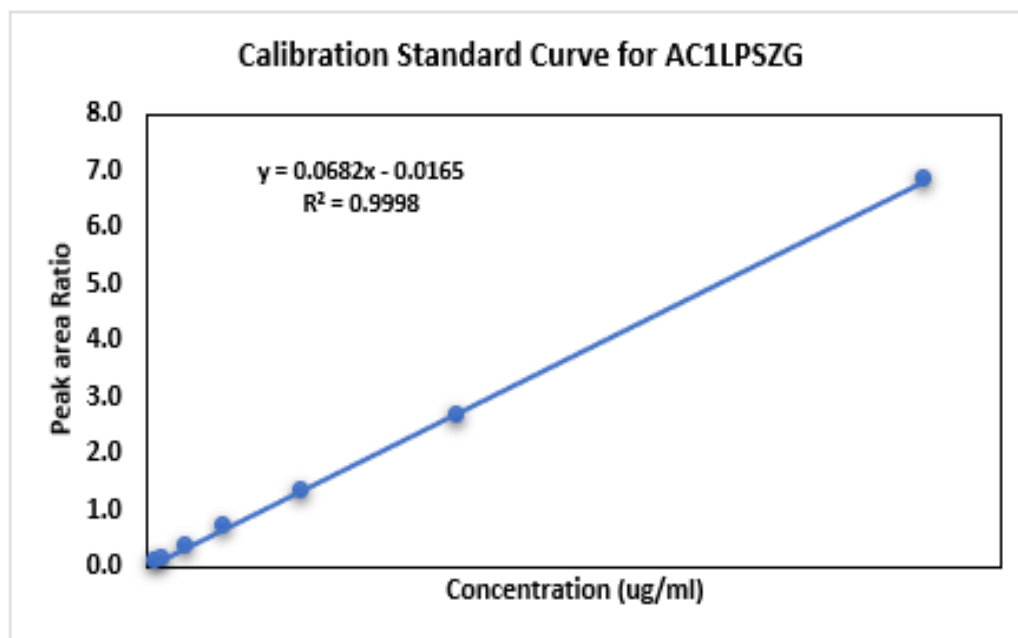
Figure 4. 1: UPLC calibration standard curve for AC1LPSZG
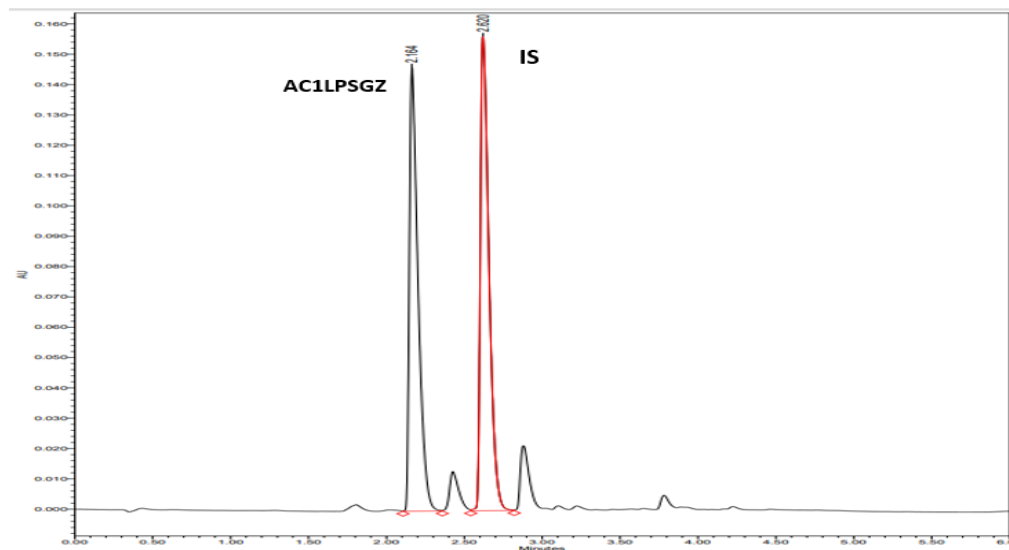
Figure 4. 2: Chromatogram for AC1LPSZG and IS both at conc = 10ug/ml

Table 4.1: Comparable Analyte and IS Properties

Property	AC1LPSZG (Analyte)	Griseofulvin (IS)
Molecular Weight (Dalton)	456	352.8
Log P	3.47	2.18
Hydrogen Bond Donor	1	0
Hydrogen Bond Acceptor	5	6

Table 4.2: Solvent Gradient Profile for UPLC Method

Time (min)	Mobile Phase A (%)	Mobile Phase B (%)
0	90	10
0.2	90	10
4.0	0	100
5.0	0	100
5.5	90	10
6.0	90	10

4.1.2 LC-MS/MS Method

Previously developed LC-MS/MS assay was used for pharmacokinetics study (Chen et al., 2022). For MS/MS analysis a 4000 QTRAP® triple quadrupole mass spectrometer with a Turbo Ion Spray source (AB Sciex, Redwood City, CA, USA) was used in the positive mode. The source parameters were set as follows: ion source temperature, 500 °C; ion spray voltage, 5000 V; curtain gas, 25 psi, nebulizer gas (Gas 1), 30 psi, heater gas, 25 psi (Gas 2), and high collision gas. The compound-dependent parameters were optimized with entrance potential (EP), 10V; declustering potential (DP), 76 V for both AC1LPSZG and the IS; Collision cell exit potential (CXE), 17V; and

collision energy (CE) 28 V for AC1LPSZG and 24 V for the IS, respectively. After collision cell fragmentation the most abundant and stable multiple reaction monitoring (MRM) transitions for $[M + H]^+$ ion of AC1LSPZG was (m/z 457.10 → 349.00) and that of Griseofulvin (IS) was (m/z 353.27 → 285.10) (Figure 4.3). The retention times of the drug and IS in in LC-MS/MS chromatograms were 1.28 minutes and 1.52 minutes, respectively (Figure 4.4). The calibration curve of LC-MS/MS assay for AC1LPSZG in rat plasma was linear ($R^2 = 0.999$) over the range of 10-5000 ng/mL. Sensitivity evaluation was done by measuring the limit of detection (LOD) and the lower limit of quantitation (LLOQ). The LOD and LLOQ of the method were established with the signal-to-noise ratio (S/N) 3:1 and 10:1, respectively. The lowest limit of quantitation of AC1LPSZG in LC-MS/MS assay was 10 ng/mL. These results indicated good linearity and sensitivity for their specific applications.

Waters ACQUITY UPLC HSS T3 C18 column (50 mm x 3 mm i.d., 1.8μm, 100 Å) UPLC column was used with retention times for AC1LPSZG and IS being 1.27min and 1.52 min respectively. Mobile phase A was 0.1% formic acid in water, Mobile phase B was 0.1% formic acid in acetonitrile at flow rate of 0.5 mL/min and injection volume of 5μL. Table 4.3 shows the solvent gradient profile.
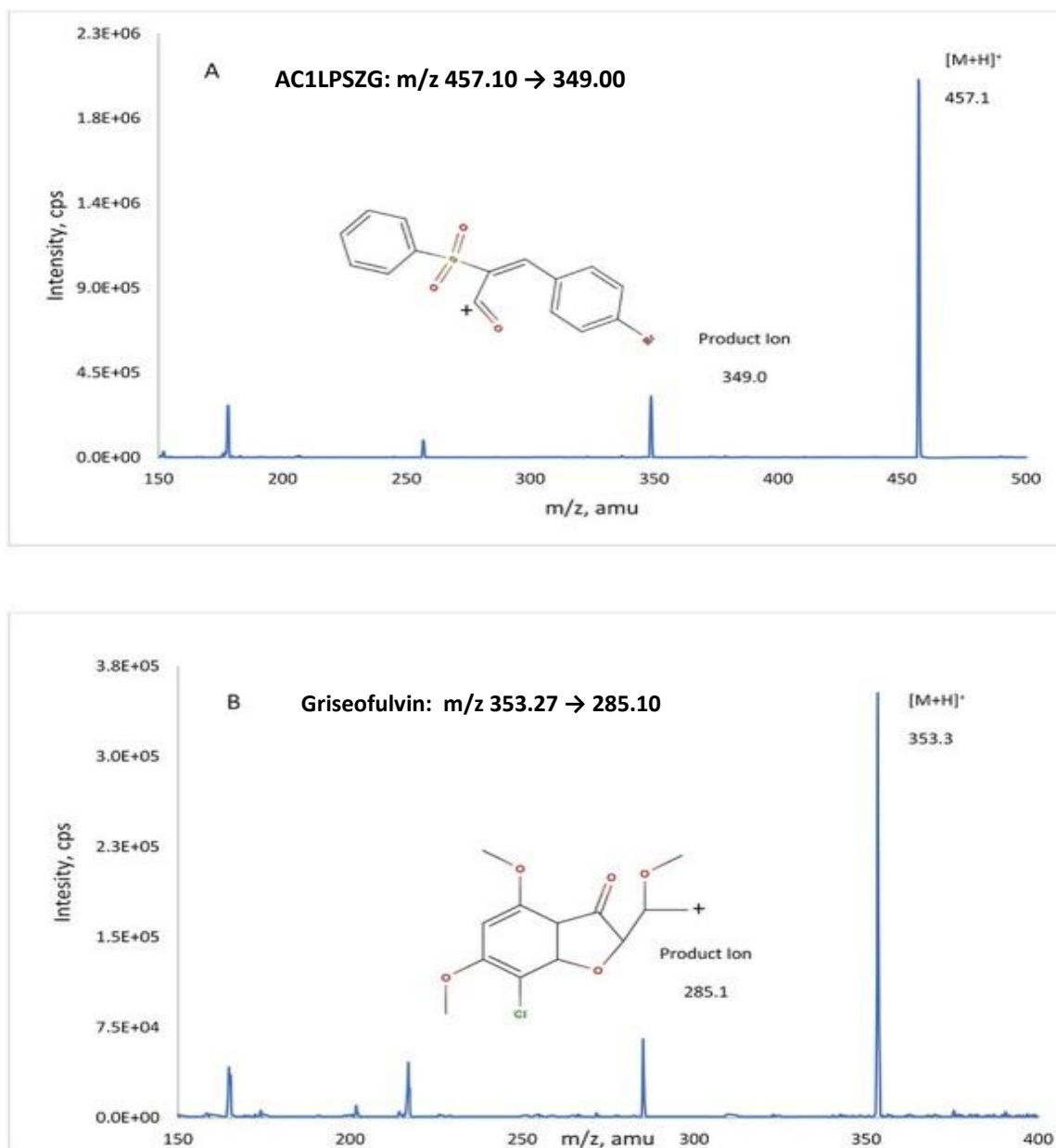
Figure 4. 3: Product ion spectra and proposed fragmentation pathways for analyte AC1LPSZG (A), internal standard Griseofulvin (B)

XIC of +MRM (4 pairs): 457.100/349.000 Da ID: 276_1 from Sample 13 (500) of 04272022276.wiff (Turbo Spray)   Max. 5.6e4 cps

(A) AC1LPSGZ

(B) IS

1.27
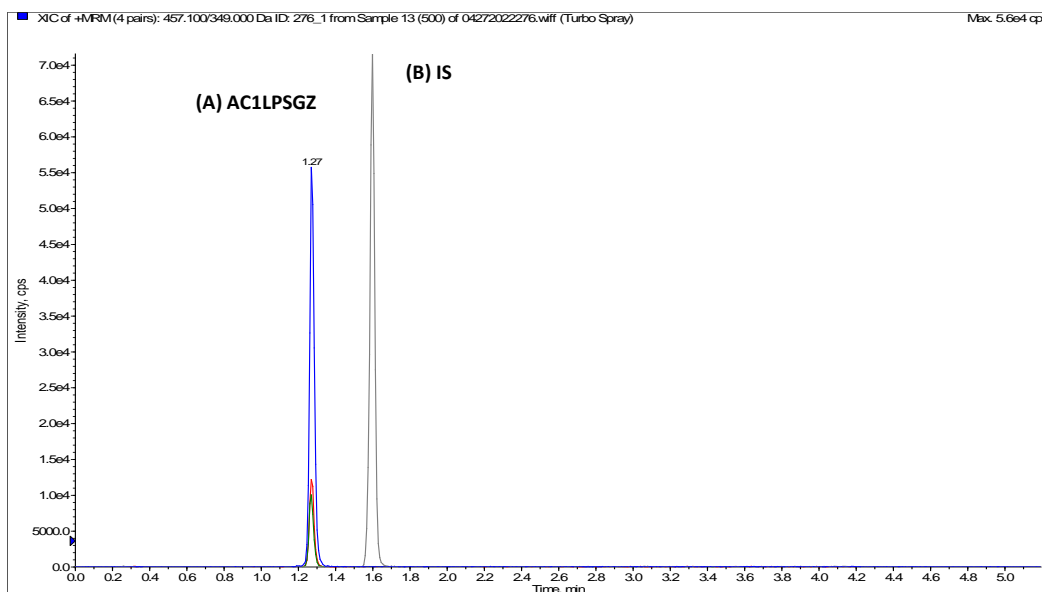
Figure 4. 4: Representative chromatogram-tandem mass spectrometry (LC-MS/MS) chromatography for (A) AC1LPSZG (500 ng/mL), (B) internal standard Griseofulvin

Table 4.3: Solvent Gradient Profile for LCMS Method

Time (min)	Mobile Phase A (%)	Mobile Phase B (%)
0	80	20
2	80	20
3.5	20	80
3.6	20	80
4.6	80	20

Recovery of AC1LPSZG in rat plasma for LLOQ and QC samples ranged from 86.87% to 102.51%. Matrix effects for all samples were less than 15% suggesting negligible enhancement or suppression signals (Table 4.4). Short-term, long-term, freeze-thaw and auto-sampler stability of AC1LPSZG in rat plasma is shown in Table 4.5. To evaluate the intra-day and inter-day assay accuracy (% RE) and precision (% CV) the QC and LLOQ samples were analyzed on the same day and repeating on three separate days. The results presented in Table 4.6 met the acceptance criteria of ±15%.

Table 4.4: Recovery and matrix effect of AC1LPSZG in rat plasma for LLOQ and QC samples

Biological samples	Nominal concentration (ng/mL)	Matrix effect (%) (n = 6)	Recovery (%) (n = 6)
Plasma	10	7.66 ± 9.93	86.87 ± 5.42
	15	2.35 ± 6.57	102.51 ± 4.98
	1000	10.64 ± 3.09	88.00 ± 3.26
	4000	10.98 ± 2.13	94.35 ± 9.12

Table 4.5: Stability of AC1LPSZG in rat plasma [n= 3; mean (±SD)]

Biological samples	Stability test	Nominal Concentration (ng/mL)	Calculated Concentration (ng/mL)		
			Mean ± SD (n = 6)	CV (%)	RE (%)
Plasma	Auto-sampler (RPEX,16 hr)	10	10.79 ± 0.66	6.11	7.94
		15	14.36 ± 1.29	8.98	-4.3
		1000	1052 ± 41.66	3.96	5.26
		4000	3980.15 ± 123.82	3.11	-0.5
	Short-term (RP, 6 hr, RT)	10	10.09 ± 0.29	10.02	3.39
		15	15.51 ± 1.55	8.22	3.15
		1000	941.07 ± 28.29	3.01	-5.89
		4000	4027.86 ± 222.85	5.53	0.7
	Freeze and thaw (RP, −80 °C to RT)	10	5.21 ± 0.64	12.3	-47.88
		15	10.78 ± 1.56	14.48	-28.12
		1000	766.65 ± 17.91	2.34	-23.33
		4000	2986.94 ± 36.76	1.23	-25.33
	Long-term (RP, −80 °C, 30 days)	10	2.16 ± 0.71	48.35	-78.4
		15	4.34 ± 0.04	16.24	-71.04
		1000	438.85 ± 46.27	10.54	-56.11
		4000	1597.18 ± 112.35	7.03	-60.07
	Long –term (RPEX, −80 °C, 30 days)	10	9.92 ± 0.02	0.2	-0.82
		15	14.46 ± 0.37	2.58	-3.57
		1000	834.28 ± 39.51	4.74	-16.57
		4000	3060.42 ± 177.06	4.91	-9.76

*RP, rat plasma; RT, room temperature; RPEX, rat plasma post extraction.

Table 4.6: Intra- and inter-day accuracy and precision of UPLC-MS/MS method for quantification of LLOQ and QC samplesAC1LPSZG in rat plasma

Nominal Conc. (ng/mL)	Intra-day (n = 6)			Inter-day (n = 18)		
	Observed concentration (mean ± SD)	Accuracy (RE%)	Precision (CV%)	Observed concentration (mean ± SD)	Accuracy (RE%)	Precision (CV%)
10	10.49 ± 0.69	4.88	6.56	9.51 ± 079	−4.85	8.29
15	15.12 ± 1.14	0.81	7.51	14.86 ± 1.28	−0.95	8.59
1000	947.68 ± 63.45	−5.23	6.69	1023.74 ± 44.07	2.37	4.3
4000	3928.42 ± 390.36	−1.79	9.94	4090.53 ± 223.94	2.26	5.79

4.2 Design of experiments (DoE) for Formulation Optimization of PLGA-AC1LPSZG-NPs

Formulation optimization involves investigation of appropriate combination of independent variables to give the product with desired response variables (Schwartz et al., 2002). Central composite design (CCD), a robust and high-resolution response surface design was used for NPs optimization using Design Expert® software (version 13). Two factors (independent variables), drug amount in organic phase (mg) and aqueous phase volume (ml) were tested over five different levels (Table 4.7) and four corresponding responses (dependent variables) viz., entrapment efficiency (EE), NP size, drug load and zeta potential were measured. CCD design layout and measured responses are shown in Table 4.8.

Table 4.7: Input Factors and their Coded Levels

Factor (Independent Variable)			Coded Factor levels		
	Low (-1)	Mean (0)	High (+1)	Min (-α)	Max (+α)
A: Drug Amount in Organic Phase (mg)	5	10	15	2.93	17.07
B: Aqueous Phase Volume (ml)	4	5	6	3.59	6.41

Table 4.8: CCD design layout and Measured Responses

Run	Coded Factors	EE (%)	Size (nm)	Drug Load (%)	Zeta Potential (mV)
1	(0,0)	19	142	2.3	-17
2	(0,0)	20	140	2.6	-14
3	(+α,0)	15	135	3.3	-16
4	(-α,0)	59	152	2.2	-18
5	(+1, +1)	21	143	3.9	-15
6	(0, -α)	16	139	2.1	-13
7	(0,0)	19	159	2.5	-19
8	(0,0)	17	145	2.1	-21
9	(-1, -1)	38	134	2.3	-20
10	(-1, +1)	22	178	1.4	-21
11	(0, +α)	30	156	3.8	-17
12	(+1, -1)	13	146	2.4	-17

4.2.1 Model Selection

The results obtained (measured responses) were fitted into increasing order of polynomial complexity of mathematical models. As shown in Table 4.9 model comparison statistics AIC (Akaike's Information Criteria) was lowest for the 2FI (2-factor interaction) model for EE, NP size and drug load. Mean model was sufficient to describe the zeta potential data.

Table 4.9: Model Comparison Statistics for Measured Responses

	Entrapment Efficiency (EE%)			Size (nm)			Drug Load (%)			Zeta Pot. (mV)
Model	Mean	Linear	2FI	Mean	Linear	2FI	Mean	Linear	2FI	Mean
PRESS	1.11E-06	5.38E-07	4.92E-08	2025	1728	681	7	5	3	90
-2 LL	-162.43	-178	-206	94	86	74	25	16	6	56
BIC	-160	-171	-196	96	93	84	28	23	16	59
AIC	-160	-169	-192	96	95	88	28	25	20	59

* PRESS: Predicted Residual Error Sum of Squares, BIC; Bayesian Information Criteria, AIC; Akaike's Information Criteria, -2LL; -2 Log Likelihood

For EE data the R^2 value of 0.973 for 2FI model (Table 4.10) indicates that it can explain 97.3% of variability around the mean. The adjusted R^2 value of 0.962 is highest for 2FI model and is reasonably close to predicted R^2 value of 0.947. High value of R^2 value, adequate precision > 10 and, CV < 15% confirm that selected model fitted the data very well.

Table 4.10: Fit Statistics for Measured Responses

Model	Entrapment Efficiency (EE%)			Size (nm)			Drug Load (%)			Zeta Potential (mV)
	Mean	**Linear**	**2FI**	**Mean**	**Linear**	**2FI**	**Mean**	**Linear**	**2FI**	**Mean**
R²	0.000	0.734	0.973	0.000	0.483	0.803	0.000	0.561	0.802	0.000
Adjusted R²	0.000	0.674	0.962	0.000	0.369	0.728	0.000	0.463	0.727	0.000
Predicted R²	-0.19	0.421	0.947	-0.19	-0.015	0.600	-0.19	0.062	0.424	-0.190
Adequate Precision	NA[1]	9.7	30.3	NA[1]	5.7	10.6	NA[1]	6.7	10.1	NA[1]
C.V. %	75.3	42.9	14.6	8.4	6.7	4.4	28.4	20.8	14.8	15.3

*Coefficient of determination (R^2) is a measure of total variability explained by the chosen model.

ANOVA (Fisher Test) was used to evaluate the significance of tested models. Best Fit model needs to be significant and Lack of Fit needs to be insignificant. Tests at 5% risk were considered significant (Table 4.11).

Table 4.11: Best Fit model

Response (Best Fit Model)		F-value	P-value	Remark
EE (2FI)	Model	94.29	< 0.0001	**significant**
	Lack of Fit	0.2759	0.9002	**not significant**
Size (2FI)	Model	10.84	0.0034	**significant**
	Lack of Fit	0.2651	0.9065	**not significant**
Drug Load (2FI)	Model	10.77	0.0035	**significant**
	Lack of Fit	5.72	0.0911	**not significant**
Zeta Potential (Mean)	Model	-	-	**significant**
	Lack of Fit	0.7024	0.6942	**not significant**

4.2.2 EE (%)

EE of the trial runs are given in the table 4.5. It ranged between 13 to 59%. The EE data was subjected to analysis of variance (ANOVA) for assessment of statistical significance (Table 4.8). Calculated model F value (94.29) was more than the tabulated F

value ($F_{0.01}$ = 7.59), implying that the model was significant at 1% α level. The residuals (quantitative difference between the observed and the predicted response) were randomly distributed around zero and there was no effect of experimental sequence on the residuals trend (Figure 4.5). The relative impact of factors on EE can be identified by comparing the factor coefficients in following equation for coded factors:

(EE)^-2.68 = 0.00039 + 0.00025 * A - 0.00016 * B - 0.00024 * AB   (Equation 4.1)

The positive coefficient of A suggested that the EE decreased with the increase of drug amount. It has been shown in other studies that drug: polymer ratio plays important role in the entrapment efficiency of particles. In the present study the amount of polymer was fixed, and the drug amount was varied to determine the influence of drug: polymer ratio on entrapment efficiency (EE). It is possible that the given amount of polymer was insufficient to encapsulate the increased amount of drug and resulted into lower EE. The results are in agreement with other studies (Cooper & Harirforoosh, 2014; Karataş et al., 2010). A negative sign for the coefficient of B suggested that the EE increased with increase of aqueous phase volume. Perturbation plot (Figure 4.6), Contour plot (Figures 4.7) and 3-D plots (Figures 4.8) demonstrate the similar pattern. The two factors interaction has a dominant effect on EE.
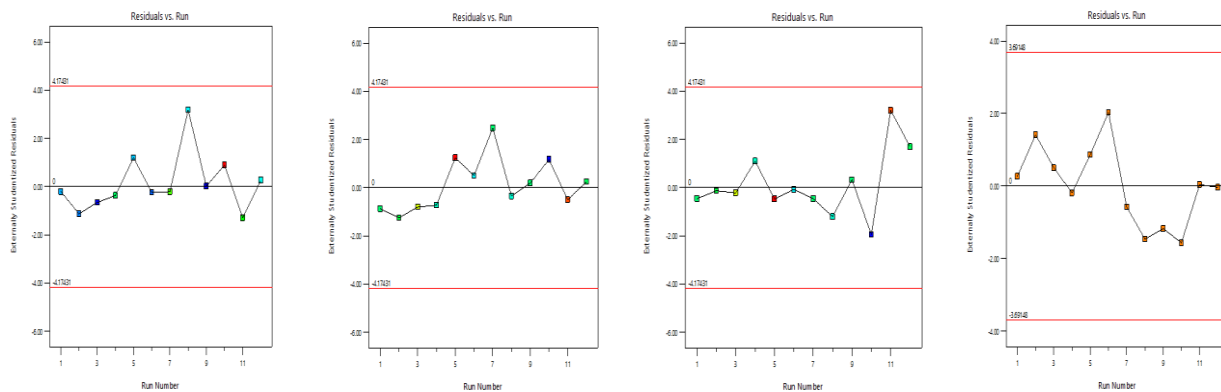
Figure 4. 5: Residual Vs Run Plots (a) EE (%), (b) Size, (c) Drug Load, (d) Zeta Potential
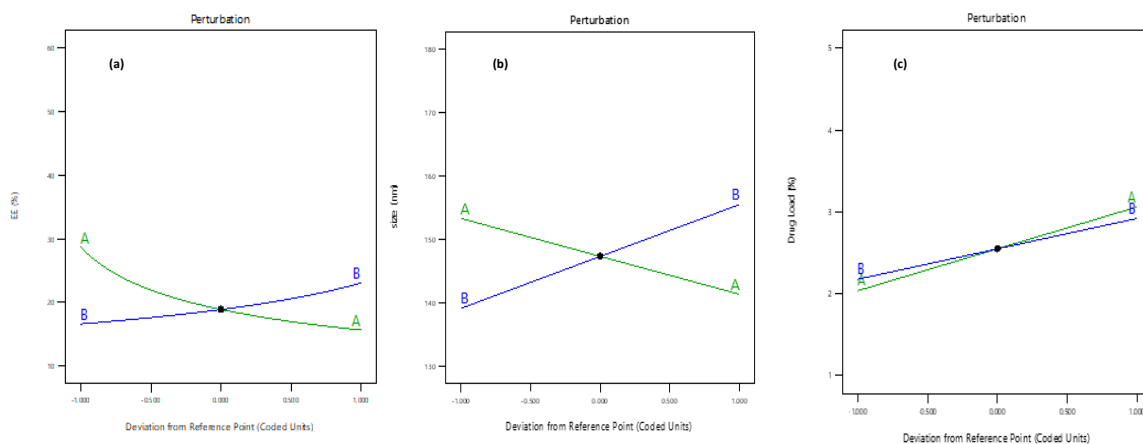
Figure 4. 6: Perturbation Plots (a) EE (%), (b) NP Size, (c) Drug Load
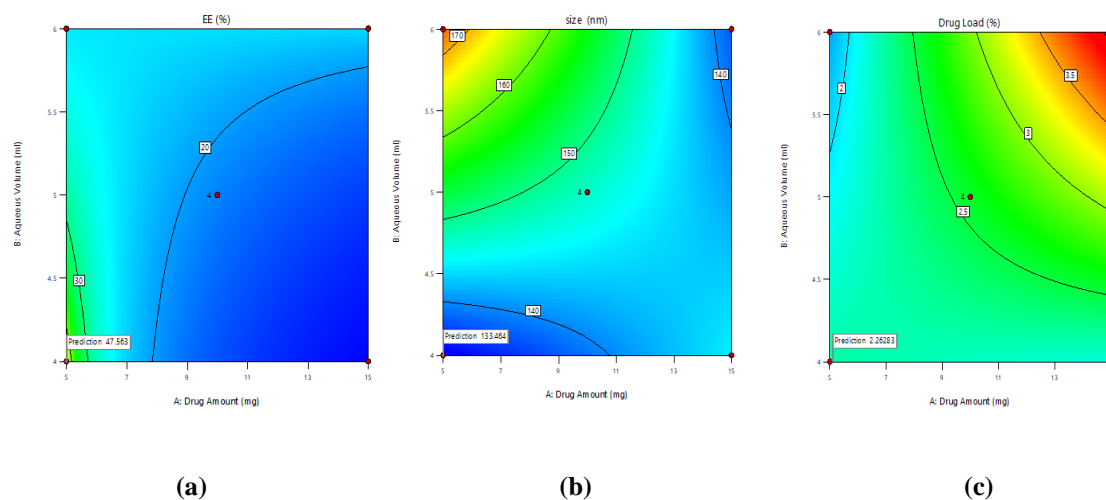
Figure 4. 7: Contour plots (a) EE (%), (b) Size, (c) Drug Load
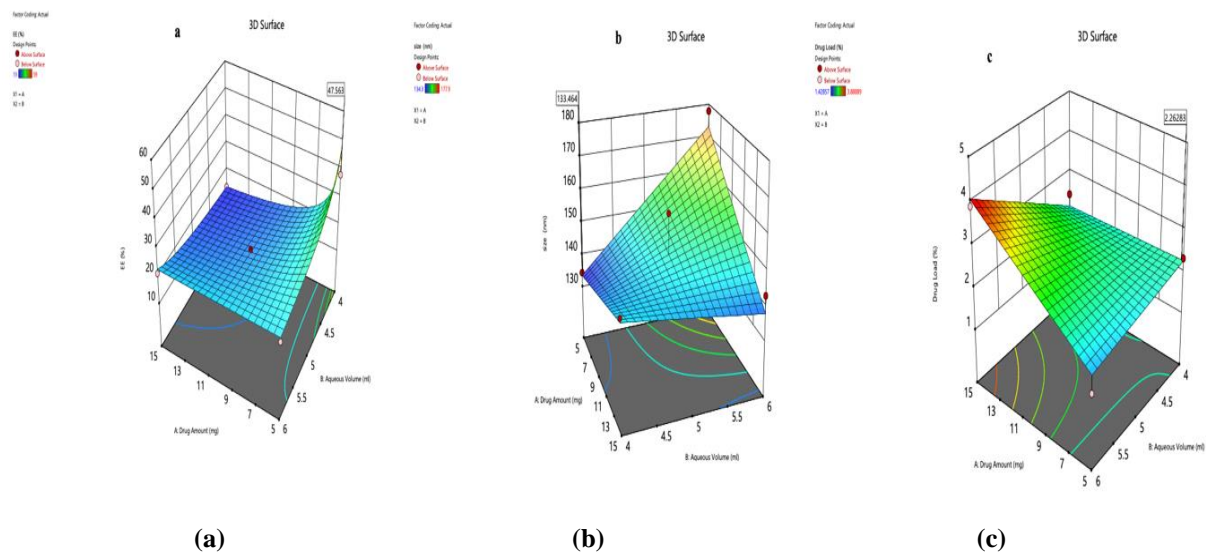
Figure 4. 8: 3-D plots (a) EE (%), (b) Size, (c) Drug Load

4.2.3 NP Size

All the particles obtained were in nano-size range (134nm to 178nm) (Figure 4.9).
Two-factor interaction (2FI) model best describes the NP size data (Table 4.6. and Table
4.7). Model F value (10.84) more than the tabulated F value (4.07), indicates that the model
is significant at 5% level (Table 4.8).

Results

		Size (d.nm):	% Intensity	Width (d.nm):
Z-Average (d.nm): 148.9	Peak 1:	161.8	100.0	47.05
PdI: 0.077	Peak 2:	0.000	0.0	0.000
Intercept: 0.950	Peak 3:	0.000	0.0	0.000
Result quality : Good				
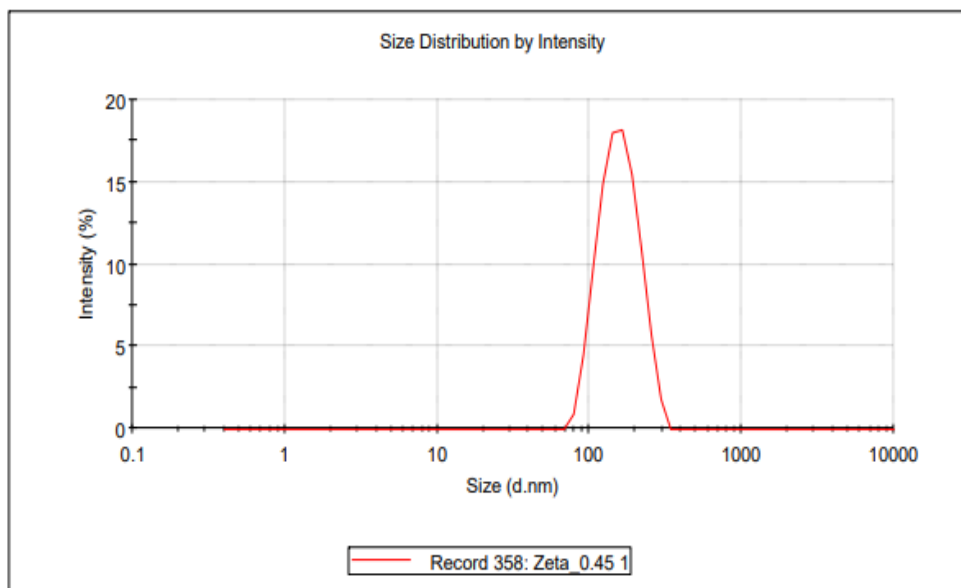
Figure 4. 9: NP Size using Malvern Zetasizer NanoZS

The relative impact of both factors on NP size can be determined by comparing the factor coefficients in following equation (Equation 4.2) for coded factors:

Size =147.32 - 5.98 * A + 8.19 * B - 11.65 * AB   (Equation 4.2)

The negative coefficient of A suggested that NP size decreased with the increase of drug amount. In contrast to reported studies (Zhang et al., 2006) the particle size decreases with increase of drug amount. Somehow, higher drug amount in organic phase improved the diffusion of solvent into aqueous phase and led to smaller particle size. A positive coefficient for the B suggested that NP size increased with the increase of aqueous phase volume. Studies have shown that during nanoprecipitation process the solvent/non-solvent (S/NS) volume ratio influences the particle size. Particle size was decreased with increasing the S/NS volume ratio (Bilati et al., 2005; Zhang et al., 2006). In our study the volume of organic phase (solvent) was kept at constant (2mL) and the volume of aqueous phase (nonsolvent) was increased (4ml to 6ml to) to decrease the S/NS ratio (0.25 to 0.17) that resulted into increase in particle size. In other word, the size increased with increase of aqueous phase volume. It was suggested that an increase in total volume of system reduces the net shear stress because of constant external energy input, resulting into bigger particle size (Song et al., 2008). Perturbation plot (Figure 4.6), Contour plot (Figures 4.7)

and 3-D plots (Figures 4.8) show a similar trend. Further, as reflected from the magnitude of coefficients two factors interaction shows much dominant negative effect on size.

4.2.4 Drug Load

2FI model is best suited to drug load data as well. The ANOVA results indicate the significance of the given model at 5% significance level as ($F_{cal} > F_{0.05}$). Model F value (10.77) more than the tabulated F value (4.07). The equation for coded factors (Equation 4.3) shows that both factors (the drug amount, the aqueous phase volume) and their interaction have a positive impact (Figures 4.6) on drug load. The volume of the aqueous phase is least controlling, and the interaction of two factors has a more pronounced effect on drug load.

Drug Load = 2.57 + 0.51 * A + 0.38 * B + 0.59 * AB   (Equation 4.3)

4.2.5 Zeta Potential

Zeta potential was insensitive to change in drug amount or aqueous phase volume. It could be explained by the fact that the type and concentration of polymer and stabilizer were kept constants throughout the experiment (Figure 4.10).

Results

	Mean (mV)	Area (%)	Width (mV)
Zeta Potential (mV): -20.1	Peak 1: -18.9	100.0	6.93
Zeta Deviation (mV): 19.2	Peak 2: 0.00	0.0	0.00
Conductivity (mS/cm): 0.0294	Peak 3: 0.00	0.0	0.00
Result quality : Good			
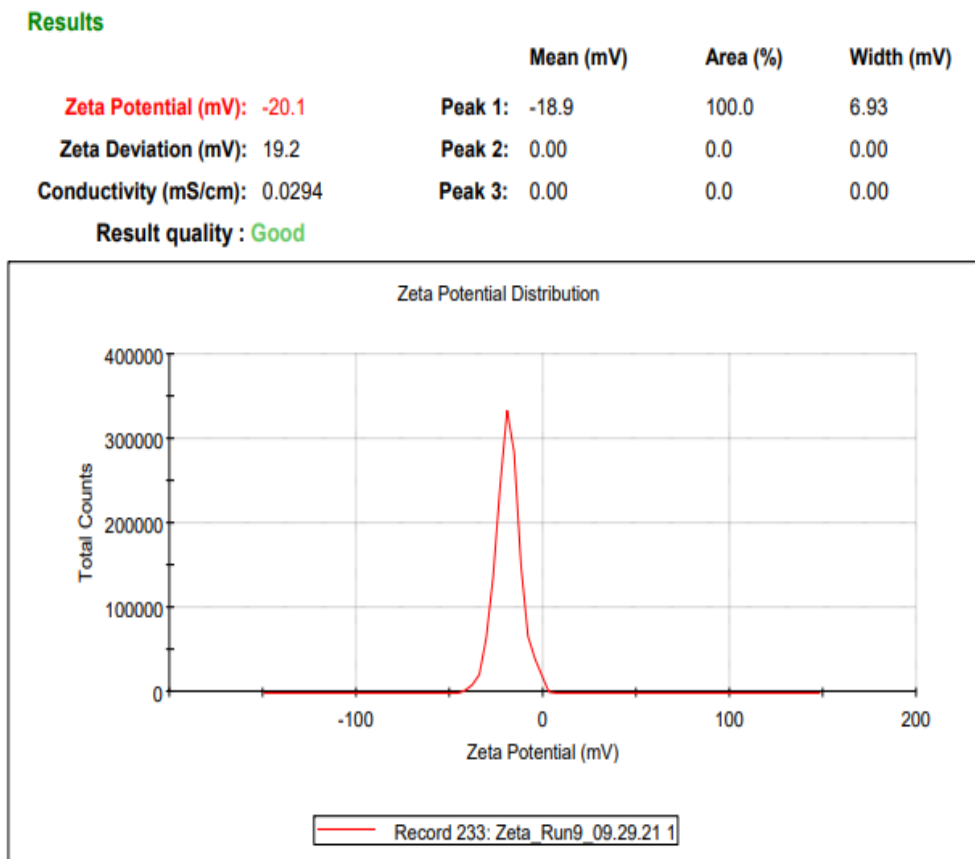
Figure 4. 10: NP Zeta Potential using Malvern Zetasizer NanoZS

4.2.6 Mathematical (numerical) Optimization and overall Desirability Function

Graphical optimization is useful in case of single response. However, mathematical optimization is preferred in cases of multiple, at times opposing, responses (Derringer & Suich, 1980; Jeong & Kim, 2009). For this formulation design we wanted to achieve NPs with maximum EE, hence the optimization goal for EE was set to "maximize" it. As all the

prepared NPs were in nano size range and zeta potential follows mean model, the goals for size and zeta potential were set to "in range". Maximum relative importance was set for EE. The software predicts a list of optimization solutions with associated desirability with each solution (Table 4.12). The optimized formulation with highest desirability value of 0.961 (Figures 4.11) was achieved using 5 mg drug amount and 4 ml aqueous phase. The resulting NPs showed the best responses of EE of 41.2 % (predicted 47.6 %), size of 124 nm (predicted 133 nm), drug load of 2.6 % (predicted 2.3 %) and zeta potential of – 15 mV (predicted – 17 mV) (Table 4.13).

Table 4.12: Numerical Optimization Solutions

Run No.	Drug Amount (mg)	Aqueous Volume (ml)	EE (%)	NP Size (nm)	Drug Load (%)	Zeta Potential (mV)	Desirability	
1	5	4	47.6	133	2.3	-17.2	0.961	Selected
2	5	4.7	31.2	148	2.1	-17.2	0.903	
3	5	4.8	30.5	149	2.1	-17.2	0.898	
4	5	5.9	24.1	170	1.8	-17.2	0.814	
5	5	6	23.6	173	1.8	-17.2	0.803	
6	5	6	23.6	173	1.8	-17.2	0.802	
7	10.6	6	23	153	3.1	-17.2	0.788	
8	11.2	6	23	151	3.2	-17.2	0.787	
9	12.3	6	22.9	148	3.4	-17.2	0.784	

Table 4.13: Optimized Formulation

Response	Predicted Mean	Observed Mean	Std Dev.	% Accuracy
EE (%)	47.6	41.2	13.3	87
NP Size (nm)	133	124	6.0	93
Drug Load (%)	2.3	2.6	0.4	113
Zeta Potential (mV)	-17	-15	3.0	87
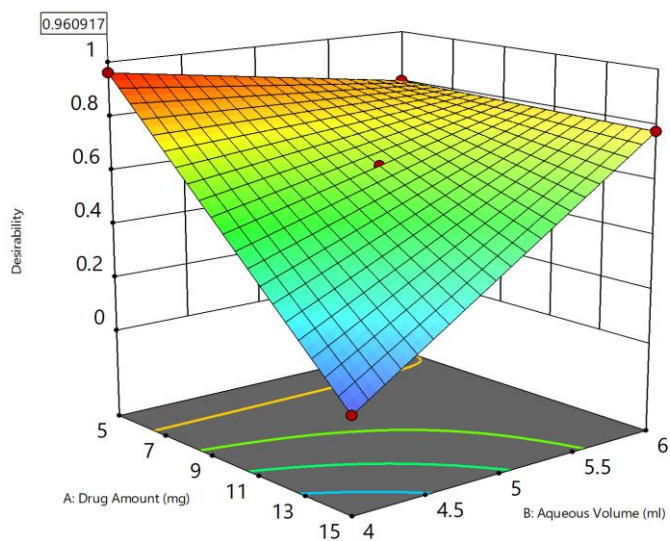
Figure 4. 11: Desirability Plot

4.2.7 Preparation of NPs using other PLGA polymer grades

Based on above optimization for PLGA (50:50) polymer grade (Table 4.11) two more polymer grades; PLGA (75:25) and Resomer RG 503H and were used to prepare NPs. Their physicochemical characterization is presented in Table 4.14.

Table 4.14: Physicochemical properties of different PLGA NPs

PLGA Type	Size	PdI	Zeta	EE%
PLGA (75:25)	133 ± 9.12	0.095 ± 0.01	-12.8 ± 3.54	38.3 ± 2.52
Resomer RG 503H	136 ± 13.21	0.060 ± 0.02	-53.6 ± 2.11	49 ± 7.55

4.3 *In vitro* drug release study

For poorly soluble drugs the absorption is dissolution-rate limited. Hence, proper choice of dissolution medium becomes very critical in developing a robust and biorelevant *in vitro* drug release method for such drugs. Closed-loop type flow through apparatus (USP apparatus 4) was used to test *in vitro* release from PLGA NPs.

4.3.1 Solubility of AC1LPSZG in Different pH Buffers

AC1LPSZG solubility was tested in five different pH buffers (1.2, 4.5, 5.5, 6.8 and 7.4). Results show pH-dependent solubility with high solubility at lower pH (Figure 4.12). The highest solubility was obtained at pH 1.2 as Strongest pKa (Base) is 4.7 ± 0.1 (*Strongest pKa (Acid): 11.0 ± 0.5).
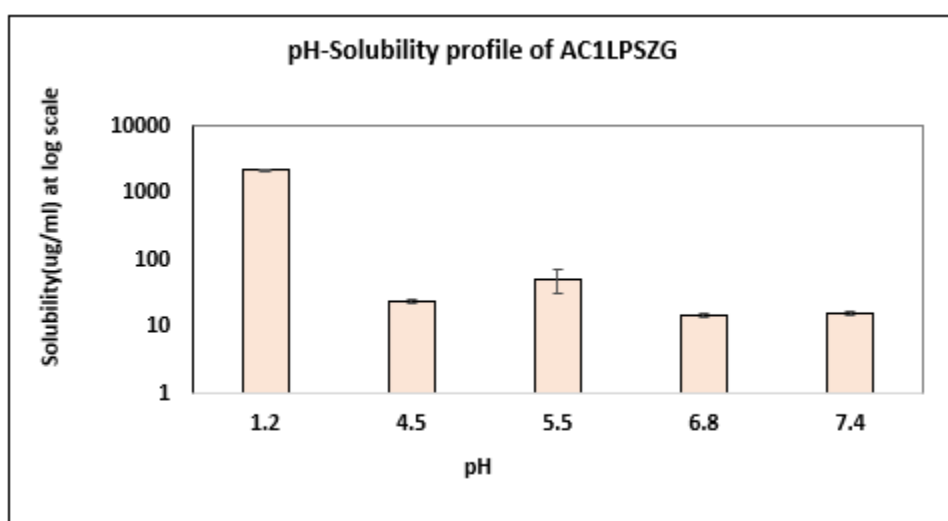
Figure 4. 12: Drug Solubility in Different pH Buffers

4.3.2 *In Vitro* Drug Release from PLGA-AC1LPSZG-NPs at pH 1.2 and 6.8

In Vitro Drug Release from PLGA-AC1LPSZG-NPs was studied at pH 1.2 and 6.8. Biphasic release pattern was obtained (Figure 4.13). Initial rapid (burst) release was obtained from drug molecules present near surface. Afterwards, slow/sustained release was

obtained probably due to drug diffusion through polymer matrix and/or polymer hydrolysis.
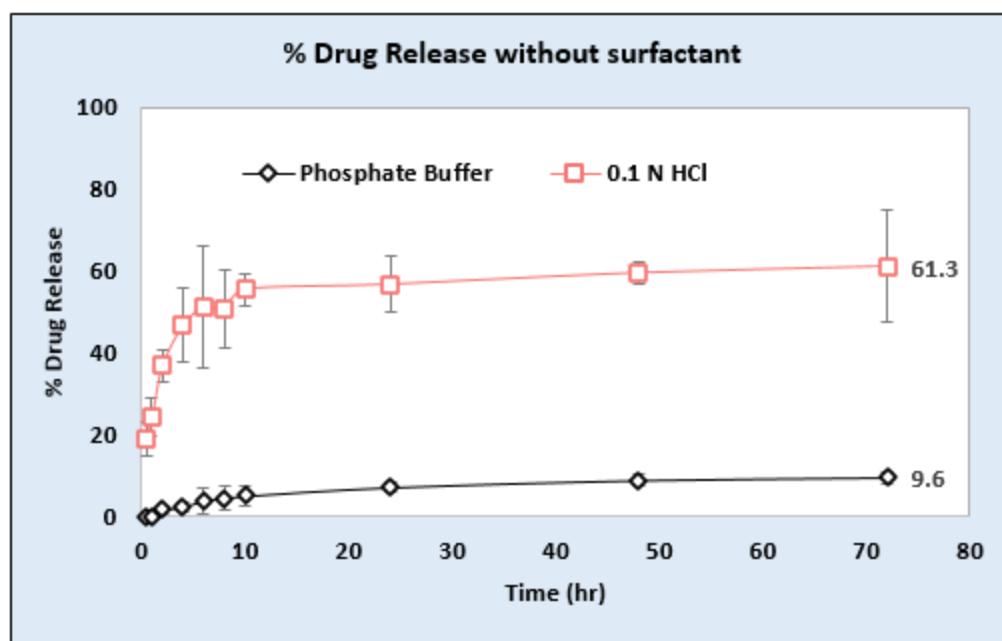
Figure 4. 13: *In Vitro* **Drug Release at pH 1.2 and 6.8**

The dissolution concentrations were very low (approximately 10 % drug was released at pH 6.8 over 72 hours), hence, LC-MS/MS method was used to analyze the dissolution samples after performing liquid-liquid extraction method (Figure 4.14).
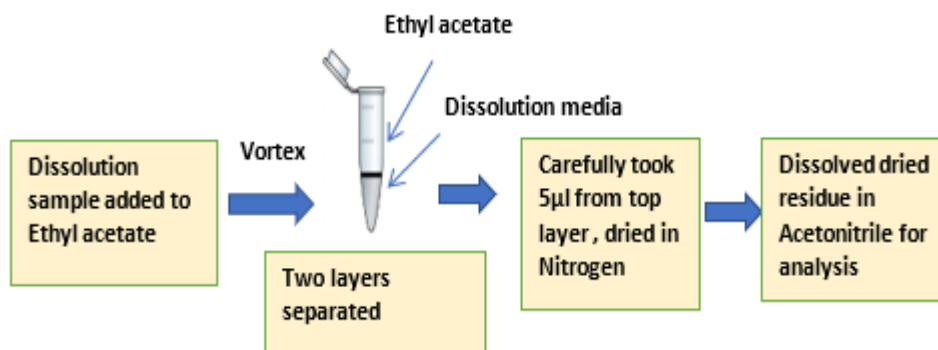
Figure 4. 14: Sample preparation for LCMS analysis by Liquid-liquid extraction

4.3.3 Approaches used to improve Sink Conditions

Absence of sink conditions may lead to unpredictable release kinetics and suppressed release profiles. In this study the effect of cosolvent (25% Ethanol) and different surfactants on the sink conditions and *in vitro* drug release has been demonstrated. Use of 25% ethanol in dissolution medium does not improve *in vitro* drug release significantly (Figure 4.15).
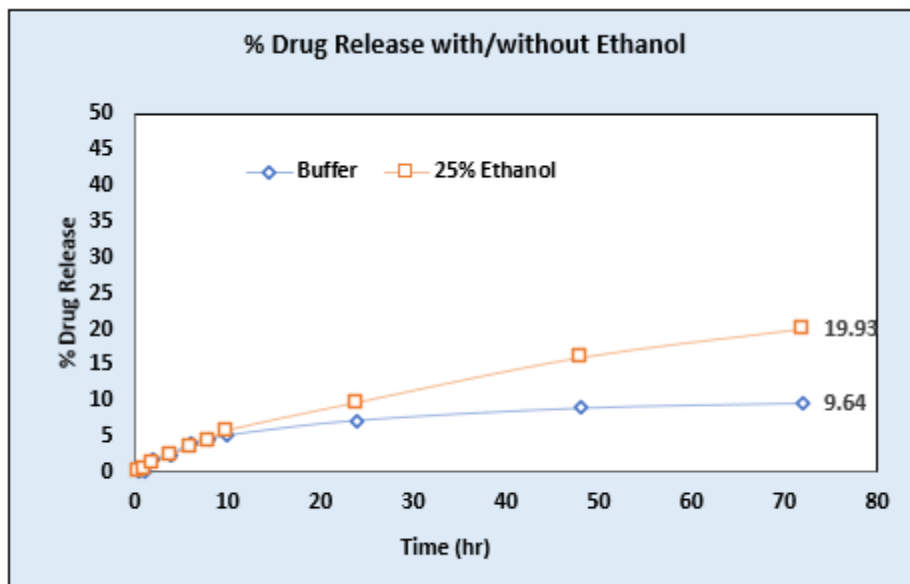
Figure 4. 15: *In Vitro* **Drug Release using Cosolvent (25% Ethanol)**

Three different surfactant types: anionic (sodium lauryl sulfate or SLS), non-ionic (Tween 80) and cationic (cetyltrimethylammonium bromide or CTAB) were tested. Figure 4.16 demonstrates the increase in drug solubility at two different levels (0.5% and 1%) of surfactants SLS and Tween 80. Figure 4.17 shows linear increase in drug solubility at four different levels (0.5%, 1%, 1.5% and 2 %) of positive surfactant CTAB. The order of solubility enhancement using surfactants was SLS > Tween80 > CTAB. Figure 4.18 demonstrates the drug stability in SLS and Tween 80. Figure 4.19 shows drug stability in CTAB. Drug was stable with Tween 80 and CTAB. Instability with SLS might be explained by ionic interaction between the cationic drug and anionic surfactant.

To achieve the sink conditions the volume of dissolution medium should be **at least three to ten times** the saturation volume. Relative sink is calculated as the ratio of Cs and Cd. Where, Cs is saturation solubility of drug and Cd is drug concentration after complete dissolution of NPs in 100 mL dissolution medium. SLS and Tween 80 were not able to achieve sink conditions at the tested concentrations. As CTAB shows significant improvement in sink conditions (Table 4.15) hence it was tested for further *in vitro* drug release studies (Figure 4.20). Drug release increased as the concentration of CTAB was increased from 0.5% (approximately 15 % drug release) to 2% (approximately 31 % drug release). The results of univariate ANOVA (Table 4.16) followed by **Student's t test (two-sided)** showed % drug release was significantly different at different levels of CTAB (P< 0.05).
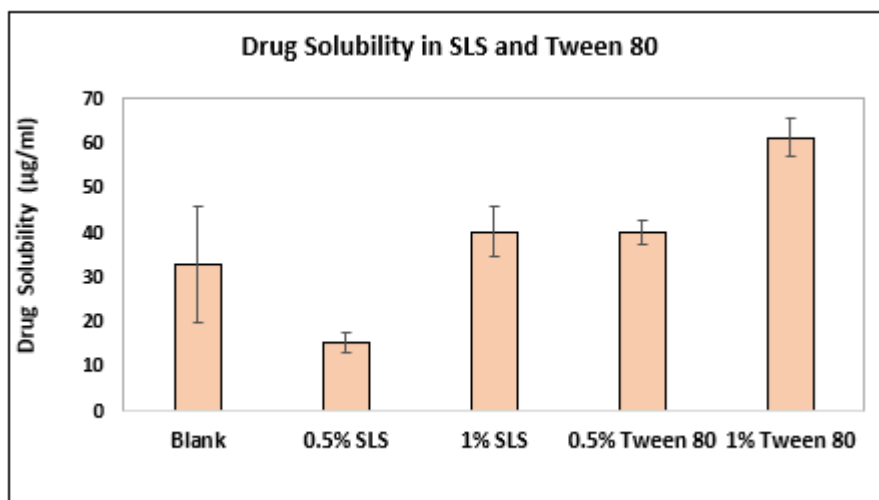
Figure 4. 16: Effect of SLS and Tween 80 on Drug Solubility
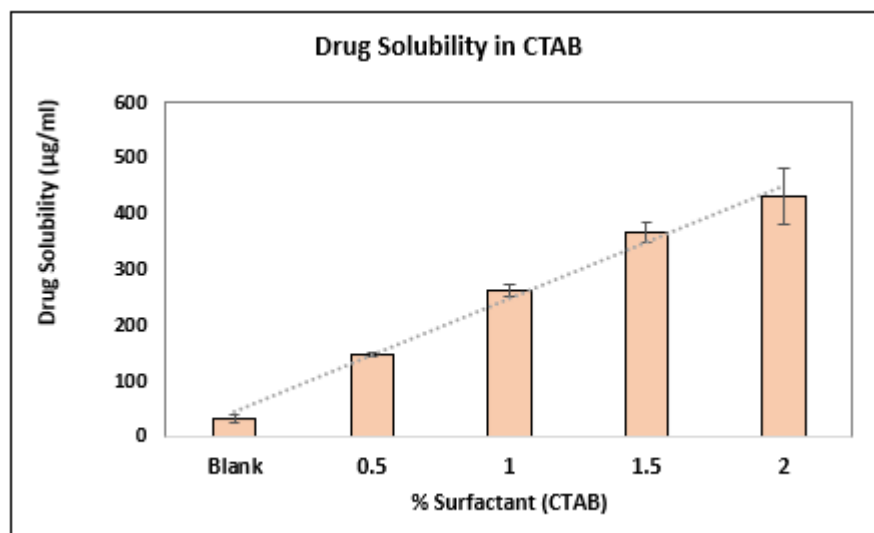
Figure 4. 17: Effect of CTAB on Drug Solubility
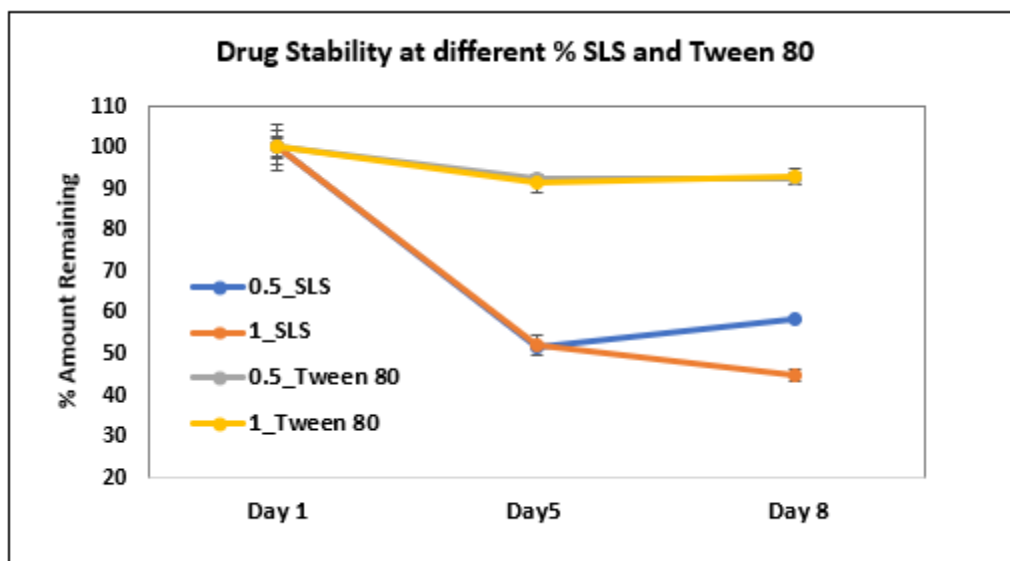
Figure 4. 18: Effect of SLS and Tween 80 on Drug Stability
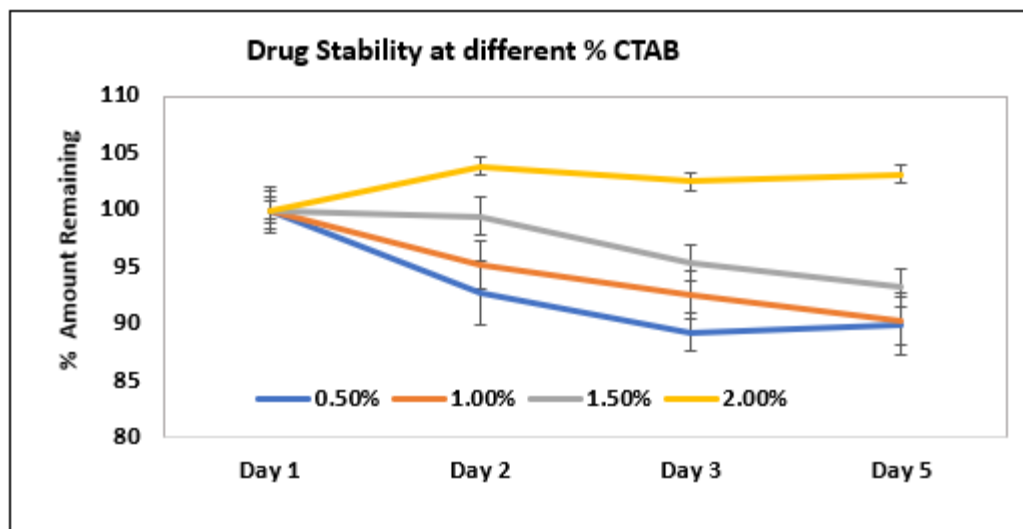
Figure 4. 19: Effect of CTAB on Drug Stability

Table 4.15: Relative Sink conditions at different Surfactant Concentrations

Surfactant	Solubility	Rel. Sink (Cs/Cd)
Blank	33	1.1
0.5_SLS	15	0.5
1_SLS	40	1.3
0.5_Tween 80	40	1.3
1_Tween 80	61	2.0
0.5_CTAB	147	4.9
1_CTAB	264	8.8
1.5_CTAB	366	12.2
2_CTAB	432	14.4
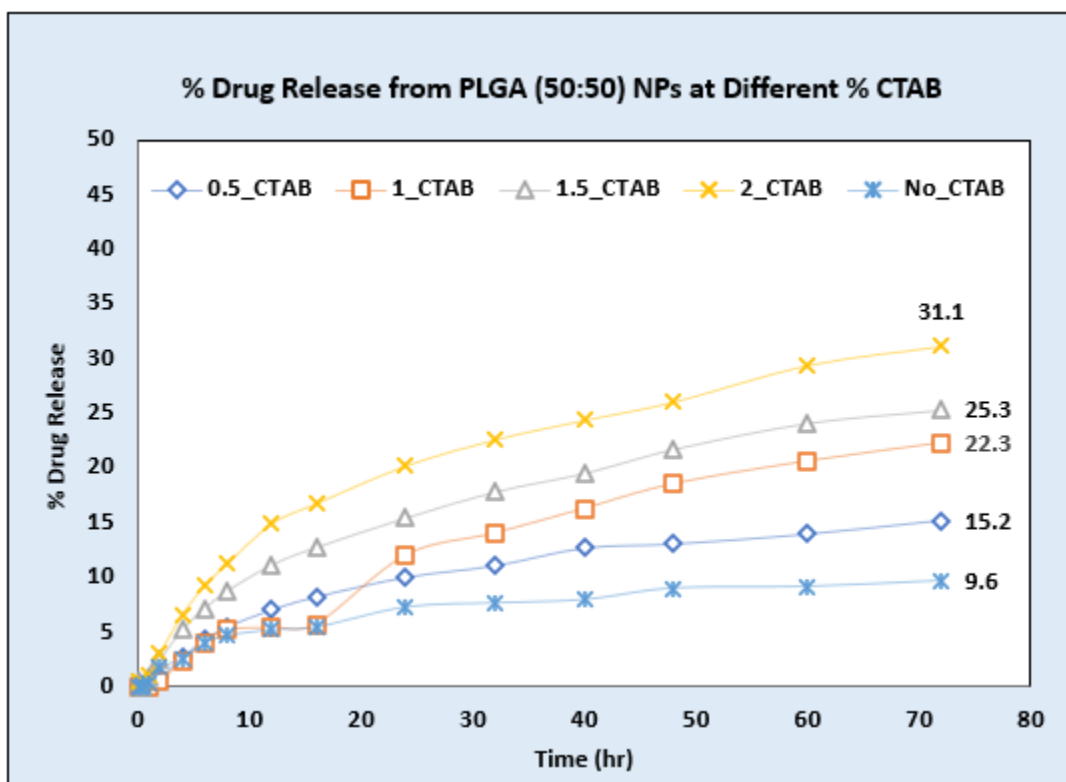
Figure 4. 20: Drug Release from PLGA (50:50) NPs at Different % CTAB (pH6.8)

Table 4.16: Comparisons for different Surfactant-pairs

Surfactant Pair		p-Value (significance) (DE)	p-Value (significance) (AUC)
1%	0%	0.0066*	0.0145*
1%	0.5%	0.2932	0.3749
1%	1.5%	0.4399	0.5052
1%	2%	0.0095*	0.0207*
1.5%	0%	0.0025*	0.0058*
1.5%	0.5%	0.0952	0.1466
1.5%	2%	0.0265*	0.0528
2%	0%	0.0002*	0.0005*
2%	0.5%	0.0027*	0.0065*
0.5%	0%	0.0310*	0.057

*$p < 0.05$ for DE; Dissolution efficiency, AUC; Area Under Dissolution Curve

4.3.4 Discriminatory *In Vitro* Drug Release Method

Drug Release from NPs prepared using different PLGA polymer grades was tested at different levels of CTAB (0.5%, 1%, 1.5%, and 2%). NPs prepared with PLGA (75:25) showed slower release than NPs prepared with PLGA (50:50). The results are in agreement with the literature suggesting that higher the L:G ratio slower the rates of degradation

(Makadia & Siegel, 2011). NPs prepared using Resomer RG 503H showed fastest release due to its hydrophilic nature. The discrimination among the release profiles was improved with the increase of surfactant concentration in dissolution medium from 0.5 % to 2 % (Figure 4.21). Student's t test (two-sided) shows that release profiles from all polymer grade NPs were different from drug release from drug suspension (Table 4.17) JMP software was used for statistical analyses (model- independent approach).

Table 4.17: Model-independent approach for release profile comparison at 2% CTAB using student's t test (two-sided)

Parameter	Mean Dissolution Time (MDT)	Dissolution Efficiency (DE)	Area Under Dissolution Curve (AUC)	Mean Residence Time (MRT)	Model-Independent Parameters	
Polymer Pair	p-Value (significance)	p-Value (significance)	p-Value (significance)	p-Value (significance)	F2- value (Similarity factor)	F1- value (Difference factor)
Suspension (50:50)	0.3815	0.0014*	0.0011*	0.0013*	52.5	54.4
Suspension (75:25)	0.5408	0.0112*	0.0081*	0.0123*	60.3	46.3
Suspension Reso	0.1361	0.0001*	<.0001*	<.0001*	43.2	64.3
(50:50) (75:25)	0.7813	0.1664	0.1868	0.1513	74.2	19.9
(50:50) Reso	0.4856	0.0518	0.0494*	0.0193*	62.6	28.5
Reso (75:25)	0.3384	0.0052*	0.0056*	0.0020*	53.9	52.4

*$p < 0.05$

% Drug Release (0.5% CTAB) (a)

% Drug Release (1% CTAB) (b)

% Drug Release (1.5% CTAB) (c)
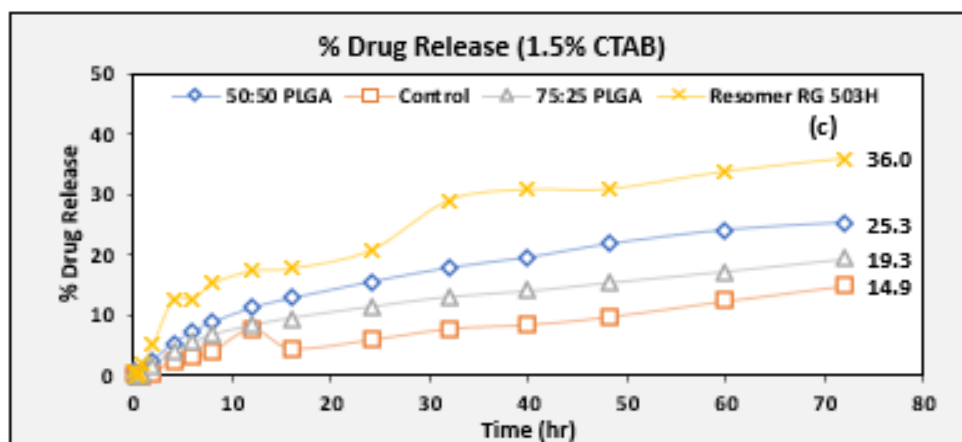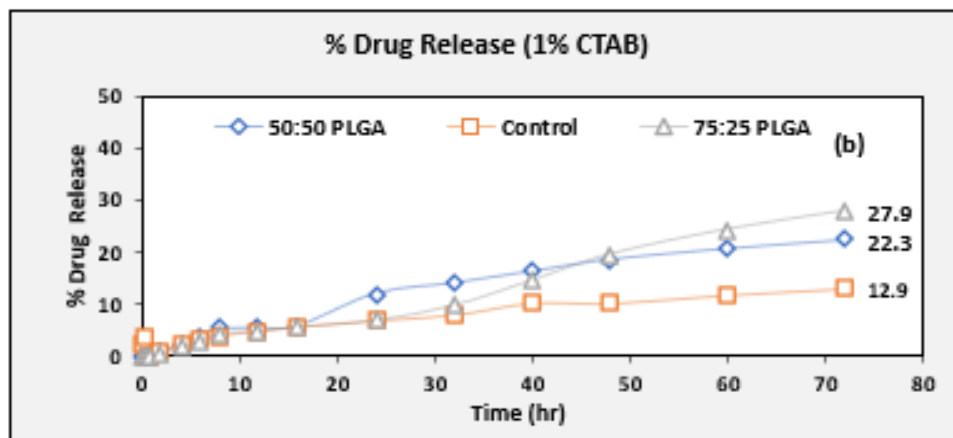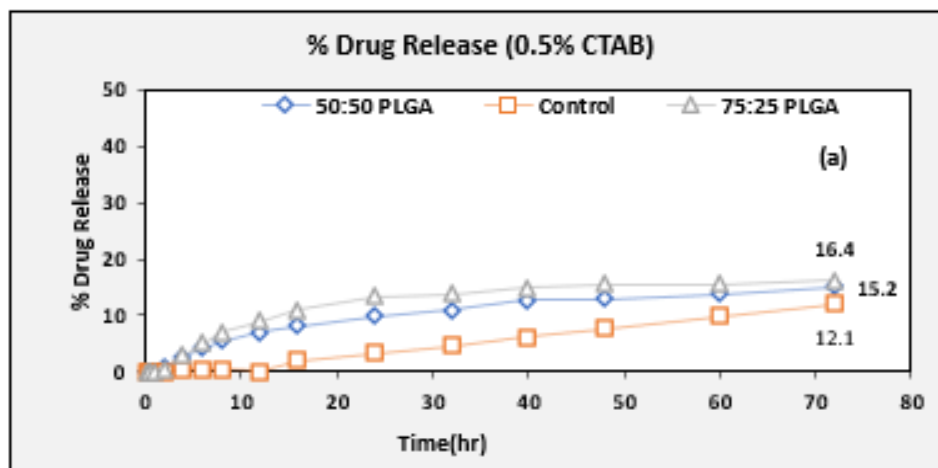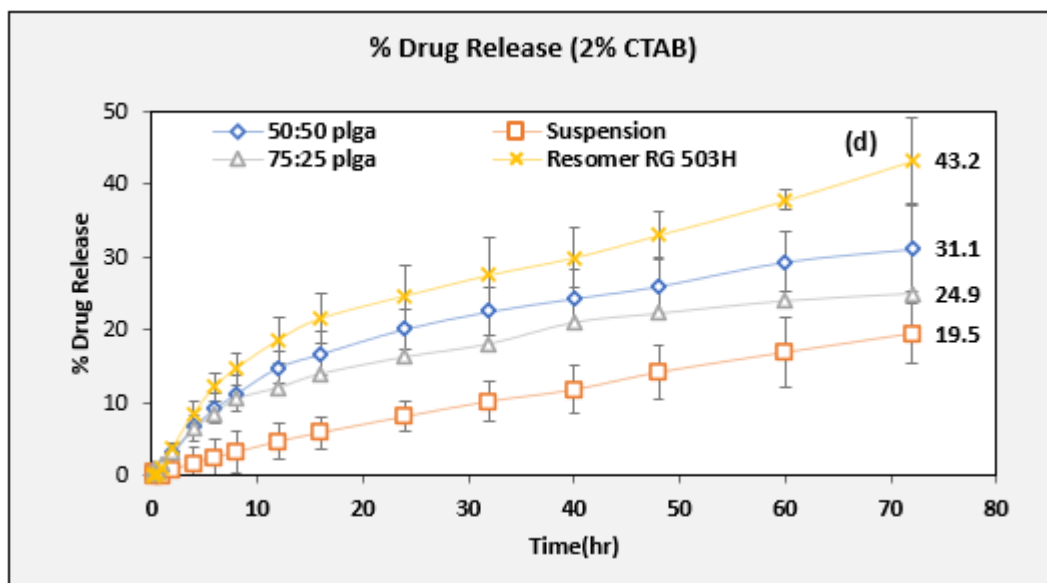
Figure 4. 21: Drug Release from different NPs (a) 0.5%, (a) 1%, (a) 1.5%, (a) 2%, CTAB

4.3.5 Fitting of different models for Release Kinetics

Various kinetic models were fitted for drug release from all three types of PLGA NPs. DDSolver software was used for kinetic modelling. Weibull model was found to best fit the dissolution data with highest values of R^2 and MSC and smallest values of AIC (Table 4.18).

Table 4.18: Kinetic models for NPs prepared using different PLGA grades

Parameter/ Model	PLGA (50:50) NPs				PLGA (75:25) NPs				Resomer RG 503H NPs			
	R^2_adj	AIC	MSE	MSC	R^2_adj	AIC	MSE	MSC	R^2_adj	AIC	MSE	MSC
Zero-order	0.76	97.31	27.95	1.28	0.71	94.12	22.6	1.03	0.8	103.3	42.85	1.4
First-order	0.83	91.44	20.03	1.65	0.77	90.2	17.77	1.28	0.87	97.22	28.13	1.78
Hixson-Crowell	0.81	93.49	22.47	3.49	0.75	91.54	19.28	1.2	0.85	99.26	32.5	1.65
Quadratic	0.95	73.39	6.32	2.78	0.92	70.41	6.08	2.52	0.94	86.72	12.87	2.44
Higuchi	0.97	65.3	3.8	3.28	0.97	58.33	2.41	3.27	0.96	79.27	9.03	2.9
Korsmeyer-Peppas	0.98	62	2.93	3.49	0.97	56.79	2.12	3.37	0.97	77.8	7.23	2.99
Weibull	0.99	35.22	0.59	5.16	0.99	42.84	0.79	4.24	0.98	54	3.96	4.48

*R^2; coefficient of determination, MSC; Model Selection Criteria, AIC; Akaike information criterion, MSE; Mean Squared Error

Weibull Model Equation can be represented by Equation 4.4. Visual fit is shown in Figure 4.22. Table 4.19 represents the model-dependent approach to compare release profiles using student's t test (two-sided).

$$F=100*\{1-Exp[-((t-Ti)^{\wedge}\beta)/\alpha]\}$$

(Equation 4.4)

Where, F = fraction dissolved, t = time, Ti = dissolution lag time, **α = time constant, β = shape parameter** (slope of the best-fit line through the data points on a Weibull plot). **β =1 indicates the curve as exponential**, β > 1 indicates S-shaped curve

with upward curvature, followed by a turning point, $\beta < 1$ indicates curve with a steeper initial slope than is consistent with the exponential. **$\beta \leq 0.75$ indicates Fickian diffusion.** $0.75 < \beta < 1$ a combined mechanism (Fickian diffusion and Case II transport). For values of β higher than 1, the drug transport follows a complex release mechanism.

Table 4.19: Model-dependent approach to compare release profiles using student's t test (two-sided)

Model-Dependent Parameters	Time constant (α)	Shape parameter (β)
Polymer Pair	p-value (significance)	p-value (significance)
Suspension and (50:50)	0.0004*	0.0539
Suspension and (75:25)	0.0005*	0.0344*
Suspension and Reso	0.0005*	0.0999
(50:50) and (75:25)	0.9242	0.7806
(50:50) and Reso	0.8508	0.7018
Reso and (75:25)	0.9258	0.5127

*$p < 0.05$, (50:50); PLGA (50:50) and (75:25), PLGA (75:25)

(a) Mean *(PLGA 50:50)_Zero Order

(b) Mean *(PLGA 50:50)_First Order

(c) Mean *PLGA 50:50)_Hixson-Crowell

(d) Mean *(PLGA 50:50)_Quadratic
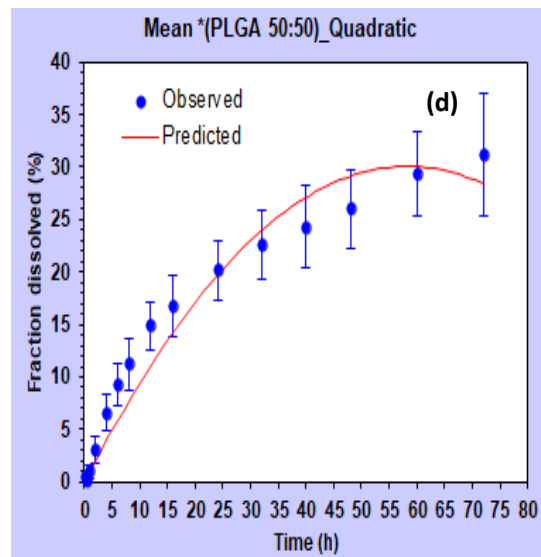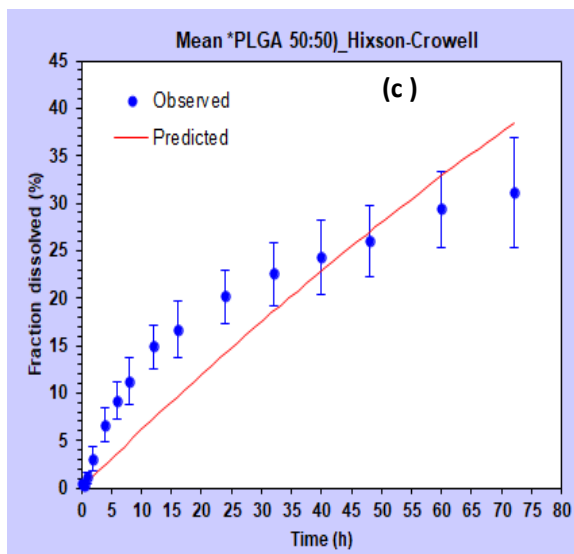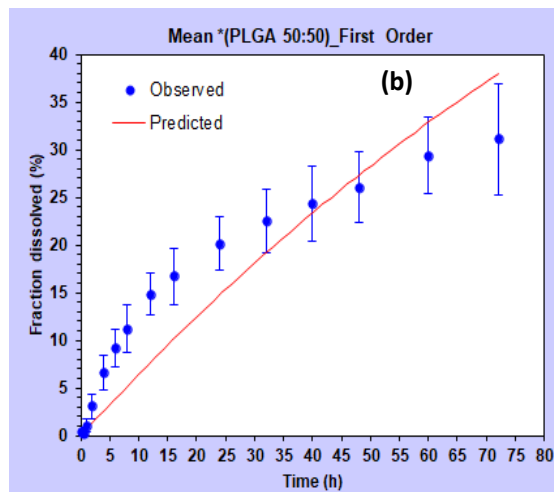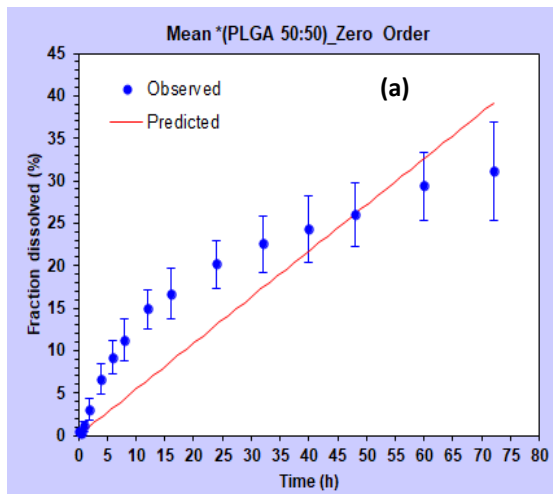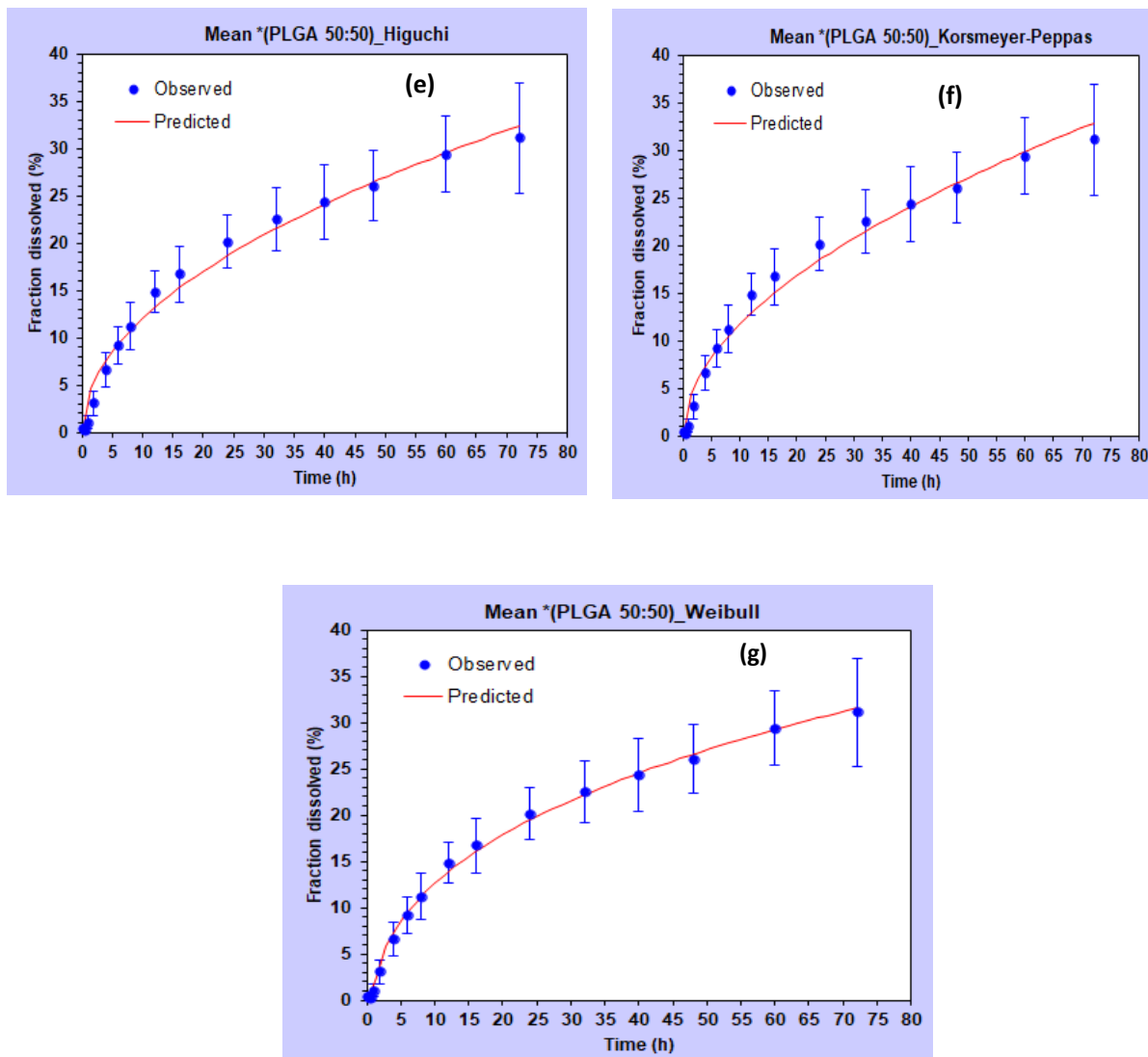
Figure 4. 22: Various kinetic models to fit dissolution data from PLGA (50:50) NPs; (a) Zero order, (b) First order, (c) Hixon Crowell, (d) Quadratic, (e) Higuchi, (f) Korshmeyer-Peppas, (g) Weibull

4.4 <u>Differential Scanning Calorimetry (DSC)</u>

No visible peak of drug was seen in in DSC thermogram (Figure 4.23) at its melting point (MP) (167.84°C) indicating amorphous dispersion of drug in NPs.
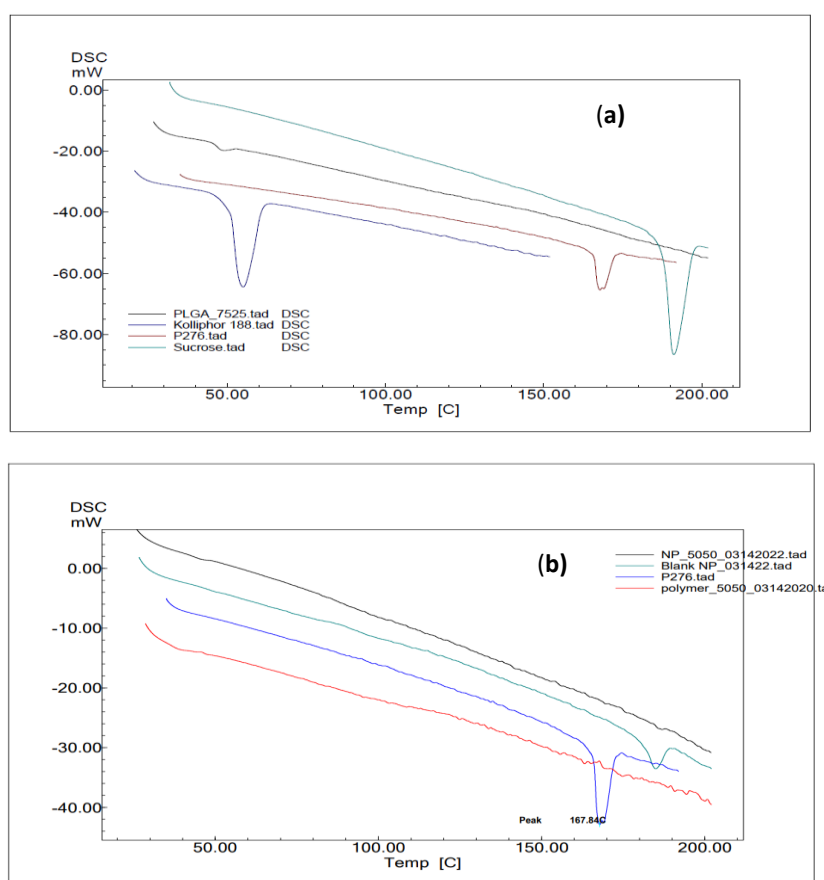
Figure 4. 23: (DSC) Thermogram using Shimadzu DSC-60A at 10°C per min and N2 atmosphere. (a) Overlay with individual components, (b) Overlay with PLGA NPs

4.5 <u>Accelerated Stability Studies</u>

Accelerated stability studies of lyophilized NPs were conducted at room temperature (RT) and at 4°C using NP size, zeta potential, and % EE as stability parameters. The results are reported in Table 4.20. It was observed that NPs were more stable at 4°C than at RT. There was a slight increase in average particle size, however it was still approximate 200 nm. It can be concluded that, prepared NPs were sufficiently stable for a total period of 2 months.

Table 4.20: Stability study of NPs at RT and 4°C

Stability Parameter	NP Size (nm)					
Polymer Grade	**PLGA (50:50)**		**PLGA (75:25)**		**Resomer**	
	4°C	RT	4°C	RT	4°C	RT
Day 1	145.9	145.9	137.9	137.9	139.8	139.8
Day 60	167.8	214	215.1	181.5	212.7	203.2
Stability Parameter	**Zeta Pot. (mV)**					
Polymer Grade	**PLGA (50:50)**		**PLGA (75:25)**		**Resomer**	
	4°C	RT	4°C	RT	4°C	RT
Day 1	-25	-25	-9.56	-9.56	-50.4	-50.4
Day 60	-25.5	-21.6	-7.06	-10.7	-43.9	-42.2
Stability Parameter	**%EE**					
Polymer Grade	**PLGA (50:50)**		**PLGA (75:25)**		**Resomer**	
	4°C	RT	4°C	RT	4°C	RT
Day 1	38.9	38.9	38.1	38.1	55.6	55.6
Day 60	37.4	35.9	37.2	32.8	53.5	50.1

4.6 *In Vivo* Studies

Figure 4.28 shows the plasma concentration versus time profiles of AC1LPSZG after intravenous administration of optimized cosolvent formulation in SD rats. Non-compartmental analysis (NCA) and two-compartmental model were applied to obtained PK profile of AC1LPSZG using Phoenix WinNonlin® 8.0 software (Table 4.21).
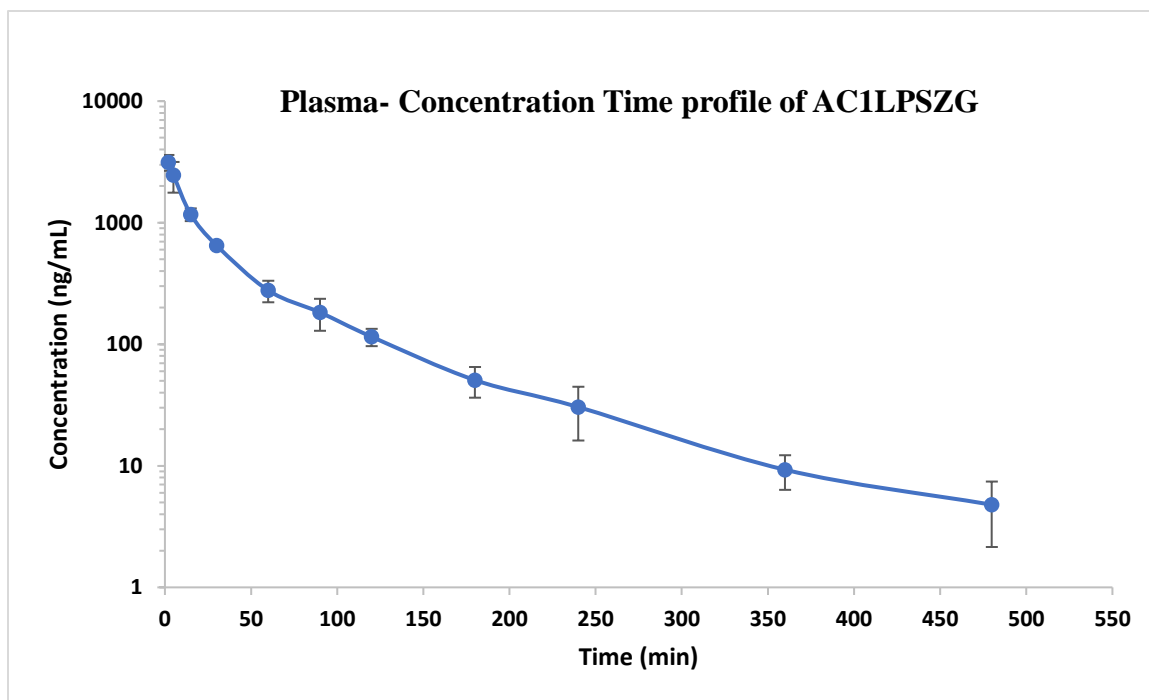
Figure 4. 24: Plasma-Concentration Time profile for AC1LPSZG in plasma after a single intravenous administration of cosolvent at 5 mg/kg to rats (n = 4)

Table 4.21: Pharmacokinetics parameters of AC1LPSZG in plasma after a single intravenous administration of cosolvent at 5 mg/kg to rats (n = 4)

PK Parameters	Non-Compartment Model	Two-Compartment Model
CL_1(ml/min/kg)	59.9 ± 8.8	63.5 ± 8.6
CL_2(ml/min/kg)	-	27.6 ± 10.0
Vss_obs (ml/kg)	3152.4 ± 430.0	3624.5 ± 379.3
V1 (ml/kg)	-	1703.3 ± 523.0
V2(ml/kg)	-	1921.2 ± 150.0
AUC∞ (min*ng/ml)	16967 ± 2351	15981 ± 2166
$t_{1/2}$ (min)	89.9 ± 35.7	-
$t_{1/2\ \alpha}$	-	12 ± 4.1
$t_{1/2\ \beta}$	-	80 ± 10.7
MRT∞ (min)	52.8 ± 3.4	57.4 ± 3.1

The terminal elimination half-life ($t_{1/2}$) of AC1LPSZG is 89.9 min. The Pharmacokinetic profile was collected for 6 h (approximate 5 elimination half-lives of the drug), for a time long enough to eliminate > 95% of the administered dose. Using NCA the values of total clearance (CL) and area under the plasma concentration-time curve to infinity (AUC∞) are 59.9 mL/min/kg and 16967 min*ng/ml, respectively. These pharmacokinetic parameters are in good agreement with the two-compartment modeling.

Continuing investigation of developed PLGA-based nano-formulation of AC1LPSZG and its pharmacokinetic studies are undergoing in our research lab for further preclinical development of AC1LPSZG.

CHAPTER 5 SUMMARY AND CONCLUSION

Design of Experiments (DOE) strategy using Design Expert® software (version 13) was successfully used to optimize Poly(dl-lactide-co-glycolide) (50:50) (PLGA) based NPs of chemotherapeutic agent AC1LPSZG. Optimized batch was prepared using 5 mg drug and 4 mL aqueous phase volume with EE of 41.2%, NP size of 124 nm, drug load of 2.6% and zeta potential of – 15 mV. We conclude similar DOE approaches can help to understand and optimize innovative manufacturing processes, needed for the quality by design (QbD) preparation of other nano-formulations.

USP apparatus 4 was used to test *in vitro* drug release of poorly water-soluble drug AC1LPSZG from PLGA-AC1LPSZG-NPs. The influence of three different surfactants: SLS (Sodium Lauryl Sulfate-anionic), Tween 80 (non-ionic) and CTAB (Cetyltrimethylammonium bromide- cationic) on drug solubility, sink conditions and dissolution behavior was demonstrated. The solubility improvement was in the order of SLS > Tween80 > CTAB and dissolution efficiency was improved with the increase of surfactant concentration. The developed *in vitro* drug release method was able to discriminate among different release profiles. In brief, similar discriminatory test method can be used as a quality control tool to identify critical formulation and process parameters and can also be used as a surrogate for bioequivalence studies if a predictive *IVIVC* (*In vitro In vivo* correlation) is obtained.

The developed UPLC and LC-MS/MS methods were simple, sensitive, accurate and suitable for quantification of AC1LPSZG in *in vitro* study samples and rat plasma, respectively. The LC-MS/MS method was further applied to determine AC1LPSZG plasma concentrations in rats after intravenous injection of cosolvent formulations. The resulting pharmacokinetic parameters were analyzed using non-compartmental analysis (NCA) and two-compartmental modeling. Further pharmacokinetic and biodistribution studies of developed PLGA-AC1LPSZG-NPs formulation are under investigation in our laboratory to test the capability of developed formulation for sustained drug release.

REFERENCES

FDA and PAT. (2004). "Guidance for Industry PAT — A Framework for Innovative Pharmaceutical Development, Manufacturing, and Quality Assurance." from https://www.fda.gov/media/71012/download.

Fukuda, I. M., C. F. F. Pinto, C. d. S. Moreira, A. M. Saviano and F. R. Lourenço (2018). "Design of experiments (DoE) applied to pharmaceutical and analytical quality by design (QbD)." Brazilian Journal of Pharmaceutical Sciences **54**.

ICH and Q8(R2). (2009). "Guidance for Industry Q8(R2) Pharmaceutical Development." Retrieved 12/27, 2020, from https://www.fda.gov/media/71535/download.

Nayak, A. K., S. A. Ahmed, S. Beg, M. Tabish and M. S. Hasnain (2019). Chapter 18 - Application of Quality by Design for the Development of Biopharmaceuticals. Pharmaceutical Quality by Design. S. Beg and M. S. Hasnain, Academic Press**:** 399-411.

NIST. "Response surface designs." Retrieved 12/27, 2020, from https://www.itl.nist.gov/div898/handbook/pri/section3/pri336.htm.

Zhang, L. and S. Mao (2017). "Application of quality by design in the current drug development." Asian Journal of Pharmaceutical Sciences **12**(1): 1-8.

Abdel-Mageed, H. M., Fouad, S. A., Teaima, M. H., Abdel-Aty, A. M., Fahmy, A. S., Shaker, D. S., & Mohamed, S. A. (2019). Optimization of nano spray drying parameters for production of α-amylase nanopowder for biotheraputic applications using factorial design. *Drying Technology*, *37*(16), 2152-2160. https://doi.org/10.1080/07373937.2019.1565576

Agrawal, C. M., Huang, D., Schmitz, J., & Athanasiou, K. (1997). Elevated temperature degradation of a 50: 50 copolymer of PLA-PGA. *Tissue engineering*, *3*(4), 345-352.

Akbari, Z., Amanlou, M., Karimi-Sabet, J., Golestani, A., & Niassar, M. S. (2020). Application of Supercritical Fluid Technology for Preparation of Drug Loaded Solid Lipid Nanoparticles. *International Journal of NanoScience and Nanotechnology*, *16*, 13-33.

Ali, M. E., & Lamprecht, A. (2014). Spray freeze drying for dry powder inhalation of nanoparticles. *Eur J Pharm Biopharm*, *87*(3), 510-517. https://doi.org/10.1016/j.ejpb.2014.03.009

Allémann, E., Gurny, R., & Doelker, E. (1992). Preparation of aqueous polymeric nanodispersions by a reversible salting-out process: influence of process parameters on particle size. *International Journal of Pharmaceutics*, *87*(1), 247-253. https://doi.org/https://doi.org/10.1016/0378-5173(92)90249-2

Alshamsan, A. (2014). Nanoprecipitation is more efficient than emulsion solvent evaporation method to encapsulate cucurbitacin I in PLGA nanoparticles. *Saudi Pharm J*, *22*(3), 219-222. https://doi.org/10.1016/j.jsps.2013.12.002

Amadeo, I., Mauro, L., Ortí, E., & Forno, G. (2014). Establishment of a design space for biopharmaceutical purification processes using DoE. In *Protein Downstream Processing* (pp. 11-27). Springer.

Amann, L. C., Gandal, M. J., Lin, R., Liang, Y., & Siegel, S. J. (2010). In vitro–in vivo correlations of scalable PLGA-risperidone implants for the treatment of schizophrenia. *Pharmaceutical Research*, *27*(8), 1730-1737.

Anand, O., Yu, L. X., Conner, D. P., & Davit, B. M. (2011). Dissolution testing for generic drugs: an FDA perspective. *AAPS J*, *13*(3), 328-335. https://doi.org/10.1208/s12248-011-9272-y

Anderson, N. H., Bauer, M., Boussac, N., Khan-Malek, R., Munden, P., & Sardaro, M. (1998). An evaluation of fit factors and dissolution efficiency for the comparison of in vitro dissolution profiles. *J Pharm Biomed Anal*, *17*(4-5), 811-822. https://doi.org/10.1016/s0731-7085(98)00011-9

Anton, N., Bally, F., Serra, C. A., Ali, A., Arntz, Y., Mely, Y., Zhao, M., Marchioni, E., Jakhmola, A., & Vandamme, T. F. (2012). A new microfluidic setup for precise control of the polymer nanoprecipitation process and lipophilic drug encapsulation [10.1039/C2SM25357G]. *Soft Matter*, *8*(41), 10628-10635. https://doi.org/10.1039/C2SM25357G

Anwer, M. K., Mohammad, M., Ezzeldin, E., Fatima, F., Alalaiwe, A., & Iqbal, M. (2019). Preparation of sustained release apremilast-loaded PLGA nanoparticles: In vitro characterization and in vivo pharmacokinetic study in rats. *International journal of nanomedicine*, *14*, 1587.

Asghar, A., Abdul Raman, A. A., & Daud, W. M. A. W. (2014). A comparison of central composite design and Taguchi method for optimizing Fenton process. *The Scientific World Journal*, *2014*.

Attia, M. F., Anton, N., Wallyn, J., Omran, Z., & Vandamme, T. F. (2019). An overview of active and passive targeting strategies to improve the nanocarriers efficiency to tumour sites. *J Pharm Pharmacol*, *71*(8), 1185-1198. https://doi.org/10.1111/jphp.13098

Awasthi, R., Roseblade, A., Hansbro, P. M., Rathbone, M. J., Dua, K., & Bebawy, M. (2018). Nanoparticles in Cancer Treatment: Opportunities and Obstacles. *Curr Drug Targets*, *19*(14), 1696-1709. https://doi.org/10.2174/1389450119666180326122831

Bagwe, R. P., Hilliard, L. R., & Tan, W. (2006). Surface Modification of Silica Nanoparticles to Reduce Aggregation and Nonspecific Binding. *Langmuir*, *22*(9), 4357-4362. https://doi.org/10.1021/la052797j

Bala, I., Bhardwaj, V., Hariharan, S., Kharade, S. V., Roy, N., & Ravi Kumar, M. N. V. (2006). Sustained release nanoparticulate formulation containing antioxidant-ellagic acid as potential prophylaxis system for oral administration. *Journal of Drug Targeting*, *14*(1), 27-34. https://doi.org/10.1080/10611860600565987

Balbi, T., Camisassi, G., Montagna, M., Fabbri, R., Franzellitti, S., Carbone, C., Dawson, K., & Canesi, L. (2017). Impact of cationic polystyrene nanoparticles (PS-NH2) on early embryo development of Mytilus galloprovincialis: Effects on shell formation. *Chemosphere*, *186*, 1-9. https://doi.org/https://doi.org/10.1016/j.chemosphere.2017.07.120

Basta, A. H., Lotfy, V. F., Micky, J. A., & Salem, A. M. (2020). Liquid crystal behavior of cellulose nanoparticles ethyl cellulose composites: Preparation, characterization, and rheology. *Journal of Applied Polymer Science*, *138*, 50067.

Bastogne, T. (2017). Quality-by-design of nanopharmaceuticals - a state of the art. *Nanomedicine*, *13*(7), 2151-2157. https://doi.org/10.1016/j.nano.2017.05.014

Behzadi, S., Serpooshan, V., Sakhtianchi, R., Müller, B., Landfester, K., Crespy, D., & Mahmoudi, M. (2014). Protein corona change the drug release profile of nanocarriers: the "overlooked" factor at the nanobio interface. *Colloids Surf B Biointerfaces*, *123*, 143-149. https://doi.org/10.1016/j.colsurfb.2014.09.009

Beisl, S., Monteiro, S., Santos, R., Figueiredo, A. S., Sánchez-Loredo, M. G., Lemos, M. A., Lemos, F., Minhalma, M., & de Pinho, M. N. (2019). Synthesis and bactericide activity of nanofiltration composite membranes – Cellulose acetate/silver nanoparticles and cellulose acetate/silver ion exchanged zeolites. *Water Research*, *149*, 225-231. https://doi.org/https://doi.org/10.1016/j.watres.2018.10.096

Bhagav, P., Upadhyay, H., & Chandran, S. (2011). Brimonidine tartrate-eudragit long-acting nanoparticles: formulation, optimization, in vitro and in vivo evaluation. *AAPS PharmSciTech*, *12*(4), 1087-1101. https://doi.org/10.1208/s12249-011-9675-1

Bhattacharjee, S. (2016). DLS and zeta potential – What they are and what they are not? *Journal of Controlled Release*, *235*, 337-351. https://doi.org/https://doi.org/10.1016/j.jconrel.2016.06.017

Bhavna, Md, S., Ali, M., Baboota, S., Sahni, J. K., Bhatnagar, A., & Ali, J. (2014). Preparation, characterization, in vivo biodistribution and pharmacokinetic studies of donepezil-loaded PLGA nanoparticles for brain targeting. *Drug development and industrial pharmacy*, *40*(2), 278-287. https://doi.org/10.3109/03639045.2012.758130

Bilati, U., Allémann, E., & Doelker, E. (2005). Development of a nanoprecipitation method intended for the entrapment of hydrophilic drugs into nanoparticles. *European Journal of Pharmaceutical Sciences*, *24*(1), 67-75. https://doi.org/https://doi.org/10.1016/j.ejps.2004.09.011

Blasi, P., D'Souza, S. S., Selmin, F., & DeLuca, P. P. (2005). Plasticizing effect of water on poly (lactide-co-glycolide). *Journal of Controlled Release*, *108*(1), 1-9.

Bootz, A., Vogel, V., Schubert, D., & Kreuter, J. (2004). Comparison of scanning electron microscopy, dynamic light scattering and analytical ultracentrifugation for the sizing of poly(butyl cyanoacrylate) nanoparticles. *European Journal of Pharmaceutics and Biopharmaceutics*, *57*(2), 369-375. https://doi.org/https://doi.org/10.1016/S0939-6411(03)00193-0

Brown, W. (2005). Apparatus 4 Flow Through Cell: Some Thoughts on Operational Characteristics. *Dissolution Technologies*(May), 3. https://doi.org/dx.doi.org/10.14227/DT120205P28

Budhian, A., Siegel, S. J., & Winey, K. I. (2005). Production of haloperidol-loaded PLGA nanoparticles for extended controlled drug release of haloperidol. *Journal of microencapsulation*, *22*(7), 773-785.

Butler, J. M., & Dressman, J. B. (2010). The developability classification system: application of biopharmaceutics concepts to formulation development. *J Pharm Sci*, *99*(12), 4940-4954. https://doi.org/10.1002/jps.22217

Calvo, P., Vila-Jato, J. L., & Alonso, M. J. (1996). Comparative in vitro evaluation of several colloidal systems, nanoparticles, nanocapsules, and nanoemulsions, as ocular drug carriers. *J Pharm Sci*, *85*(5), 530-536. https://doi.org/10.1021/js950474+

Campardelli, R., Baldino, L., & Reverchon, E. (2015). Supercritical fluids applications in nanomedicine. *The Journal of Supercritical Fluids*, *101*, 193-214. https://doi.org/https://doi.org/10.1016/j.supflu.2015.01.030

Cargnello, M., Tcherkezian, J., & Roux, P. P. (2015). The expanding role of mTOR in cancer cell growth and proliferation. *Mutagenesis*, *30*(2), 169-176.

Carvalho, P. M., Felício, M. R., Santos, N. C., Gonçalves, S., & Domingues, M. M. (2018). Application of Light Scattering Techniques to Nanoparticle Characterization and Development [Review]. *Frontiers in Chemistry*, *6*(237). https://doi.org/10.3389/fchem.2018.00237

Chakravarty, P., Famili, A., Nagapudi, K., & Al-Sayah, M. A. (2019). Using Supercritical Fluid Technology as a Green Alternative During the Preparation of Drug Delivery Systems. *Pharmaceutics*, *11*(12). https://doi.org/10.3390/pharmaceutics11120629

Chen, C., Yang, W., Wang, D.-T., Chen, C.-L., Zhuang, Q.-Y., & Kong, X.-D. (2014). A modified spontaneous emulsification solvent diffusion method for the preparation of curcumin-loaded PLGA nanoparticles with enhanced in vitro anti-tumor activity. *Frontiers of Materials Science*, *8*(4), 332-342. https://doi.org/10.1007/s11706-014-0268-2

Chen, Y., Gao, X., Gupta, R., Ma, J., Dere, R., Liang, D., & Xie, H. (2022). Development and Validation of an LC-MS/MS Method for AC1LPSZG and Pharmacokinetics Application in Rats. *Journal of chromatographic science*, *60*(1), 26-34. https://doi.org/10.1093/chromsci/bmab020

Chidambaram, N., & Burgess, D. J. (1999). A novel in vitro release method for submicron sized dispersed systems. *AAPS PharmSci*, *1*(3), E11. https://doi.org/10.1208/ps010311

Chiesa, E., Dorati, R., Modena, T., Conti, B., & Genta, I. (2018). Multivariate analysis for the optimization of microfluidics-assisted nanoprecipitation method intended for the loading of small hydrophilic drugs into PLGA nanoparticles. *International Journal of Pharmaceutics*, *536*(1), 165-177. https://doi.org/https://doi.org/10.1016/j.ijpharm.2017.11.044

Choi, K. Y., Chung, H., Min, K. H., Yoon, H. Y., Kim, K., Park, J. H., Kwon, I. C., & Jeong, S. Y. (2010). Self-assembled hyaluronic acid nanoparticles for active tumor targeting. *Biomaterials*, *31*(1), 106-114. https://doi.org/https://doi.org/10.1016/j.biomaterials.2009.09.030

Cohen-Sela, E., Chorny, M., Koroukhov, N., Danenberg, H. D., & Golomb, G. (2009). A new double emulsion solvent diffusion technique for encapsulating hydrophilic molecules in PLGA nanoparticles. *Journal of Controlled Release*, *133*(2), 90-95.

Cooper, D. L., & Harirforoosh, S. (2014). Effect of formulation variables on preparation of celecoxib loaded polylactide-co-glycolide nanoparticles. *PLoS One*, *9*(12), e113558. https://doi.org/10.1371/journal.pone.0113558

Corrigan, O. I., & Li, X. (2009). Quantifying drug release from PLGA nanoparticulates. *European Journal of Pharmaceutical Sciences*, *37*(3), 477-485. https://doi.org/https://doi.org/10.1016/j.ejps.2009.04.004

D'Arcy, D. M., Liu, B., Bradley, G., Healy, A. M., & Corrigan, O. I. (2010). Hydrodynamic and species transfer simulations in the USP 4 dissolution apparatus: considerations for dissolution in a low velocity pulsing flow. *Pharm Res*, *27*(2), 246-258. https://doi.org/10.1007/s11095-009-0010-4

D'Souza, S. (2014). A Review of In Vitro Drug Release Test Methods for Nano-Sized Dosage Forms. *Advances in Pharmaceutics*, *2014*, 304757. https://doi.org/10.1155/2014/304757

Danhier, F., Ansorena, E., Silva, J. M., Coco, R., Le Breton, A., & Préat, V. (2012). PLGA-based nanoparticles: An overview of biomedical applications. *Journal of Controlled Release*, *161*(2), 505-522. https://doi.org/https://doi.org/10.1016/j.jconrel.2012.01.043

del Castillo-Santaella, T., Ortega-Oller, I., Padial-Molina, M., O'Valle, F., Galindo-Moreno, P., Jódar-Reyes, A. B., & Peula-García, J. M. (2019). Formulation, colloidal characterization, and in vitro biological effect of BMP-2 Loaded PLGA nanoparticles for bone regeneration. *Pharmaceutics*, *11*(8), 388.

Deng, Y., Zhang, X., Shen, H., He, Q., Wu, Z., Liao, W., & Yuan, M. (2019). Application of the Nano-Drug Delivery System in Treatment of Cardiovascular Diseases. *Front Bioeng Biotechnol*, *7*, 489. https://doi.org/10.3389/fbioe.2019.00489

Derringer, G., & Suich, R. (1980). Simultaneous optimization of several response variables. *Journal of Quality Technology*, *12*(4), 214-219.

Desgouilles, S., Vauthier, C., Bazile, D., Vacus, J., Grossiord, J.-L., Veillard, M., & Couvreur, P. (2003). The Design of Nanoparticles Obtained by Solvent Evaporation: A Comprehensive Study. *Langmuir*, *19*(22), 9504-9510. https://doi.org/10.1021/la034999q

Dikpati, A., Mohammadi, F., Greffard, K., Quéant, C., Arnaud, P., Bastiat, G., Rudkowska, I., & Bertrand, N. (2020). Residual Solvents in Nanomedicine and Lipid-Based Drug Delivery Systems: a Case Study to Better Understand Processes. *Pharm Res*, *37*(8), 149. https://doi.org/10.1007/s11095-020-02877-x

Dong, D., Hsiao, C.-H., Giovanella, B. C., Wang, Y., Chow, D. S., & Li, Z. (2019). Sustained delivery of a camptothecin prodrug - CZ48 by nanosuspensions with improved pharmacokinetics and enhanced anticancer activity. *International journal of nanomedicine*, *14*, 3799-3817. https://doi.org/10.2147/IJN.S196453

Draheim, C., de Crécy, F., Hansen, S., Collnot, E.-M., & Lehr, C.-M. (2015). A Design of Experiment Study of Nanoprecipitation and Nano Spray Drying as Processes to Prepare PLGA Nano- and Microparticles with Defined Sizes and Size Distributions. *Pharmaceutical Research*, *32*(8), 2609-2624. https://doi.org/10.1007/s11095-015-1647-9

Duse, L., Agel, M. R., Pinnapireddy, S. R., Schäfer, J., Selo, M. A., Ehrhardt, C., & Bakowsky, U. (2019). Photodynamic therapy of ovarian carcinoma cells with curcumin-loaded biodegradable polymeric nanoparticles. *Pharmaceutics*, *11*(6), 282.

Dutka, M., Ditaranto, M., & Løvås, T. (2015). Application of a central composite design for the study of NOx emission performance of a low NOx burner. *Energies*, *8*(5), 3606-3627.

E.I, J., Etuk, E., Iwundu, M., & Amos, E. (2021). Robustness of Central Composite Design and Modified Central Composite Design to a Missing Observation for Non-Standard Models. *African Journal of Mathematics and Statistics Studies*, *4*, 25-40. https://doi.org/10.52589/AJMSS-C5NKOI81

Eaton, J. W., Tran, D., Hauck, W. W., & Stippler, E. S. (2012). Development of a performance verification test for USP apparatus 4. *Pharm Res*, *29*(2), 345-351. https://doi.org/10.1007/s11095-011-0559-6

Esfandiari, N., & Ghoreishi, S. M. (2013). Synthesis of 5-Fluorouracil nanoparticles via supercritical gas antisolvent process. *The Journal of Supercritical Fluids*, *84*, 205-210. https://doi.org/https://doi.org/10.1016/j.supflu.2013.10.008

Fam, S. Y., Chee, C. F., Yong, C. Y., Ho, K. L., Mariatulqabtiah, A. R., & Tan, W. S. (2020). Stealth Coating of Nanoparticles in Drug-Delivery Systems. *Nanomaterials (Basel)*, *10*(4). https://doi.org/10.3390/nano10040787

FDA, & ICHQ3C. (2017). *ICH Q3C Maintenance Procedures for the Guidance for Industry Q3C Impurities: Residual Solvents*. Retrieved April 14 from https://www.fda.gov/regulatory-information/search-fda-guidance-documents/ich-q3c-maintenance-procedures-guidance-industry-q3c-impurities-residual-solvents

FDA, & Liposome. (2018). *Liposome Drug Products Chemistry, Manufacturing, and Controls; Human Pharmacokinetics and Bioavailability; and Labeling Documentation*. Retrieved May 05 from https://www.fda.gov/media/70837/download

FDA, & M9. (2018). *M9 BIOPHARMACEUTICS CLASSIFICATION SYSTEM-BASED BIOWAIVERS*. Retrieved April 28 from https://www.fda.gov/media/117974/download

FDA, & Nanotechnology. (2014). *Considering Whether an FDA-Regulated Product Involves the Application of Nanotechnology*.

Office of the Commissioner, Office of Policy, Legislation, and International Affairs, Office of Policy

FDA, & PAT. (2004). *Guidance for Industry PAT — A Framework for Innovative Pharmaceutical Development, Manufacturing, and Quality Assurance*. https://www.fda.gov/media/71012/download

FDA, & Q3C. (2018). *Q3C — Tables and List Guidance for Industry*. Retrieved April 04 from https://www.fda.gov/media/133650/download

FDA, & Safety. (2014). *Safety of Nanomaterials in Cosmetic Products*. Retrieved Jan 03 from https://www.fda.gov/media/83957/download

FDA, & SUPAC. (1997). *SUPAC-MR: Modified Release Solid Oral Dosage Forms*. Retrieved April 28 from https://www.fda.gov/media/70956/download

Fontdecaba, S., Grima, P., & Tort-Martorell, X. (2014). Analyzing DOE With Statistical Software Packages: Controversies and Proposals. *The American Statistician*, *68*(3), 205-211. https://doi.org/10.1080/00031305.2014.923784

Forrest, W. P., Reuter, K. G., Shah, V., Kazakevich, I., Heslinga, M., Dudhat, S., Patel, S., Neri, C., & Mao, Y. (2018). USP Apparatus 4: a Valuable In Vitro Tool to Enable Formulation

Development of Long-Acting Parenteral (LAP) Nanosuspension Formulations of Poorly Water-Soluble Compounds. *AAPS PharmSciTech*, *19*(1), 413-424. https://doi.org/10.1208/s12249-017-0842-x

Fredenberg, S., Wahlgren, M., Reslow, M., & Axelsson, A. (2011). The mechanisms of drug release in poly(lactic-co-glycolic acid)-based drug delivery systems--a review. *Int J Pharm*, *415*(1-2), 34-52. https://doi.org/10.1016/j.ijpharm.2011.05.049

Fukuda, I. M., Pinto, C. F. F., Moreira, C. d. S., Saviano, A. M., & Lourenço, F. R. (2018). Design of experiments (DoE) applied to pharmaceutical and analytical quality by design (QbD). *Brazilian Journal of Pharmaceutical Sciences*, *54*.

Fumarola, C., Bonelli, M. A., Petronini, P. G., & Alfieri, R. R. (2014). Targeting PI3K/AKT/mTOR pathway in non small cell lung cancer. *Biochemical pharmacology*, *90*(3), 197-207.

Galindo-Rodriguez, S., Allémann, E., Fessi, H., & Doelker, E. (2004). Physicochemical Parameters Associated with Nanoparticle Formation in the Salting-Out, Emulsification-Diffusion, and Nanoprecipitation Methods. *Pharmaceutical Research*, *21*(8), 1428-1439. https://doi.org/10.1023/B:PHAM.0000036917.75634.be

Galindo-Rodríguez, S. A., Puel, F., Briançon, S., Allémann, E., Doelker, E., & Fessi, H. (2005). Comparative scale-up of three methods for producing ibuprofen-loaded nanoparticles. *European Journal of Pharmaceutical Sciences*, *25*(4), 357-367. https://doi.org/https://doi.org/10.1016/j.ejps.2005.03.013

Gao, X., Wu, L., Tsai, R. Y. L., Ma, J., Liu, X., Chow, D. S. L., Liang, D., & Xie, H. (2021). Pharmacokinetic Model Analysis of Supralingual, Oral and Intravenous Deliveries of Mycophenolic Acid. *Pharmaceutics*, *13*(4), 574. https://doi.org/10.3390/pharmaceutics13040574

Gao, Y., Zuo, J., Bou-Chacra, N., Pinto, T. d. J. A., Clas, S.-D., Walker, R. B., & Löbenberg, R. (2013). In Vitro Release Kinetics of Antituberculosis Drugs from Nanoparticles Assessed Using a Modified Dissolution Apparatus. *BioMed Research International*, *2013*, 136590. https://doi.org/10.1155/2013/136590

Gaonkar, R. H., Ganguly, S., Dewanjee, S., Sinha, S., Gupta, A., Ganguly, S., Chattopadhyay, D., & Chatterjee Debnath, M. (2017). Garcinol loaded vitamin E TPGS emulsified PLGA nanoparticles: preparation, physicochemical characterization, in vitro and in vivo studies. *Sci Rep*, *7*(1), 530. https://doi.org/10.1038/s41598-017-00696-6

Gill, P., Moghadam, T. T., & Ranjbar, B. (2010). Differential scanning calorimetry techniques: applications in biology and nanoscience. *Journal of biomolecular techniques : JBT*, *21 4*, 167-193.

Grant, S. A., Spradling, C. S., Grant, D. N., Fox, D. B., Jimenez, L., Grant, D. A., & Rone, R. J. (2014). Assessment of the biocompatibility and stability of a gold nanoparticle collagen bioscaffold. *J Biomed Mater Res A*, *102*(2), 332-339. https://doi.org/10.1002/jbm.a.34698

Grune, C., Zens, C., Czapka, A., Scheuer, K., Thamm, J., Hoeppener, S., Jandt, K. D., Werz, O., Neugebauer, U., & Fischer, D. (2021). Sustainable preparation of anti-inflammatory atorvastatin PLGA nanoparticles. *International Journal of Pharmaceutics*, *599*, 120404.

Gu, B., Sun, X., Papadimitrakopoulos, F., & Burgess, D. J. (2016). Seeing is believing, PLGA microsphere degradation revealed in PLGA microsphere/PVA hydrogel composites. *Journal of Controlled Release*, *228*, 170-178. https://doi.org/https://doi.org/10.1016/j.jconrel.2016.03.011

Guo, Q., Dasgupta, D., Doll, T. A. P. F., Burkhard, P., & Lanar, D. E. (2013). Expression, purification and refolding of a self-assembling protein nanoparticle (SAPN) malaria vaccine. *Methods*, *60*(3), 242-247. https://doi.org/https://doi.org/10.1016/j.ymeth.2013.03.025

Gupta, R., Chen, Y., & Xie, H. (2021). In vitro dissolution considerations associated with nano drug delivery systems. *Wiley Interdiscip Rev Nanomed Nanobiotechnol*, *13*(6), e1732. https://doi.org/10.1002/wnan.1732

Haggag, Y. A., Abosalha, A. K., Tambuwala, M. M., Osman, E. Y., El-Gizawy, S. A., Essa, E. A., & Donia, A. A. (2021). Polymeric nanoencapsulation of zaleplon into PLGA nanoparticles for enhanced pharmacokinetics and pharmacological activity. *Biopharmaceutics & Drug Disposition*, *42*(1), 12-23.

Ham, A. S., Cost, M. R., Sassi, A. B., Dezzutti, C. S., & Rohan, L. C. (2009). Targeted delivery of PSC-RANTES for HIV-1 prevention using biodegradable nanoparticles. *Pharm Res*, *26*(3), 502-511. https://doi.org/10.1007/s11095-008-9765-2

Heng, D., Cutler, D. J., Chan, H. K., Yun, J., & Raper, J. A. (2008). What is a suitable dissolution method for drug nanoparticles? *Pharm Res*, *25*(7), 1696-1701. https://doi.org/10.1007/s11095-008-9560-0

Holzer, M., Vogel, V., Mäntele, W., Schwartz, D., Haase, W., & Langer, K. (2009). Physico-chemical characterisation of PLGA nanoparticles after freeze-drying and storage. *European Journal of Pharmaceutics and Biopharmaceutics*, *72*(2), 428-437. https://doi.org/https://doi.org/10.1016/j.ejpb.2009.02.002

Honigford, C. R., Aburub, A., & Fadda, H. M. (2019). A Simulated Stomach Duodenum Model Predicting the Effect of Fluid Volume and Prandial Gastric Flow Patterns on Nifedipine Pharmacokinetics From Cosolvent-Based Capsules. *Journal of Pharmaceutical Sciences*, *108*(1), 288-294. https://doi.org/https://doi.org/10.1016/j.xphs.2018.07.023

Hu, X., Zhang, J., Tang, X., Li, M., Ma, S., Liu, C., Gao, Y., Zhang, Y., Liu, Y., & Yu, F. (2018). An accelerated release method of risperidone loaded PLGA microspheres with good IVIVC. *Current drug delivery*, *15*(1), 87-96.

Hua, H., Kong, Q., Zhang, H., Wang, J., Luo, T., & Jiang, Y. (2019). Targeting mTOR for cancer therapy. *Journal of hematology & oncology*, *12*(1), 1-19.

Huang, Z., Parikh, S., & Fish, W. P. (2018). Interactions between a poorly soluble cationic drug and sodium dodecyl sulfate in dissolution medium and their impact on in vitro dissolution behavior. *Int J Pharm*, *535*(1-2), 350-359. https://doi.org/10.1016/j.ijpharm.2017.10.063

Hwang, A. A., Lee, B. Y., Clemens, D. L., Dillon, B. J., Zink, J. I., & Horwitz, M. A. (2015). Tuberculosis: pH-Responsive Isoniazid-Loaded Nanoparticles Markedly Improve Tuberculosis Treatment in Mice (Small 38/2015). *Small*, *11*(38), 5065. https://doi.org/10.1002/smll.201570235

ICH. (2019). *ICH guideline Q3C (R6) on impurities: guideline for residual solvents*. Retrieved April 14 from https://www.ema.europa.eu/en/documents/scientific-guideline/international-conference-harmonisation-technical-requirements-registration-pharmaceuticals-human-use_en-33.pdf

ICH, & Q8(R2). (2009). *Guidance for Industry Q8(R2) Pharmaceutical Development*. Retrieved 12/27 from https://www.fda.gov/media/71535/download

In Pyo Park, P., & Jonnalagadda, S. (2006). Predictors of glass transition in the biodegradable poly-lactide and poly-lactide-co-glycolide polymers. *Journal of Applied Polymer Science*, *100*(3), 1983-1987.

Iqbal, M., Zafar, N., Fessi, H., & Elaissari, A. (2015). Double emulsion solvent evaporation techniques used for drug encapsulation. *International Journal of Pharmaceutics*, *496*(2), 173-190. https://doi.org/https://doi.org/10.1016/j.ijpharm.2015.10.057

Italia, J. L., Bhatt, D. K., Bhardwaj, V., Tikoo, K., & Kumar, M. N. V. R. (2007). PLGA nanoparticles for oral delivery of cyclosporine: Nephrotoxicity and pharmacokinetic studies in comparison to Sandimmune Neoral®. *Journal of Controlled Release*, *119*(2), 197-206. https://doi.org/https://doi.org/10.1016/j.jconrel.2007.02.004

Jafari, S. M., Assadpoor, E., Bhandari, B., & He, Y. (2008). Nano-particle encapsulation of fish oil by spray drying. *Food Research International*, *41*(2), 172-183. https://doi.org/https://doi.org/10.1016/j.foodres.2007.11.002

Jain, G. K., Pathan, S. A., Akhter, S., Ahmad, N., Jain, N., Talegaonkar, S., Khar, R. K., & Ahmad, F. J. (2010). Mechanistic study of hydrolytic erosion and drug release behaviour of PLGA nanoparticles: Influence of chitosan. *Polymer degradation and stability*, *95*(12), 2360-2366. https://doi.org/https://doi.org/10.1016/j.polymdegradstab.2010.08.015

Jain, P., Pawar, R. S., Pandey, R. S., Madan, J., Pawar, S., Lakshmi, P. K., & Sudheesh, M. S. (2017). In-vitro in-vivo correlation (IVIVC) in nanomedicine: Is protein corona the missing link? *Biotechnol Adv*, *35*(7), 889-904. https://doi.org/10.1016/j.biotechadv.2017.08.003

Jeong, I.-J., & Kim, K.-J. (2009). An interactive desirability function method to multiresponse optimization. *European Journal of Operational Research*, *195*(2), 412-426.

Joshi, M. D., & Muller, R. H. (2009). Lipid nanoparticles for parenteral delivery of actives. *Eur J Pharm Biopharm*, *71*(2), 161-172. https://doi.org/10.1016/j.ejpb.2008.09.003

Kade, M. J., & Tirrell, M. V. (2014). Free Radical and Condensation Polymerizations.

Kakhi, M. (2009). Mathematical modeling of the fluid dynamics in the flow-through cell. *Int J Pharm*, *376*(1-2), 22-40. https://doi.org/10.1016/j.ijpharm.2009.04.012

Kamaly, N., Yameen, B., Wu, J., & Farokhzad, O. C. (2016). Degradable Controlled-Release Polymers and Polymeric Nanoparticles: Mechanisms of Controlling Drug Release. *Chem Rev*, *116*(4), 2602-2663. https://doi.org/10.1021/acs.chemrev.5b00346

Kammari, R., Das, N. G., & Das, S. K. (2017). Chapter 6 - Nanoparticulate Systems for Therapeutic and Diagnostic Applications. In (pp. 105-144): Elsevier Inc.

Karataş, A., Sonakin, Ö., Kiliçarslan, M., & Baykara, T. (2010). EFFECTS OF STIRRING RATE AND DRUG: POISMER RATIO (ON THE CHARACTERISTICS OF LEVOBUNOLOL HCL LOADED POLY (ε-CAPROLACTONE) MICROPARTICLES. *Turkish Journal of Pharmaceutical Sciences*, *7*(3).

Karlsson, O., Stubbs, J., Karlsson, L., & Sundberg, D. (2001). Estimating diffusion coefficients for small molecules in polymers and polymer solutions. *Polymer*, *42*(11), 4915-4923.

Kassaye, L., & Genete, G. (2013). Evaluation and comparison of in-vitro dissolution profiles for different brands of amoxicillin capsules. *Afr Health Sci*, *13*(2), 369-375. https://doi.org/10.4314/ahs.v13i2.25

Kaszuba, M., Corbett, J., Watson, F. M., & Jones, A. (2010). High-concentration zeta potential measurements using light-scattering techniques. *Philos Trans A Math Phys Eng Sci*, *368*(1927), 4439-4451. https://doi.org/10.1098/rsta.2010.0175

Kauffman, K. J., Dorkin, J. R., Yang, J. H., Heartlein, M. W., DeRosa, F., Mir, F. F., Fenton, O. S., & Anderson, D. G. (2015). Optimization of Lipid Nanoparticle Formulations for mRNA Delivery in Vivo with Fractional Factorial and Definitive Screening Designs. *Nano Letters*, *15*(11), 7300-7306. https://doi.org/10.1021/acs.nanolett.5b02497

Keles, H., Naylor, A., Clegg, F., & Sammon, C. (2015). Investigation of factors influencing the hydrolytic degradation of single PLGA microparticles. *Polymer degradation and stability*, *119*, 228-241.

Khalil, N. M., Nascimento, T. C. F. d., Casa, D. M., Dalmolin, L. F., Mattos, A. C. d., Hoss, I., Romano, M. A., & Mainardes, R. M. (2013). Pharmacokinetics of curcumin-loaded PLGA and PLGA–PEG blend nanoparticles after oral administration in rats. *Colloids and Surfaces B: Biointerfaces*, *101*, 353-360. https://doi.org/https://doi.org/10.1016/j.colsurfb.2012.06.024

Khan, K. A. (2011). The concept of dissolution efficiency. *Journal of Pharmacy and Pharmacology*, *27*(1), 48-49. https://doi.org/10.1111/j.2042-7158.1975.tb09378.x

Kim, Y. I., Fluckiger, L., Hoffman, M., Lartaud-Idjouadiene, I., Atkinson, J., & Maincent, P. (1997). The antihypertensive effect of orally administered nifedipine-loaded nanoparticles in spontaneously hypertensive rats. *Br J Pharmacol*, *120*(3), 399-404. https://doi.org/10.1038/sj.bjp.0700910

Kitchell, J. P., & Wise, D. L. (1985). [32] Poly(lactic/glycolic acid) biodegradable drug—polymer matrix systems. In *Methods in Enzymology* (Vol. 112, pp. 436-448). Academic Press. https://doi.org/https://doi.org/10.1016/S0076-6879(85)12034-3

Klose, D., Siepmann, F., Elkharraz, K., Krenzlin, S., & Siepmann, J. (2006). How porosity and size affect the drug release mechanisms from PLGA-based microparticles. *International Journal of Pharmaceutics*, *314*(2), 198-206. https://doi.org/https://doi.org/10.1016/j.ijpharm.2005.07.031

Körber, M. (2010). PLGA Erosion: Solubility- or Diffusion-Controlled? *Pharmaceutical Research*, *27*(11), 2414-2420. https://doi.org/10.1007/s11095-010-0232-5

Kotti, K., & Kiparissides, C. (2010). Synthesis of Composite Polystyrene/Silica Nanoparticles via Precipitation and Emulsion Polymerization Methods. *Macromolecular Reaction Engineering*, *4*, 347-357. https://doi.org/10.1002/mren.200900054

Kowalski, S. M., Cornell, J. A., & Vining, G. G. (2002). Split-Plot Designs and Estimation Methods for Mixture Experiments With Process Variables. *Technometrics*, *44*(1), 72-79. https://doi.org/10.1198/004017002753398344

Krull, S. M., Ammirata, J., Bawa, S., Li, M., Bilgili, E., & Davé, R. N. (2017). Critical Material Attributes of Strip Films Loaded With Poorly Water-Soluble Drug Nanoparticles: II. Impact of Polymer Molecular Weight. *J Pharm Sci*, *106*(2), 619-628. https://doi.org/10.1016/j.xphs.2016.10.009

Lamprecht, A., Ubrich, N., Hombreiro Pérez, M., Lehr, C. M., Hoffman, M., & Maincent, P. (2000). Influences of process parameters on nanoparticle preparation performed by a double emulsion pressure homogenization technique. *International Journal of Pharmaceutics*, *196*(2), 177-182. https://doi.org/https://doi.org/10.1016/S0378-5173(99)00422-6

Legrand, P., Lesieur, S., Bochot, A., Gref, R., Raatjes, W., Barratt, G., & Vauthier, C. (2007). Influence of polymer behaviour in organic solution on the production of polylactide nanoparticles by nanoprecipitation. *International Journal of Pharmaceutics*, *344*(1), 33-43. https://doi.org/https://doi.org/10.1016/j.ijpharm.2007.05.054

Leyva-Gomez, G., Pinon-Segundo, E., Mendoza-Munoz, N., Zambrano-Zaragoza, M. L., Mendoza-Elvira, S., & Quintanar-Guerrero, D. (2018). Approaches in Polymeric Nanoparticles for Vaginal Drug Delivery: A Review of the State of the Art. *Int J Mol Sci*, *19*(6). https://doi.org/10.3390/ijms19061549

Li, M.-C., Wu, Q., Song, K., Lee, S., Qing, Y., & Wu, Y. (2015). Cellulose Nanoparticles: Structure–Morphology–Rheology Relationships. *ACS Sustainable Chemistry & Engineering*, *3*(5), 821-832. https://doi.org/10.1021/acssuschemeng.5b00144

Li, X., Anton, N., Arpagaus, C., Belleteix, F., & Vandamme, T. F. (2010). Nanoparticles by spray drying using innovative new technology: The Büchi Nano Spray Dryer B-90. *Journal of Controlled Release*, *147*(2), 304-310. https://doi.org/https://doi.org/10.1016/j.jconrel.2010.07.113

Lim, K., & Hamid, Z. A. A. (2018). 10 - Polymer nanoparticle carriers in drug delivery systems: Research trend. In Inamuddin, A. M. Asiri, & A. Mohammad (Eds.), *Applications of Nanocomposite Materials in Drug Delivery* (pp. 217-237). Woodhead Publishing. https://doi.org/https://doi.org/10.1016/B978-0-12-813741-3.00010-8

Lima, I. A., Khalil, N. M., Tominaga, T. T., Lechanteur, A., Sarmento, B., & Mainardes, R. M. (2018). Mucoadhesive chitosan-coated PLGA nanoparticles for oral delivery of ferulic acid. *Artif Cells Nanomed Biotechnol*, *46*(sup2), 993-1002. https://doi.org/10.1080/21691401.2018.1477788

Liu, J., Xu, Y., Liu, Z., Ren, H., Meng, Z., Liu, K., Liu, Z., Yong, J., Wang, Y., & Li, X. (2019). A modified hydrophobic ion-pairing complex strategy for long-term peptide delivery with high drug encapsulation and reduced burst release from PLGA microspheres. *European Journal of Pharmaceutics and Biopharmaceutics*, *144*, 217-229. https://doi.org/https://doi.org/10.1016/j.ejpb.2019.09.022

Liu, P., De Wulf, O., Laru, J., Heikkilä, T., van Veen, B., Kiesvaara, J., Hirvonen, J., Peltonen, L., & Laaksonen, T. (2013). Dissolution studies of poorly soluble drug nanosuspensions in non-sink conditions. *AAPS PharmSciTech*, *14*(2), 748-756. https://doi.org/10.1208/s12249-013-9960-2

Loo, S. C. J., Ooi, C. P., & Boey, Y. C. F. (2004). Radiation effects on poly(lactide-co-glycolide) (PLGA) and poly(l-lactide) (PLLA). *Polymer degradation and stability*, *83*(2), 259-265. https://doi.org/https://doi.org/10.1016/S0141-3910(03)00271-4

Lovell, P. A., & Schork, F. J. (2020). Fundamentals of Emulsion Polymerization. *Biomacromolecules*, *21*(11), 4396-4441. https://doi.org/10.1021/acs.biomac.0c00769

Lu, X., Xu, P., Ding, H. M., Yu, Y. S., Huo, D., & Ma, Y. Q. (2019). Tailoring the component of protein corona via simple chemistry. *Nat Commun*, *10*(1), 4520. https://doi.org/10.1038/s41467-019-12470-5

Mabuchi, S., Kuroda, H., Takahashi, R., & Sasano, T. (2015). The PI3K/AKT/mTOR pathway as a therapeutic target in ovarian cancer. *Gynecologic oncology*, *137*(1), 173-179.

Madani, F., Esnaashari, S. S., Bergonzi, M. C., Webster, T. J., Younes, H. M., Khosravani, M., & Adabi, M. (2020). Paclitaxel/methotrexate co-loaded PLGA nanoparticles in glioblastoma treatment: Formulation development and in vitro antitumor activity evaluation. *Life Sci*, *256*, 117943. https://doi.org/10.1016/j.lfs.2020.117943

Mahato, R. (2017). Chapter 2 - Multifunctional Micro- and Nanoparticles. In (pp. 21-43): Elsevier Inc.

Makadia, H. K., & Siegel, S. J. (2011). Poly Lactic-co-Glycolic Acid (PLGA) as Biodegradable Controlled Drug Delivery Carrier. *Polymers*, *3*(3), 1377-1397. https://doi.org/10.3390/polym3031377

MalvernZetasizer, & Performance.).

. https://www.malvernpanalytical.com/en/assets/MRK1839_tcm50-17228.pdf

Mendoza-Muñoz, N., Quintanar-Guerrero, D., & Allémann, E. (2012). The impact of the salting-out technique on the preparation of colloidal particulate systems for pharmaceutical applications. *Recent Pat Drug Deliv Formul*, *6*(3), 236-249. https://doi.org/10.2174/187221112802652688

Meziani, M. J., Pathak, P., & Sun, Y.-P. (2009). Supercritical Fluid Technology for Nanotechnology in Drug Delivery. In M. M. de Villiers, P. Aramwit, & G. S. Kwon (Eds.), *Nanotechnology in Drug Delivery* (pp. 69-104). Springer New York. https://doi.org/10.1007/978-0-387-77668-2_3

Mo, Y., & Lim, L. Y. (2005). Paclitaxel-loaded PLGA nanoparticles: potentiation of anticancer activity by surface conjugation with wheat germ agglutinin. *J Control Release*, *108*(2-3), 244-262. https://doi.org/10.1016/j.jconrel.2005.08.013

Mochizuki, A., Niikawa, T., Omura, I., & Yamashita, S. (2008). Controlled release of argatroban from PLA film—Effect of hydroxylesters as additives on enhancement of drug release. *Journal of Applied Polymer Science*, *108*(5), 3353-3360.

Monge, M., Fornaguera, C., Quero, C., Dols-Perez, A., Calderó, G., Grijalvo, S., García-Celma, M. J., Rodríguez-Abreu, C., & Solans, C. (2020). Functionalized PLGA nanoparticles prepared by nano-emulsion templating interact selectively with proteins involved in the transport through the blood-brain barrier. *European Journal of Pharmaceutics and Biopharmaceutics*, *156*, 155-164. https://doi.org/https://doi.org/10.1016/j.ejpb.2020.09.003

Morales-Cruz, M., Flores-Fernández, G. M., Orellano, E. A., Rodriguez-Martinez, J. A., Ruiz, M., & Griebenow, K. (2012). Two-step nanoprecipitation for the production of protein-loaded PLGA nanospheres. *Results Pharma Sci*, *2*, 79-85. https://doi.org/10.1016/j.rinphs.2012.11.001

Morelli, L., Gimondi, S., Sevieri, M., Salvioni, L., Guizzetti, M., Colzani, B., Palugan, L., Foppoli, A., Talamini, L., & Morosi, L. (2019). Monitoring the fate of orally administered PLGA nanoformulation for local delivery of therapeutic drugs. *Pharmaceutics*, *11*(12), 658.

Murakami, H., Kobayashi, M., Takeuchi, H., & Kawashima, Y. (1999). Preparation of poly(DL-lactide-co-glycolide) nanoparticles by modified spontaneous emulsification solvent diffusion method. *Int J Pharm*, *187*(2), 143-152. https://doi.org/10.1016/s0378-5173(99)00187-8

Murphy, N. P., & Lampe, K. J. (2018). Fabricating PLGA microparticles with high loads of the small molecule antioxidant N-acetylcysteine that rescue oligodendrocyte progenitor cells from oxidative stress. *Biotechnology and bioengineering*, *115*(1), 246-256.

N. Politis, S., Colombo, P., Colombo, G., & M. Rekkas, D. (2017). Design of experiments (DoE) in pharmaceutical development. *Drug development and industrial pharmacy*, *43*(6), 889-901.

Nayak, A. K., Ahmed, S. A., Beg, S., Tabish, M., & Hasnain, M. S. (2019). Chapter 18 - Application of Quality by Design for the Development of Biopharmaceuticals. In S. Beg & M. S. Hasnain (Eds.), *Pharmaceutical Quality by Design* (pp. 399-411). Academic Press. https://doi.org/https://doi.org/10.1016/B978-0-12-815799-2.00019-8

NIST. *Response surface designs*. Retrieved 12/27 from https://www.itl.nist.gov/div898/handbook/pri/section3/pri336.htm

Oladugba, A. V., & Nwanonobi, O. C. (2021). Robustness of definitive screening composite designs to missing observations. *Communications in Statistics-Theory and Methods*, 1-15.

Ozturk, A. A., & Kiyan, H. T. (2020). Treatment of oxidative stress-induced pain and inflammation with dexketoprofen trometamol loaded different molecular weight chitosan nanoparticles: Formulation, characterization and anti-inflammatory activity by using in vivo HET-CAM assay. *Microvasc Res*, *128*, 103961. https://doi.org/10.1016/j.mvr.2019.103961

Paliwal, R., Babu, R. J., & Palakurthi, S. (2014). Nanomedicine scale-up technologies: feasibilities and challenges. *AAPS PharmSciTech*, *15*(6), 1527-1534. https://doi.org/10.1208/s12249-014-0177-9

Panyam, J., Williams, D., Dash, A., Leslie-Pelecky, D., & Labhasetwar, V. (2004). Solid-state Solubility Influences Encapsulation and Release of Hydrophobic Drugs from PLGA/PLA Nanoparticles. *Journal of Pharmaceutical Sciences*, *93*(7), 1804-1814. https://doi.org/https://doi.org/10.1002/jps.20094

Paoloni, M. C., Mazcko, C., Fox, E., Fan, T., Lana, S., Kisseberth, W., Vail, D. M., Nuckolls, K., Osborne, T., Yalkowsy, S., Gustafson, D., Yu, Y., Cao, L., & Khanna, C. (2010). Rapamycin pharmacokinetic and pharmacodynamic relationships in osteosarcoma: a comparative

oncology study in dogs. *PLoS One*, *5*(6), e11013-e11013. https://doi.org/10.1371/journal.pone.0011013

Pardeshi, S. R., Nikam, A., Chandak, P., Mandale, V., Naik, J. B., & Giram, P. S. (2021). Recent advances in PLGA based nanocarriers for drug delivery system: a state of the art review. *International journal of polymeric materials*, *ahead-of-print*(ahead-of-print), 1-30. https://doi.org/10.1080/00914037.2021.1985495

Patel, J., Amrutiya, J., Bhatt, P., Javia, A., Jain, M., & Misra, A. (2018). Targeted delivery of monoclonal antibody conjugated docetaxel loaded PLGA nanoparticles into EGFR overexpressed lung tumour cells. *Journal of microencapsulation*, *35*(2), 204-217.

Pavel, F. M. (2004). Microemulsion Polymerization. *Journal of dispersion science and technology*, *25*(1), 1-16. https://doi.org/10.1081/DIS-120027662

Phillips, D. J., Pygall, S. R., Cooper, V. B., & Mann, J. C. (2012). Overcoming sink limitations in dissolution testing: a review of traditional methods and the potential utility of biphasic systems. *J Pharm Pharmacol*, *64*(11), 1549-1559. https://doi.org/10.1111/j.2042-7158.2012.01523.x

Quintanar-Guerrero, D., Zambrano-Zaragoza Mde, L., Gutierrez-Cortez, E., & Mendoza-Munoz, N. (2012). Impact of the emulsification-diffusion method on the development of pharmaceutical nanoparticles. *Recent Pat Drug Deliv Formul*, *6*(3), 184-194. https://doi.org/10.2174/187221112802652642

Rafiei, P., & Haddadi, A. (2017). Docetaxel-loaded PLGA and PLGA-PEG nanoparticles for intravenous application: pharmacokinetics and biodistribution profile. *International journal of nanomedicine*, *12*, 935.

Rao, Y. F., Chen, W., Liang, X. G., Huang, Y. Z., Miao, J., Liu, L., Lou, Y., Zhang, X. G., Wang, B., Tang, R. K., Chen, Z., & Lu, X. Y. (2015). Epirubicin-loaded superparamagnetic iron-oxide nanoparticles for transdermal delivery: cancer therapy by circumventing the skin barrier. *Small*, *11*(2), 239-247. https://doi.org/10.1002/smll.201400775

Ribeiro, S. B., de Araújo, A. A., Oliveira, M. M. B., Santos Silva, A. M. d., da Silva-Júnior, A. A., Guerra, G. C. B., Brito, G. A. d. C., Leitão, R. F. d. C., Araújo Júnior, R. F. d., & Garcia, V. B. (2021). Effect of dexamethasone-loaded PLGA nanoparticles on oral mucositis induced by 5-fluorouracil. *Pharmaceutics*, *13*(1), 53.

Ricci, M., Blasi, P., Giovagnoli, S., Rossi, C., Macchiarulo, G., Luca, G., Basta, G., & Calafiore, R. (2005). Ketoprofen controlled release from composite microcapsules for cell encapsulation: effect on post-transplant acute inflammation. *Journal of Controlled Release*, *107*(3), 395-407.

Ritu, G., & Meenakshi, B. (2013). Preparation and Physicochemical Characterization of Tizanidine Hydrochloride Nanoparticles. *Journal of Pharmaceutical Research*, *12*(1), 15-22.

Robertson, J. D., Rizzello, L., Avila-Olias, M., Gaitzsch, J., Contini, C., Magoń, M. S., Renshaw, S. A., & Battaglia, G. (2016). Purification of Nanoparticles by Size and Shape. *Sci Rep*, *6*, 27494. https://doi.org/10.1038/srep27494

Rüttimann, B. G., & Wegener, K. (2015). The power of DOE: How to increase experimental design success and avoid pitfalls. *Journal of Service Science and Management*, *8*(02), 250.

Saadati, R., & Dadashzadeh, S. (2014). Marked effects of combined TPGS and PVA emulsifiers in the fabrication of etoposide-loaded PLGA-PEG nanoparticles: in vitro and in vivo evaluation. *Int J Pharm*, *464*(1-2), 135-144. https://doi.org/10.1016/j.ijpharm.2014.01.014

Sadhukhan, B., Mondal, N. K., & Chattoraj, S. (2016). Optimisation using central composite design (CCD) and the desirability function for sorption of methylene blue from aqueous solution onto Lemna major. *Karbala International Journal of Modern Science*, *2*(3), 145-155.

Sahin, A., Spiroux, F., Guedon, I., Arslan, F. B., Sarcan, E. T., Ozkan, T., Colak, N., Yuksel, S., Ozdemir, S., Ozdemir, B., Akbas, S., Ultav, G., Aktas, Y., & Capan, Y. (2017). Using PVA and TPGS as combined emulsifier in nanoprecipitation method improves characteristics and anticancer activity of ibuprofen loaded PLGA nanoparticles. *Pharmazie*, *72*(9), 525-528. https://doi.org/10.1691/ph.2017.7015

Sahoo, N., Sahoo, R. K., Biswas, N., Guha, A., & Kuotsu, K. (2015). Recent advancement of gelatin nanoparticles in drug and vaccine delivery. *Int J Biol Macromol*, *81*, 317-331. https://doi.org/10.1016/j.ijbiomac.2015.08.006

Sánchez-López, E., Espina, M., Doktorovova, S., Souto, E. B., & García, M. L. (2017). Lipid nanoparticles (SLN, NLC): Overcoming the anatomical and physiological barriers of the eye – Part II - Ocular drug-loaded lipid nanoparticles. *European Journal of Pharmaceutics and Biopharmaceutics*, *110*, 58-69. https://doi.org/https://doi.org/10.1016/j.ejpb.2016.10.013

Sandland, J., Savoie, H., Boyle, R. W., & Murray, B. S. (2021). RAPTA-Decorated Polyacrylamide Nanoparticles: Exploring their Synthesis, Physical Properties and Effect on Cell Viability. *Chembiochem*, *22*(5), 931-936. https://doi.org/10.1002/cbic.202000704

Sangshetti, J. N., Deshpande, M., Zaheer, Z., Shinde, D. B., & Arote, R. (2017). Quality by design approach: Regulatory need. *Arabian Journal of Chemistry*, *10*, S3412-S3425.

Sanna, V., Roggio, A. M., Siliani, S., Piccinini, M., Marceddu, S., Mariani, A., & Sechi, M. (2012). Development of novel cationic chitosan-and anionic alginate-coated poly(D,L-lactide-co-glycolide) nanoparticles for controlled release and light protection of resveratrol. *Int J Nanomedicine*, *7*, 5501-5516. https://doi.org/10.2147/IJN.S36684

Sarkar, M., Grossman, R. G., Toups, E. G., & Chow, D. S. L. (2018). Rational design and development of a stable liquid formulation of riluzole and its pharmacokinetic evaluation after oral and IV administrations in rats. *European Journal of Pharmaceutical Sciences*, *125*, 1-10. https://doi.org/https://doi.org/10.1016/j.ejps.2018.09.004

Saroj, S., & Rajput, S. J. (2018). Etoposide encapsulated functionalized mesoporous silica nanoparticles: Synthesis, characterization and effect of functionalization on dissolution kinetics in simulated and biorelevant media. *Journal of Drug Delivery Science and Technology*, *44*, 27-40. https://doi.org/https://doi.org/10.1016/j.jddst.2017.11.020

Schubert, M. A., & Müller-Goymann, C. C. (2003). Solvent injection as a new approach for manufacturing lipid nanoparticles – evaluation of the method and process parameters. *European Journal of Pharmaceutics and Biopharmaceutics*, *55*(1), 125-131. https://doi.org/https://doi.org/10.1016/S0939-6411(02)00130-3

Schwartz, J. B., O'Connor, R. E., & Schnaare, R. L. (2002). Optimization techniques in pharmaceutical formulation and processing. In *Modern pharmaceutics* (pp. 921-950). CRC Press.

Sedighi, M., Sieber, S., Rahimi, F., Shahbazi, M. A., Rezayan, A. H., Huwyler, J., & Witzigmann, D. (2019). Rapid optimization of liposome characteristics using a combined microfluidics and design-of-experiment approach. *Drug Deliv Transl Res*, *9*(1), 404-413. https://doi.org/10.1007/s13346-018-0587-4

Seju, U., Kumar, A., & Sawant, K. K. (2011). Development and evaluation of olanzapine-loaded PLGA nanoparticles for nose-to-brain delivery: In vitro and in vivo studies. *Acta Biomaterialia*, *7*(12), 4169-4176. https://doi.org/https://doi.org/10.1016/j.actbio.2011.07.025

Shabbits, J. A., Chiu, G. N., & Mayer, L. D. (2002). Development of an in vitro drug release assay that accurately predicts in vivo drug retention for liposome-based delivery systems. *J Control Release*, *84*(3), 161-170. https://doi.org/10.1016/s0168-3659(02)00294-8

Shah, S. M., Jain, A. S., Kaushik, R., Nagarsenker, M. S., & Nerurkar, M. J. (2014). Preclinical formulations: insight, strategies, and practical considerations. *AAPS PharmSciTech*, *15*(5), 1307-1323. https://doi.org/10.1208/s12249-014-0156-1

Shah, S. S., Cha, Y., & Pitt, C. G. (1992). Poly (glycolic acid-co-dl-lactic acid): diffusion or degradation controlled drug delivery? *Journal of Controlled Release*, *18*(3), 261-270. https://doi.org/https://doi.org/10.1016/0168-3659(92)90171-M

Shah, V. P., Tsong, Y., Sathe, P., & Liu, J. P. (1998). In vitro dissolution profile comparison--statistics and analysis of the similarity factor, f2. *Pharm Res*, *15*(6), 889-896. https://doi.org/10.1023/a:1011976615750

Shameem, M., Lee, H., & DeLuca, P. P. (1999). A short term (accelerated release) approach to evaluate peptide release from PLGA depot-formulations. *AAPS PharmSci*, *1*(3), E7. https://doi.org/10.1208/ps010307

Sharma, D., Maheshwari, D., Philip, G., Rana, R., Bhatia, S., Singh, M., Gabrani, R., Sharma, S. K., Ali, J., Sharma, R. K., & Dang, S. (2014). Formulation and optimization of polymeric nanoparticles for intranasal delivery of lorazepam using Box-Behnken design: in vitro and in vivo evaluation. *Biomed Res Int*, *2014*, 156010. https://doi.org/10.1155/2014/156010

Shen, J., & Burgess, D. J. (2013). Dissolution Testing Strategies for Nanoparticulate Drug Delivery Systems: Recent Developments and Challenges. *Drug Deliv Transl Res*, *3*(5), 409-415. https://doi.org/10.1007/s13346-013-0129-z

Shen, J., Lee, K., Choi, S., Qu, W., Wang, Y., & Burgess, D. J. (2016). A reproducible accelerated in vitro release testing method for PLGA microspheres. *Int J Pharm*, *498*(1-2), 274-282. https://doi.org/10.1016/j.ijpharm.2015.12.031

Shi, Y., xue, J., Jia, L., Du, Q., Niu, J., & Zhang, D. (2018). Surface-modified PLGA nanoparticles with chitosan for oral delivery of tolbutamide. *Colloids and Surfaces B: Biointerfaces*, *161*, 67-72. https://doi.org/https://doi.org/10.1016/j.colsurfb.2017.10.037

Shubhra, Q. T., Feczko, T., Kardos, A. F., Toth, J., Mackova, H., Horak, D., Dosa, G., & Gyenis, J. (2014). Co-encapsulation of human serum albumin and superparamagnetic iron oxide in

PLGA nanoparticles: part II. Effect of process variables on protein model drug encapsulation efficiency. *J Microencapsul*, *31*(2), 156-165. https://doi.org/10.3109/02652048.2013.814730

Siegel, S. J., Kahn, J. B., Metzger, K., Winey, K. I., Werner, K., & Dan, N. (2006). Effect of drug type on the degradation rate of PLGA matrices. *European Journal of Pharmaceutics and Biopharmaceutics*, *64*(3), 287-293.

Siepmann, J., Elkharraz, K., Siepmann, F., & Klose, D. (2005). How Autocatalysis Accelerates Drug Release from PLGA-Based Microparticles: A Quantitative Treatment. *Biomacromolecules*, *6*(4), 2312-2319. https://doi.org/10.1021/bm050228k

Sievens-Figueroa, L., Pandya, N., Bhakay, A., Keyvan, G., Michniak-Kohn, B., Bilgili, E., & Davé, R. N. (2012). Using USP I and USP IV for Discriminating Dissolution Rates of Nano- and Microparticle-Loaded Pharmaceutical Strip-Films. *AAPS PharmSciTech*, *13*(4), 1473-1482. https://doi.org/10.1208/s12249-012-9875-3

Sindhu, R., Binod, P., & Pandey, A. (2015). Chapter 17 - Microbial Poly-3-Hydroxybutyrate and Related Copolymers. In A. Pandey, R. Höfer, M. Taherzadeh, K. M. Nampoothiri, & C. Larroche (Eds.), *Industrial Biorefineries & White Biotechnology* (pp. 575-605). Elsevier. https://doi.org/https://doi.org/10.1016/B978-0-444-63453-5.00019-7

Singh, B., Bhatowa, R., Tripathi, C. B., & Kapil, R. (2011). Developing micro-/nanoparticulate drug delivery systems using "design of experiments". *International journal of pharmaceutical investigation*, *1*(2), 75.

Singh, I., & Aboul-Enein, H. Y. (2006). Advantages of USP Apparatus IV (flow-through cell apparatus) in dissolution studies. *Journal of the Iranian Chemical Society*, *3*(3), 220-222. https://doi.org/10.1007/BF03247211

Soh, S. H., & Lee, L. Y. (2019). Microencapsulation and Nanoencapsulation Using Supercritical Fluid (SCF) Techniques. *Pharmaceutics*, *11*(1). https://doi.org/10.3390/pharmaceutics11010021

Sonaje, K., Chen, Y.-J., Chen, H.-L., Wey, S.-P., Juang, J.-H., Nguyen, H.-N., Hsu, C.-W., Lin, K.-J., & Sung, H.-W. (2010). Enteric-coated capsules filled with freeze-dried chitosan/poly(γ-glutamic acid) nanoparticles for oral insulin delivery. *Biomaterials*, *31*(12), 3384-3394. https://doi.org/https://doi.org/10.1016/j.biomaterials.2010.01.042

Song, X., Zhao, Y., Hou, S., Xu, F., Zhao, R., He, J., Cai, Z., Li, Y., & Chen, Q. (2008). Dual agents loaded PLGA nanoparticles: Systematic study of particle size and drug entrapment efficiency. *European Journal of Pharmaceutics and Biopharmaceutics*, *69*(2), 445-453. https://doi.org/https://doi.org/10.1016/j.ejpb.2008.01.013

Stevens, R. E., Gray, V., Dorantes, A., Gold, L., & Pham, L. (2015). Scientific and regulatory standards for assessing product performance using the similarity factor, f2. *AAPS J*, *17*(2), 301-306. https://doi.org/10.1208/s12248-015-9723-y

Subra, P., & Jestin, P. (2000). Screening Design of Experiment (DOE) Applied to Supercritical Antisolvent Process. *Industrial & Engineering Chemistry Research*, *39*(11), 4178-4184. https://doi.org/10.1021/ie990940w

Suk, J. S., Xu, Q., Kim, N., Hanes, J., & Ensign, L. M. (2016). PEGylation as a strategy for improving nanoparticle-based drug and gene delivery. *Adv Drug Deliv Rev*, *99*(Pt A), 28-51. https://doi.org/10.1016/j.addr.2015.09.012

Sun, L.-G., Xie, Z.-Y., Zhao, Y.-J., Wei, H.-M., & Gu, Z.-Z. (2013). Optical monitoring the degradation of PLGA inverse opal film. *Chinese Chemical Letters*, *24*(1), 9-12. https://doi.org/https://doi.org/10.1016/j.cclet.2013.01.012

Sun, S. B., Liu, P., Shao, F. M., & Miao, Q. L. (2015). Formulation and evaluation of PLGA nanoparticles loaded capecitabine for prostate cancer. *Int J Clin Exp Med*, *8*(10), 19670-19681.

Sun, Y.-P., Atorngitjawat, P., & Meziani, M. J. (2001). Preparation of Silver Nanoparticles via Rapid Expansion of Water in Carbon Dioxide Microemulsion into Reductant Solution. *Langmuir*, *17*(19), 5707-5710. https://doi.org/10.1021/la0103057

Sun, Y., Bhattacharjee, A., Reynolds, M., & Li, Y. V. (2021). Synthesis and characterizations of gentamicin-loaded poly-lactic-co-glycolic (PLGA) nanoparticles. *Journal of Nanoparticle Research*, *23*(8), 155. https://doi.org/10.1007/s11051-021-05293-3

Taghavi, S., Ramezani, M., Alibolandi, M., Abnous, K., & Taghdisi, S. M. (2017). Chitosan-modified PLGA nanoparticles tagged with 5TR1 aptamer for in vivo tumor-targeted drug delivery. *Cancer letters*, *400*, 1-8. https://doi.org/10.1016/j.canlet.2017.04.008

Tang, J., Srinivasan, S., Yuan, W., Ming, R., Liu, Y., Dai, Z., Noble, C. O., Hayes, M. E., Zheng, N., Jiang, W., Szoka, F. C., & Schwendeman, A. (2019). Development of a flow-through USP 4 apparatus drug release assay for the evaluation of amphotericin B liposome. *European Journal of Pharmaceutics and Biopharmaceutics*, *134*, 107-116. https://doi.org/https://doi.org/10.1016/j.ejpb.2018.11.010

Tansık, G., Yakar, A., & Gündüz, U. (2013). Tailoring magnetic PLGA nanoparticles suitable for doxorubicin delivery. *Journal of Nanoparticle Research*, *16*(1), 2171. https://doi.org/10.1007/s11051-013-2171-7

Tomoda, B. T., Yassue-Cordeiro, P. H., Ernesto, J. V., Lopes, P. S., Péres, L. O., da Silva, C. F., & de Moraes, M. A. (2020). Chapter 3 - Characterization of biopolymer membranes and films: Physicochemical, mechanical, barrier, and biological properties. In M. A. de Moraes, C. F. da Silva, & R. S. Vieira (Eds.), *Biopolymer Membranes and Films* (pp. 67-95). Elsevier. https://doi.org/https://doi.org/10.1016/B978-0-12-818134-8.00003-1

Tukulula, M., Hayeshi, R., Fonteh, P., Meyer, D., Ndamase, A., Madziva, M. T., Khumalo, V., Lubuschagne, P., Naicker, B., Swai, H., & Dube, A. (2015). Curdlan-Conjugated PLGA Nanoparticles Possess Macrophage Stimulant Activity and Drug Delivery Capabilities. *Pharmaceutical Research*, *32*(8), 2713-2726. https://doi.org/10.1007/s11095-015-1655-9

Urbaniak, T., & Musiał, W. (2019). Influence of Solvent Evaporation Technique Parameters on Diameter of Submicron Lamivudine-Poly-ε-Caprolactone Conjugate Particles. *Nanomaterials*, *9*(9), 1240. https://www.mdpi.com/2079-4991/9/9/1240

USP43NF38. (2020). 〈*1092*〉*THE DISSOLUTION PROCEDURE: DEVELOPMENT AND VALIDATION*. text-autospace:none">https://online.uspnf.com/uspnf/document/1_GUID-CE0902BA-77AC-422D-8BF0-A221B5DE6012_5_en-US

Varga, N., Turcsányi, Á., Hornok, V., & Csapó, E. (2019). Vitamin E-loaded PLA-and PLGA-based core-shell nanoparticles: synthesis, structure optimization and controlled drug release. *Pharmaceutics*, *11*(7), 357.

Ventola, C. L. (2017). Progress in Nanomedicine: Approved and Investigational Nanodrugs. *P T*, *42*(12), 742-755. https://www.ncbi.nlm.nih.gov/pubmed/29234213

Vera Candioti, L., De Zan, M. M., Cámara, M. S., & Goicoechea, H. C. (2014). Experimental design and multiple response optimization. Using the desirability function in analytical methods development. *Talanta*, *124*, 123-138. https://doi.org/https://doi.org/10.1016/j.talanta.2014.01.034

Vining, G. G., Kowalski, S. M., & Montgomery, D. C. (2005). Response surface designs within a split-plot structure. *Journal of Quality Technology*, *37*(2), 115-129.

Wallenwein, C. M., Nova, M. V., Janas, C., Jablonka, L., Gao, G. F., Thurn, M., Albrecht, V., Wiehe, A., & Wacker, M. G. (2019). A dialysis-based in vitro drug release assay to study dynamics of the drug-protein transfer of temoporfin liposomes. *Eur J Pharm Biopharm*, *143*, 44-50. https://doi.org/10.1016/j.ejpb.2019.08.010

Wang, Y., Kho, K., Cheow, W. S., & Hadinoto, K. (2012). A comparison between spray drying and spray freeze drying for dry powder inhaler formulation of drug-loaded lipid-polymer hybrid nanoparticles. *Int J Pharm*, *424*(1-2), 98-106. https://doi.org/10.1016/j.ijpharm.2011.12.045

Wang, Y., Li, P., Truong-Dinh Tran, T., Zhang, J., & Kong, L. (2016). Manufacturing Techniques and Surface Engineering of Polymer Based Nanoparticles for Targeted Drug Delivery to Cancer. *Nanomaterials (Basel)*, *6*(2). https://doi.org/10.3390/nano6020026

Weng, J., Tong, H. H. Y., & Chow, S. F. (2020). In Vitro Release Study of the Polymeric Drug Nanoparticles: Development and Validation of a Novel Method. *Pharmaceutics*, *12*(8). https://doi.org/10.3390/pharmaceutics12080732

Wischke, C., & Schwendeman, S. P. (2008). Principles of encapsulating hydrophobic drugs in PLA/PLGA microparticles. *International Journal of Pharmaceutics*, *364*(2), 298-327.

Wong, C. Y., Al-Salami, H., & Dass, C. R. (2020). Lyophilisation Improves Bioactivity and Stability of Insulin-Loaded Polymeric-Oligonucleotide Nanoparticles for Diabetes Treatment. *AAPS PharmSciTech*, *21*(3), 108. https://doi.org/10.1208/s12249-020-01648-6

Wong, H. M., Wang, J. J., & Wang, C.-H. (2001). In vitro sustained release of human immunoglobulin G from biodegradable microspheres. *Industrial & Engineering Chemistry Research*, *40*(3), 933-948.

Xiong, S., George, S., Yu, H., Damoiseaux, R., France, B., Ng, K. W., & Loo, J. S. (2013). Size influences the cytotoxicity of poly (lactic-co-glycolic acid) (PLGA) and titanium dioxide (TiO(2)) nanoparticles. *Arch Toxicol*, *87*(6), 1075-1086. https://doi.org/10.1007/s00204-012-0938-8

Xu, X., Khan, M. A., & Burgess, D. J. (2012). A two-stage reverse dialysis in vitro dissolution testing method for passive targeted liposomes. *Int J Pharm*, *426*(1-2), 211-218. https://doi.org/10.1016/j.ijpharm.2012.01.030

Yallapu, M. M., Gupta, B. K., Jaggi, M., & Chauhan, S. C. (2010). Fabrication of curcumin encapsulated PLGA nanoparticles for improved therapeutic effects in metastatic cancer

cells. *Journal of Colloid and Interface Science*, *351*(1), 19-29. https://doi.org/https://doi.org/10.1016/j.jcis.2010.05.022

Yeo, E. L. L., Cheah, J. U. J., Thong, P. S. P., Soo, K. C., & Kah, J. C. Y. (2019). Gold Nanorods Coated with Apolipoprotein E Protein Corona for Drug Delivery. *ACS Applied Nano Materials*, *2*(10), 6220-6229. https://doi.org/10.1021/acsanm.9b01196

Yoon, M.-S., & Choi, C. S. (2016). The role of amino acid-induced mammalian target of rapamycin complex 1 (mTORC1) signaling in insulin resistance. *Experimental & molecular medicine*, *48*(1), e201-e201.

Yoshida, H., Kuwana, A., Shibata, H., Izutsu, K., & Goda, Y. (2015). Particle Image Velocimetry Evaluation of Fluid Flow Profiles in USP 4 Flow-Through Dissolution Cells. *Pharm Res*, *32*(9), 2950-2959. https://doi.org/10.1007/s11095-015-1676-4

Yuan, W., Kuai, R., Dai, Z., Yuan, Y., Zheng, N., Jiang, W., Noble, C., Hayes, M., Szoka, F. C., & Schwendeman, A. (2017). Development of a Flow-Through USP-4 Apparatus Drug Release Assay to Evaluate Doxorubicin Liposomes. *The AAPS journal*, *19*(1), 150-160. https://doi.org/10.1208/s12248-016-9958-2

Zackrisson, G., Östling, G., Skagerberg, B., & Anfält, T. (1995). ACcelerated Dissolution Rate Analysis (ACDRA) for controlled release drugs. Application to Roxiam®. *Journal of Pharmaceutical and Biomedical Analysis*, *13*(4), 377-383. https://doi.org/https://doi.org/10.1016/0731-7085(95)01293-T

ZetasizerNano, & Manual. (2003). *ZetasizerNanoUserManual*. https://physics.nyu.edu/grierlab/manuals/ZetasizerNanoUserManual.pdf

Zhang, B., Sai Lung, P., Zhao, S., Chu, Z., Chrzanowski, W., & Li, Q. (2017). Shape dependent cytotoxicity of PLGA-PEG nanoparticles on human cells. *Sci Rep*, *7*(1), 7315. https://doi.org/10.1038/s41598-017-07588-9

Zhang, D., & Yang, X. (2015). Precipitation Polymerization. In S. Kobayashi & K. Müllen (Eds.), *Encyclopedia of Polymeric Nanomaterials* (pp. 2108-2116). Springer Berlin Heidelberg. https://doi.org/10.1007/978-3-642-29648-2_282

Zhang, H., Pu, C., Wang, Q., Tan, X., Gou, J., He, H., Zhang, Y., Yin, T., Wang, Y., & Tang, X. (2018). Physicochemical Characterization and Pharmacokinetics of Agomelatine-Loaded PLGA Microspheres for Intramuscular Injection. *Pharmaceutical Research*, *36*(1), 9. https://doi.org/10.1007/s11095-018-2538-7

Zhang, J.-Y., Shen, Z.-G., Zhong, J., Hu, T.-T., Chen, J.-F., Ma, Z.-Q., & Yun, J. (2006). Preparation of amorphous cefuroxime axetil nanoparticles by controlled nanoprecipitation method without surfactants. *International Journal of Pharmaceutics*, *323*(1), 153-160. https://doi.org/https://doi.org/10.1016/j.ijpharm.2006.05.048

Zhang, L., & Mao, S. (2017). Application of quality by design in the current drug development. *Asian Journal of Pharmaceutical Sciences*, *12*(1), 1-8. https://doi.org/https://doi.org/10.1016/j.ajps.2016.07.006

Zhang, X., Sun, M., Zheng, A., Cao, D., Bi, Y., & Sun, J. (2012). Preparation and characterization of insulin-loaded bioadhesive PLGA nanoparticles for oral administration. *European Journal of Pharmaceutical Sciences*, *45*(5), 632-638.

Zhang, Y., Huo, M., Zhou, J., Zou, A., Li, W., Yao, C., & Xie, S. (2010). DDSolver: an add-in program for modeling and comparison of drug dissolution profiles. *The AAPS journal*, *12*(3), 263-271.

Zhang, Y., Zhuang, X., Gu, W., & Zhao, J. (2015). Synthesis of polyacrylonitrile nanoparticles at high monomer concentrations by AIBN-initiated semi-continuous emulsion polymerization method. *European Polymer Journal*, *67*, 57-65. https://doi.org/https://doi.org/10.1016/j.eurpolymj.2015.03.057

Zhang, Z., Guan, J., Jiang, Z., Yang, Y., Liu, J., Hua, W., Mao, Y., Li, C., Lu, W., Qian, J., & Zhan, C. (2019). Brain-targeted drug delivery by manipulating protein corona functions. *Nature Communications*, *10*(1), 3561. https://doi.org/10.1038/s41467-019-11593-z

Zhang, Z., & Xiaofeng, B. (2009, 22-24 Jan. 2009). Comparison about the Three Central Composite Designs with Simulation. 2009 International Conference on Advanced Computer Control,

Zhang, Z. B., Shen, Z. G., Wang, J. X., Zhang, H. X., Zhao, H., Chen, J. F., & Yun, J. (2009). Micronization of silybin by the emulsion solvent diffusion method. *Int J Pharm*, *376*(1-2), 116-122. https://doi.org/10.1016/j.ijpharm.2009.04.028

Zielinska, A., Carreiro, F., Oliveira, A. M., Neves, A., Pires, B., Venkatesh, D. N., Durazzo, A., Lucarini, M., Eder, P., Silva, A. M., Santini, A., & Souto, E. B. (2020). Polymeric Nanoparticles: Production, Characterization, Toxicology and Ecotoxicology. *Molecules*, *25*(16). https://doi.org/10.3390/molecules25163731

Zolnik, B. S., & Burgess, D. J. (2008). *In Vitro–In Vivo Correlation on Parenteral Dosage Forms.* . Springer. https://doi.org/https://doi.org/10.1007/978-0-387-72379-2_11

Zolnik, B. S., Leary, P. E., & Burgess, D. J. (2006). Elevated temperature accelerated release testing of PLGA microspheres. *J Control Release*, *112*(3), 293-300. https://doi.org/10.1016/j.jconrel.2006.02.015

Zuo, J., Gao, Y., Bou-Chacra, N., & Löbenberg, R. (2014). Evaluation of the DDSolver Software Applications. *BioMed Research International*, *2014*, 204925. https://doi.org/10.1155/2014/204925